ELECTROCHEMICAL ACTIVATION OF PROTEINS

AT ELECTRODE SURFACES THROUGH

ELECTROSTATIC PROMOTION

AND DISCRIMINATION

By

MARC-OLIVER SASCHA WIRTZ

Bachelor of Science

Cameron University
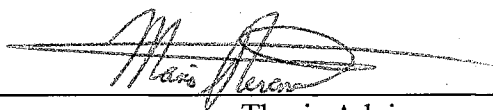
Lawton, Oklahoma

1996

Submitted to the Faculty of the
Graduate College of the
Oklahoma State University
in partial fulfillment of
the requirements for
the Degree of
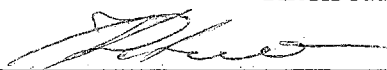DOCTOR OF PHILOSOPHY
December, 2000

DEDICATION

*Dedicated
To the two most wonderful
women in my life,
my mother and my wife*

ELECTROCHEMICAL ACTIVATION OF PROTEINS

AT ELECTRODE SURFACES THROUGH

ELECTROSTATIC PROMOTION
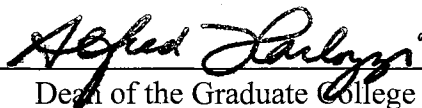
AND DISCRIMINATION

Thesis Approved:

_____

Thesis Advisor

_____

Andrew Mort

_____

Richard A. Bunce

_____

Dean of the Graduate College

ACKNOWLEDGMENTS

I would like to acknowledge several people, without whose help and input this thesis would never have materialized, at least not as quickly. First, I would like to thank my advisor Dr. Mario Rivera for his guidance, support, and encouragement. It is due to his philosophy, and through his example, that I have achieved the position I am at today.

I am extremely grateful for the assistance offered by my committee members, Drs. Richard Bunce, Andrew Mort and Nick Kotov. I would especially like to thank Dr. Nick Kotov who has always assisted me whenever I asked. I would like to thank Dr. Isabelle Lagadic who never hesitated in making herself or her lab available to further my research.

I would like to express my gratitude for the Presidential Fellowship for Water, Energy and the Environment given to me by the Environmental Institute at Oklahoma State University. I also appreciate the support given by the Chemistry Department through teaching assistantships. Mike Lucas' effort in constructing all of the electrochemical cells over the years is greatly appreciated. I also would like to give credit to Vaheh Oganeyan and Xuejun Zhang for the determination of the X-ray crystal structure of the V45I/V61I mutant of OM cytochrome b_5.

Last I would like to thank my wife Rebecca for her love, support, encouragement, and the help that she provided over this stressful time. I could not have done this without her.

TABLE OF CONTENTS

LIST OF FIGURES

Chapter IV

Chapter V

LIST OF SYMBOLS AND ABBREVIATIONS

ALA	δ-Aminolevulinic acid
α	Transfer coefficient
ATP	Adenosine Triphosphate
Cyt c	Cytochrome c
D_o	Diffusion coefficient of oxidized species
D_r	Diffusion coefficient of reduced species
DDAB	Didodecyldimethylammonium bromide
ΔE_p	Peak to peak separation
ε	Extinction coefficient
$E^{o'}$	Formal reduction potential
EC	Electrochemical
EDTA	Ethylenediaminetetraacetic acid
GC	Gas chromatography
i_{pa}	Peak anodic current
i_{pc}	Peak cathodic current
IPTG	Isopropyl-β-thiogalactoside
ITO	Indium tin oxide
k_s	Heterogeneous electron transfer rate constant
k_f	Forward homogeneous electron transfer rate constant

k_b	Backward homogeneous electron transfer rate constant
μ	Ionic strength
MOPS	3-[N-Morpholino]propane sulfonic acid
MS	Mass spectrometry
MW	Molecular weight
n	Number of electrons transferred
NADH	Nicotinamide adenine dinucleotide
NADP	Nicotinamide adenine dinuleotide phosphate
NHE	Normal hydrogen electrode
OM	Outer mitochondrial
Ox	Oxidized
PMAT	Poly(methacryloxyethyltrimethyl ammonium bromide)
Red	Reduced
rpm	revolutions per minute
UV-Vis	Ultraviolet-visible
υ	Scan rate

CHAPTER I

INTRODUCTION

Photosynthesis and Cellular Respiration

Life on this planet is based upon several fundamental energy acquiring processes. One of the major processes that is essential to life is cellular respiration, whereby nonphotosynthetic organisms use oxygen and the energy stored in the bonds of carbohydrates in order to carry out biochemical processes [1]. In cellular respiration, organic compounds are broken down and the stored energy is released. The energy is not released all at once, but in a series of discrete steps. This released energy is utilized by enzymes to carry out biochemical reactions. The equation describing cellular respiration is shown below:

$$C_6H_{12}O_6 + 6O_2 \rightarrow 6CO_2 + 6H_2O + energy$$
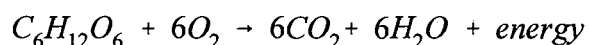
Glucose is converted to carbon dioxide and water in several catabolic pathways, thereby releasing energy stored in its chemical bonds. This energy is eventually utilized to produce nicotinamide adenine dinucleotide, (NADH). In oxidative phosphorylation [1], NADH acts as an initial electron source, and a series of electron transfer steps are initiated through the electron transport chain. This electron transport chain is composed of membrane-bound multi-subunit enzyme complexes containing several proteins which

1

H^+

H^+ H^+ H^+

H^+ H^+ H^+ H^+ H^+

H^+ H^+ H^+ H^+ H^+

e^- Membrane

                                H_2O ATP

H^+ H^+ H^+ H^+ $2O_2 + 4H^+$ synthase

ADP   ATP
+
Pi
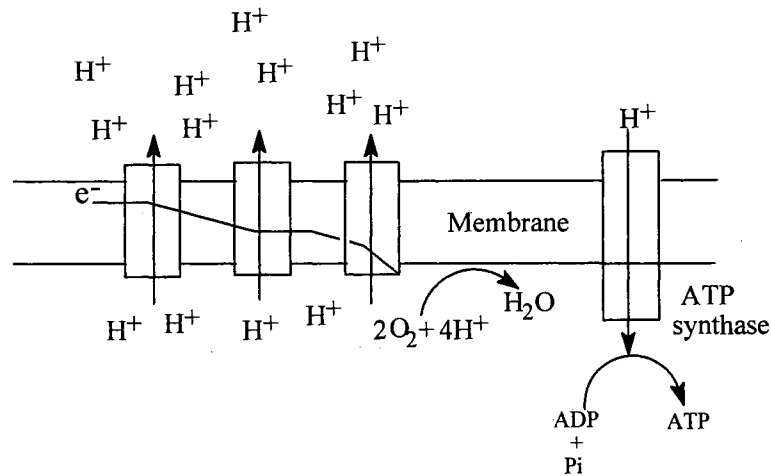
Figure 1. Mitochondrial electron transport. (Adapted from ref. 1).

transfer the electron onto a final electron acceptor, dioxygen [1]; dioxygen is reduced to water in this final step. This is shown schematically in Figure 1.

The electron transfer process is coupled to proton transfer, where protons are pumped across the mitochondrial membrane by the membrane-bound multi-subunit enzyme complexes. These protons are eventually transported back through the membrane and provide the energy source for the synthesis of adenosine triphosphate (ATP) by the enzyme ATP synthase [1]. The controlled transfer of the electrons along the electron transport chain is also shown in Figure 1. The flow of an electron along the electron transport chain proceeds through redox reactions involving proteins and cofactors. These molecules undergo cyclic oxidations and reductions that are essential to the survival of the organism.

Another essential process, for the assimilation of energy, is photosynthesis. In this process, photosynthetic organisms use carbon dioxide and water, along with light, to synthesize carbohydrates [2]. This is shown in the equation below:

$$CO_2 + 6H_2O + light \rightarrow C_6H_{12}O_6 + 6O$$
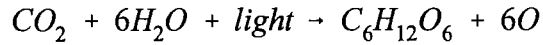
In photosynthesis, radiant energy is stored in the form of chemical bonds [2]. It should

be noted that oxygen is only a byproduct of photosynthesis. Photosynthesis takes place in

specialized organelles termed chloroplasts [1]. The thylakoid membrane is a continuous

membrane network found inside chloroplasts [1]. This membrane contains two protein

photosystems, (photosystem I and photosystem II) which carry out the light dependent

reactions of photosynthesis [1]. As seen in Figure 2, electrons originate from the

oxidation of water at photosystem II (PSII complex). These electrons are then transported

to chlorophyll molecules inside the PSII complex. Light excites the electron in chlorophyll

to a higher (excited) energy level. The excited electron is then shuttled to photosystem I
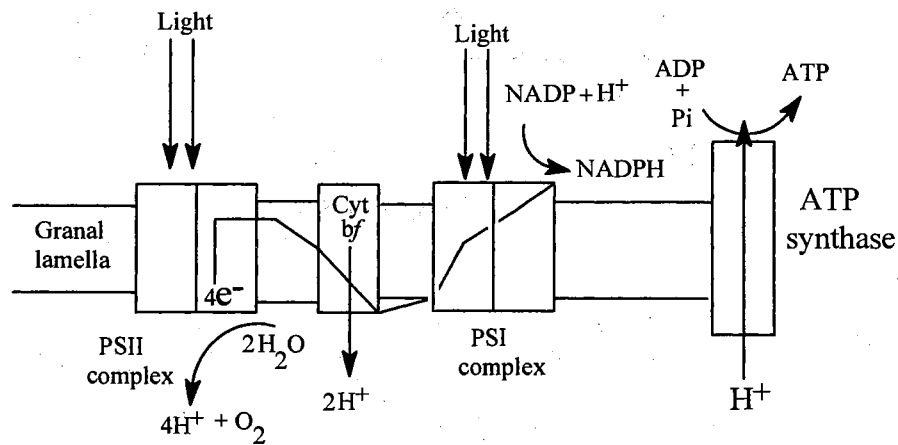
Figure 2. Photosynthetic electron transport. (Adapted from ref. 1)

(PSI complex) by an electron transport chain consisting of proteins and small organic

molecules [1]. The path that an electron takes is shown (Fig. 2) by the line originating at the oxidation of water and terminating at the reduction of NADP. At photosystem I, specialized chlorophyll molecules that contain the electron are excited by light, and the electron is once again shuttled away by electron transport molecules. In noncyclic electron transport, the terminal acceptor of the electron is nicotinamide adenine dinucleotide phosphate (NADP) (Fig. 2). During electron transport, protons are also transported across the membrane (similar to the mitochondrial electron transport chain) and are used in the production of ATP. At the heart of photosynthesis and cellular respiration lie oxidation reduction (redox) reactions, where an electron is transferred from one species to another. Countless number of times the proteins in these electron transport chains are reduced and oxidized as they contribute to energy production in the organism. Nature has accomplished this feat by using proteins that are very specific in their interaction with physiological partner molecules. This specific interaction among members of the electron transport chains ensures that the electrons are passed efficiently and precisely to the next appropriate carrier molecule. The magnitude of the reduction potential difference between partner proteins is, among other factors, central for electron transfer in photosynthesis and cellular respiration. Electron transfer proceeds from carrier molecules exhibiting low reduction potentials to carriers molecules exhibiting higher reduction potential [1]. The flow of electrons from low to high reduction potential carriers makes this transfer of the electron thermodynamically feasible, as is shown schematically in Figure 3. Where the four major complexes of the mitochrondrial electron transport chain, along with the relative reduction potentials of the complexes, are depicted. NADH is the initial source of the electron, and oxygen is the terminal acceptor. The four complexes are immobilized in the

4
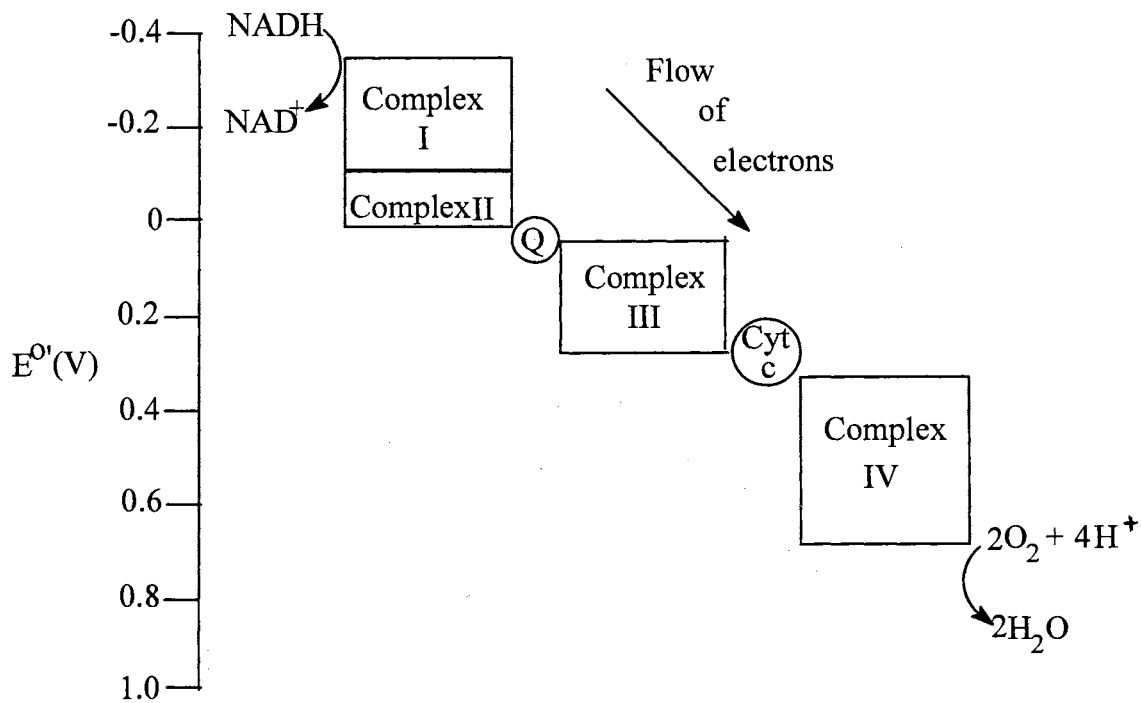
Figure 3. Representation of the flow of electrons in the mitochondrial electron transport chain, along with the relative reduction potentials of the species involved. Note that the transfer of electrons proceeds from species of lower reduction potential to species of higher reduction potential. (Adapted from ref.1)

membrane, and small molecules such as ubiquinone (Q) and cytochrome c (Cyt c), aid in transferring electrons between the major complexes.

Metalloproteins

The pathways that are involved in the production of chemical energy utilize two main categories of metalloproteins: 1) those that are electron transfer proteins and 2) enzymes that catalyze reactions, those that combine electron acceptor roles and chemical transformations, (e.g. can perform oxidation-reduction chemistry on substrate molecules) [3]. Nature also uses other small organic molecules, such as ubiquinone, to carry out

electron transfer in the energy generation pathways. We will only be concerned with some of the redox chemistry of the metal containing proteins.

Redox Metalloproteins

This class of proteins, whose sole function is to act as electron transfer proteins, can be divided into three basic groups according to their prosthetic center [3]. The three classes of electron transfer proteins are: 1) the iron-sulfur proteins; 2) cytochromes; and 3) blue copper proteins.

The iron-sulfur proteins constitute a class of redox proteins that are found in plants, animals, and bacteria [4]. They are characterized by the number of irons in the prosthetic center. In the prosthetic center, iron is coordinated to cysteine and arranged as a cluster with bridging sulfides. Some of the active sites (clusters), along with the species names, are shown in Figure 4 [5]. One of the characteristics of this class of proteins is that they have some of the most negative reduction potentials among metalloproteins [2]. They span the potential region from 350 mV to -490 mV. Rubredoxin shuttles the iron between 2^+ and 3^+ oxidation states, and has a reduction potential of 60 mV. Both types of ferredoxins shown in Fig. 3 have reduction potentials around -400 mV vs. NHE.

A second class of electron transfer proteins are the cytochromes, such as cytochrome c (E^o = 265 mV), and cytochrome b_5 (E^o= 0 mV). The active site of these types of molecules is heme. Heme b (Iron-protoporphyrin IX) is shown in Figure 5.

There are four different types of hemes classified according to the substituents on the ring [8]. In cytochromes possessing redox roles, the iron atom is coordinated by four pyrrole nitrogens, as well as by two axial ligands originating from the polypeptide. The oxidation state of the iron atom changes from 3^+ to 2^+ upon reduction. The cytochromes are
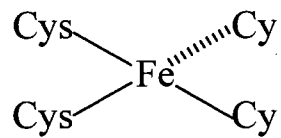
Rubredoxin
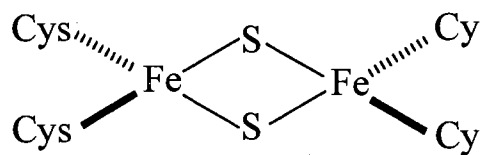
Fe$_2$S$_2$ Ferredoxin
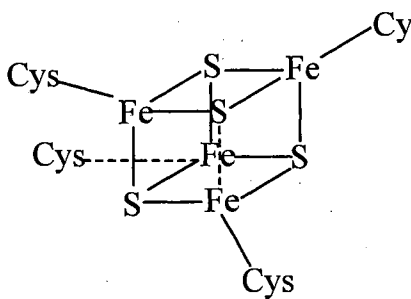
Fe$_4$S$_4$ Ferredoxin

Figure 4. Structures of the various iron-sulfur prosthetic centers found in simple redox metalloproteins
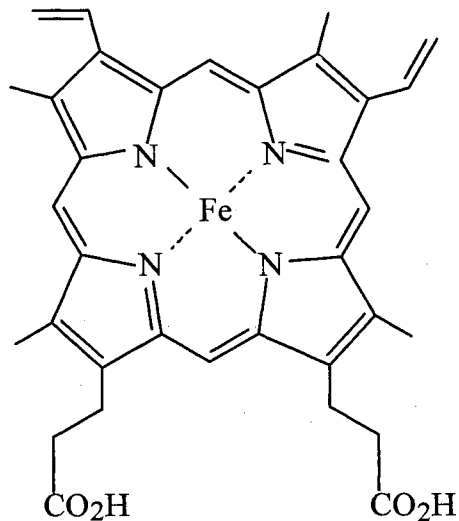
Figure 5. Structure of Heme b

characterized by having a reduction potential that is more positive than the ferredoxins, and span the potential region from +800 mV to -300 mV.

The third class of proteins, which function strictly as electron transfer proteins, are the copper or blue proteins [26]. A typical active site structure of these proteins is shown in Figure 6. This tetrahedrally coordinated copper is coordinated by two nitrogens from the two histidine amino acids, and by two sulfur atoms from a methionine and a cysteine. This coordination is found in simple electron transfer proteins such as plastocyanin $E^\circ = 360$ mV, and azurin $E^\circ = 250$ mV [26]. The copper oxidation state changes between 1^+ and 2^+. These proteins exhibit some of the most positive reduction potentials and range from 180 mV to 780 mV.

8
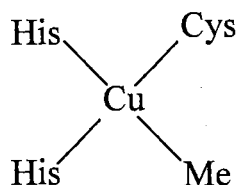
Figure 6. Prosthetic center found in copper metalloproteins
(His=histidine, Met=methionine, Cys=cysteine).

Metalloproteins-Enzymes

The second class of metalloproteins, used in the cellular and photosynthetic pathways, are the enzymes. They encompass a large number of proteins, with a diversity of metal co-factors, which catalyze a vast number of reactions. A couple of examples from this group are cytochrome c oxidase and nitrogenase. Cytochrome c oxidase constitutes the last component of the respiratory electron transport chain. It is a complex, membrane-bound protein that has four prosthetic groups consisting of heme a, heme a_3, Cu_a, and Cu_b [1]. This enzyme catalyzes the reduction of oxygen to water, as shown in the equation below:

$$O_2 + 4H^+ + 4e^- \rightarrow 2H_2O$$
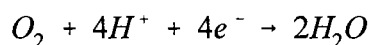
Nitrogenase is an enzyme utilized by soil microorganisms for nitrogen fixation, and is a complex enzyme containing multiple iron and molybdenum centers. It catalyzes the reduction of nitrogen to ammonia [4] as shown by the equation below:

$$N_2 + 6H^+ + 6e^- \rightarrow 2NH_3$$
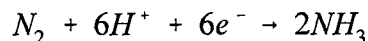
As noted from both of the equations above, reducing equivalents (electrons) are required

9

in order for the enzymes to carry out their respective reactions. For cytochrome c oxidase, the electrons are provided by its physiological partner protein cytochrome c. Nitrogense receives its electrons from certain ferredoxins. These two examples serve the purpose of showing a general scheme found in biochemical pathways; namely that enzymes, including those involved in anabolic and catabolic pathways, receive their necessary reducing equivalents from the smaller electron transfer proteins. The enzymes are directly dependent on the redox electron transfer proteins to carry out their reactions. The general scheme of electron flow for a wide variety of enzymes is shown in Figure 7; where Mox and Mred represent the oxidized and reduced forms, respectively, of the small redox proteins discussed earlier. This representation is intended to illustrate how redox proteins shuttle electrons from an electron donor to the enzyme. Electron transfer proteins are continuously shuttled between oxidation states as they are reduced by the electron donor and then reoxidized by the enzyme. In order for cytochrome c to transfer its reducing equivalents to cytochrome c oxidase, it must form an intimate complex with cytochome c oxidase to allow the electron transfer to occur. This selective docking of physiological partner proteins is believed to be guided by a complementary distribution of charged residues on their respective surfaces [7,8-12]. Structural complexes between physiological partner proteins have been well studied (e.g. cytochrome c and b_5 [7], cytochrome c and cytochrome c peroxidase [6]), and the hypothesis of complementary charge on the surface of each partner protein has been substantiated [6,7]. This complementary charge distribution is shown in Figure 8, with physiological partner proteins cytochrome c and cytochrome b_5. It is believed that this type of ionic interaction is a common means by which physiological partner proteins recognize each other [6].
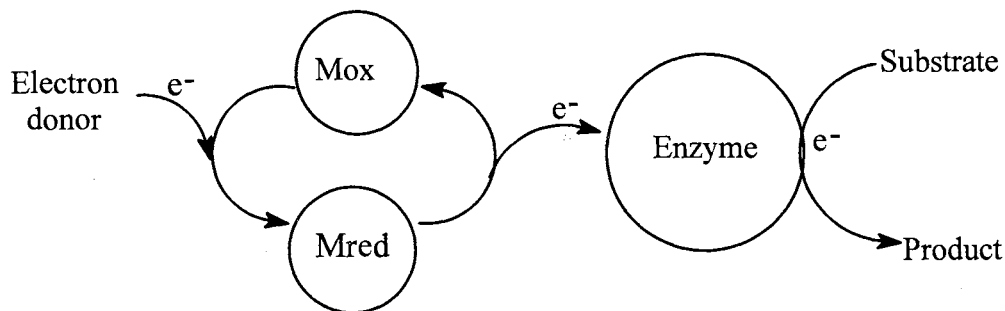
Figure 7. Schematic representation of small metalloproteins as electron carriers.

Electrochemistry

Redox reactions taking place in photosynthesis and cellular respiration occur, by way of

proteins, through well defined paths. Consequently, studying the proteins that underlie

these processes is of considerable interest. In order to study these fundamental processes,

electrochemical techniques have been applied to probe the mechanistic aspect of these

systems. Researchers initially tried to obtain electrochemical communication from

enzymes and proteins by utilizing metal electrodes. The conventional electrodes used in

obtaining the electrochemistry of small inorganic molecules consisted of gold, platinum,

and mercury. These electrodes were initially utilized to obtain electrochemical

communication with proteins, as represented in Figure 9. It was initially believed that

proteins were not directly compatible with electrode surfaces for direct electrochemistry.

This was attributed to several characteristics of the proteins, such as slow rate of charge

transfer, small diffusion coefficient, adsorption of the protein onto the electrode surface, and

a buried or inaccessible active site [21]. It was not until 1977 that a major breakthrough

11
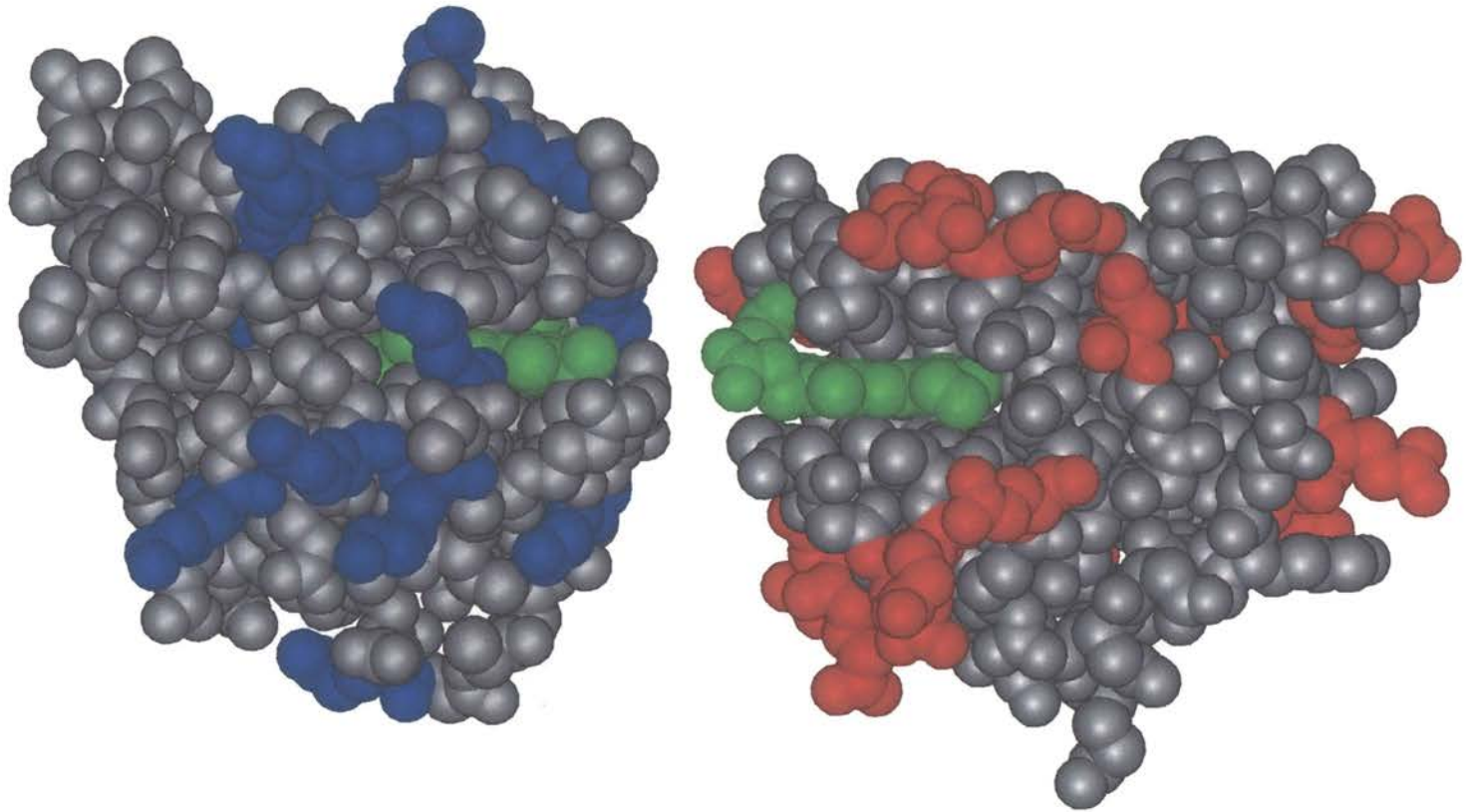
Figure 8. Space filling structure of cytochrome c and cytochrome b_5. Positively charged amino acids are highlighted blue on the surface of cytochrome c. Negatively charged amino acids are represented as red on the surface of b_5.
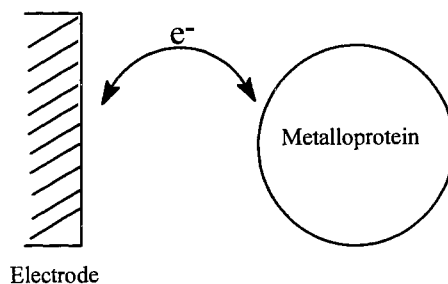
Figure 9. Schematic of electrochemical communication of protein with electrode

occurred in obtaining electrochemical communication with proteins. Two separate groups reported the direct reversible electrochemistry of cytochrome c (a small electron transfer protein involved in oxidative phosphorylation) [1]. One group utilized an indium oxide electrode to obtain the reversible electrochemistry of cytochrome c [23]. The other group used a conventional gold electrode, but included 4,4'-bipyridyl in the solution containing the protein and obtained the reversible electrochemical response of the protein [19]. These same researchers later showed that the 4,4'-bipyridyl modified the gold electrode surface by forming a monolayer on the surface. [18,31]. The initial successes in obtaining the direct electrochemistry of proteins provided the first evidence suggesting that the nature of the electrode solution interface is of central importance in obtaining the reversible electrochemistry of proteins [14-16,24].

A revealing study [28,22] that measured the kinetics of adsorption of cytochrome c in the oxidized and reduced form, utilizing rotating-disk and ring disk electrodes, was undertaken to understand the electrochemical response of cytochrome c at 4,4'-bipyridyl

modified gold electrode. The authors concluded that there are several steps that must occur in order to observe reversible electrochemistry of cytochrome c [28,22], namely:

1. diffusion of cytochrome c to the electrode surface;

2. association of oxidized cytochrome c with the electrode surface, in an optimum orientation for electron transfer;

3. electron transfer;

4. dissociation of reduced cytochrome c from the electrode surface;

5. diffusion of reduced cytochrome c away from the electrode surface.

Each of the above mentioned processes must be rapid in order for reversible electrochemistry of the protein to be observed. Most important is the transient complex formed between the protein and the electrode surface. This complex ensures that the protein is bound briefly in an orientation optimum for facile electron transfer to occur. The surface modifiers further help in preventing the irreversible adsorption and denaturation of the protein at the electrode surface. Figure 10 shows a schematic representation of a gold electrode surface modified with 4,4'-bipyridyl, and the interaction of cytochrome c with the electrode. This favorable interaction can be interpreted by considering some of the characteristics of cytochrome c. Cytochrome c is a heme containing protein with molecular weight of approximately 12,000 daltons. It contains one heme that is substantially buried, and is surrounded by a patch of lysines that form an uninterrupted positive patch (Fig. 8) [7]. It has an overall charge of +9 at pH close to 7 [13]. This positive patch of amino acids has been implicated in interprotein docking with physiological partner proteins who exhibit complementary charged amino acids. It was suggested that the lysine residues on the protein surface form hydrogen bonds with the bipyridyl nitrogen, thus enabling the protein to be

oriented at the electrode surface for optimum electron transfer, and preventing its denaturation [13,18]. There is a striking similarity between the interaction of the protein
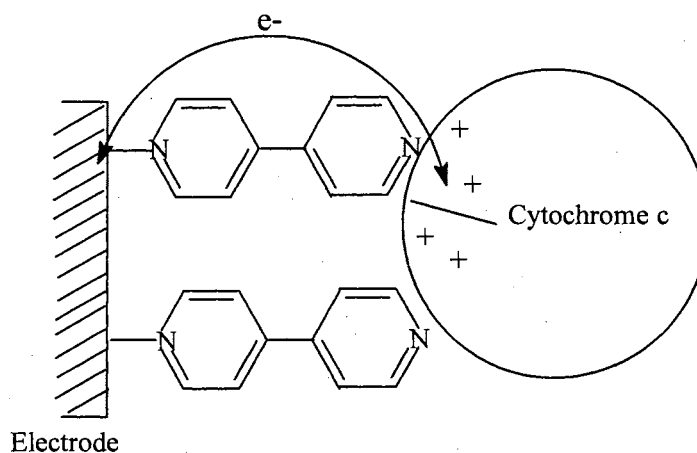
Figure 10. Gold electrode modified with 4,4'-bipyridyl. Positive charges on cytochrome c represent the lysine amino acids surrounding the active site.

with the modified electrode and its interaction with physiological partner proteins. It was therefore suggested that reversible electrochemistry of cytochrome c and other proteins could be obtained by mimicking the surface features exhibited by physiological partner proteins [32,33].

After the initial discovery of the surface modifier 4,4'-bipyridyl, a large number of surface modifiers have been reported that can promote the electrochemistry of cytochrome c, for example, bis(4-pyridyl) [29], and β-mercaptopropionic acid [30]. For a review describing some of the surface modifiers, see Armstrong et. al.[34]. The main characteristic of these modifiers is that one end binds to the electrode surface, and the other end presents a functional group to the solution. This solution end must interact favorably with the protein.

Understanding the reversible electrochemical response obtained for cytochrome c at an

15

indium oxide electrode lies in the structure of the electrode surface. Indium oxide is a semiconductor electrode, and consists of an extensive oxide network. It has been shown that in an aqueous solution with the pH approaching neutral, this oxide surfaces possess negative charges due to acid base equilibria of surface hydroxide groups [27,35]. The surface hydroxyl groups would be expected to be deprotonated at neutral pH, making the electrode interface negatively charged. The reversible electrochemistry of cytochrome c at an indium oxide electrode can be explained by favorable electrostatic interactions between the negatively charged surface groups and the positively charged amino acids around the active site of the protein. In this context, the indium oxide surface is thought to mimic the characteristics of cytochrome c physiological partner proteins.

The two initial papers reporting the direct electrochemistry of cytochrome c [19, 23] started a period of intense investigation aimed at elucidating what molecular factors are necessary to obtain reversible electrochemical communication between protein and electrode, including the role played by electrode modifiers in promoting rapid heterogeneous electron transfer. The research efforts carried out by many investigators have been reviewed [40-42]. Through this intense investigation, certain aspects of the electrode have proved to be crucial in obtaining the electrochemistry of proteins. These aspects are: 1) the electrode should be modified in such a way that it is electrostatically compatible with the surface of the protein by possessing functional groups that exhibit a high degree of charge density and hydrophilicity [16], and 2) the modified electrode surface should contribute to prevent the denaturation of proteins at the electrode surface.

In addition to metal oxide and modified metal (gold and platinum) surfaces, pyrolytic graphite has also been extensively used to promote the electrochemistry of proteins. Similar

16

to metal oxides, acid-base behavior of surface functionalities has been observed at pyrolytic graphite electrodes, which have been used to promote the electrochemistry of cytochrome c [34,36-39]. These electrodes were shown to have C-O functionalities which helped to promote the electrochemistry of positively charged proteins, such as cytochrome c.[36]. Unlike cytochrome c, several electron transfer proteins possess overall negative surface charges. These include, spinach ferredoxin and cytochrome b_5. The electrochemistry of these negatively charged proteins was also promoted, at edge plane pyrolytic graphite, by utilizing positively charged cations, such as divalent magnesium. Due to their surface functionalities (carboxyl and hydroxyl groups), the pyrolytic graphite electrode contains negative charge density. This is schematically shown in Figure 11. The positively charged cations are believed to suppress the coulombic repulsion between the negatively charged surface and the negatively charged protein (Fig. 11.) Many different types of divalent and trivalent cations have successfully promoted the electrochemistry of proteins bearing overall negative charges at negatively charged electrode surfaces. Polylysine, a polymer of the amino acid lysine, is a promoter which was used to obtain the direct electrochemistry of outer mitochondrial cytochrome b_5 [30]. The mode of promotion is similar to that offered by the smaller cations.

Most of the success in obtaining the direct electrochemistry of proteins has dealt with the small electron transfer proteins, whose sole function is the transfer of electrons. The next challenge lies in obtaining electrochemical communication with enzymes, so that the latter can be used in bioremediation, biosensors, and bioelectrosynthesis. The direct electrochemistry of enzymes has been, and continues to be, rather difficult to obtain [21,22]. This can be attributed to several aspects, one of which is the buried active site that makes it
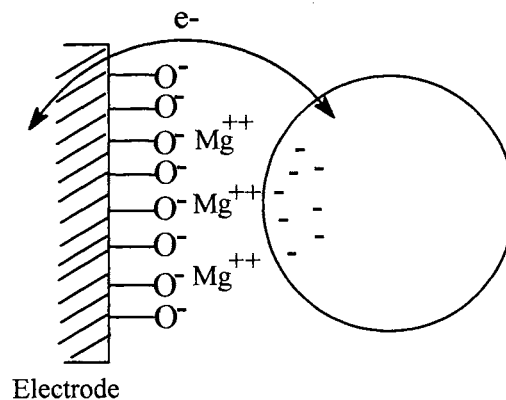
Figure 11. Schematic representation of the screening of cations between negatively charged surface and negatively charged protein.

difficult for facile electron exchange to occur. The direct electrochemistry of enzymes is further complicated by the complex surface electrostatic potentials exhibited by these proteins, as compared to the smaller electron transfer proteins. The intricate surface potentials displayed by enzymes makes the construction of electrode surfaces more challenging. It seems that the larger the enzyme, the more complicated the molecular interaction of the enzyme with the surface and the harder it is to obtain the electrochemical communication with the enzyme. Even though there are a large variety of modified electrodes, there are still a great number of enzymes that are not compatible with solid electrodes.

The difficulty in obtaining the direct electrochemistry of enzymes has been briefly described above. An alternate approach to harness the catalytic ability of the enzymes is to use a mediator in shuttling the electrons from the electrode to the enzyme. This

approach will alleviate the need for the enzyme to make an intimate complex with the electrode surface and simplify the structural requirements of the electrode surface. A schematic representation of this mediated approach is shown in Figure 12. This approach
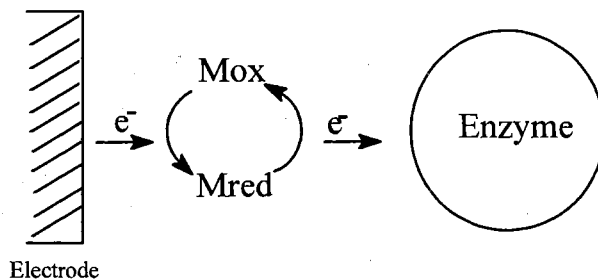
Electrode

Figure 12. Schematic representation of the mediated electrochemical approach to activate enzymes.

resembles the means by which many enzymes receive their reducing equivalents in the catabolic and anabolic pathways (Fig. 7), where Mox and Mred represent the oxidized and reduced forms of the mediator, respectively.

This thesis will focus on two aspects: 1) the continued exploration of surfaces that will interact favorable with small electron transfer proteins, and 2) the utilization of the mediated electrochemical approach to activate enzymes. The new surfaces explored, as well as the mediated electrochemical approach, will enhance our current understanding of the molecular factors that are necessary to obtain electrochemical communication between proteins and electrodes.

Purpose

The previous discussion provided a brief account of what has been learned in obtaining

direct electrochemical communication between proteins and electrodes. The electrostatic compatibility between the electrode and protein was emphasized. Even though researchers have had a great deal of success in obtaining electrochemical responses from small redox proteins, there is no universal surface that can be used to obtain direct electrochemistry of all proteins and enzymes. Each surface, to a degree, is somewhat specific to a particular protein being investigated. Consequently, there is continuing interest and need in developing surfaces that are stable, easy to use, and communicate with a diversity of proteins. Therefore, Chapters II and III of this thesis are devoted to surfaces which are compatible for protein electrochemistry. Both chapters discuss new modifiers and new ways of conditioning the electrode to obtain direct electrochemistry of proteins. Chapter III further explores the mediated electrochemical approach to measure the second order homogeneous electron transfer rate constant between cytochromes c and outer mitochondrial cytochrome b_5 at different electrode surfaces.

Harnessing the catalytic properties of the enzyme cytochrome $P450_{cam}$ for reductive dehalogenation reactions has been accomplished by utilizing the above mentioned mediated approach, and is described in Chapter IV. This investigation marks the successful activation of the enzyme for reductive dehalogenation and provides significant insight into the mechanistic aspects of reductive dehalogenation reactions carried out by the enzyme.

The final Chapter looks at the structural aspect of a V45I/V61I mutant of outer mitochondrial cytochrome b_5, and the effects the mutations have on the measured reduction potential, as well as factors that control it.

References

1. Horton, R. H., Moran, L. A., Ochs, R. S., Rawn, J. D., and Scrimgeour, K. G. *Principles of Biochemistry;* Prentice-Hall: New Jersey, 1993.

2. Harrison, P.M., Hoare, R.J. *Metals in Biochemistry;* Chapman and Hall: New York, 1980.

3. Cowan, J. A. *Inorganic Biochemistry, An Introduction;* VCH Publishers: New York, 1993.

4. Berg, J. A.; Holm, R. H. Structure and Reactions of Iron-Sulfur Protein Clusters and Their Synthetic Analogs. In *Iron-Sulfur Proteins;* Spiro, T. G., Ed.; John-Wiley & Sons: New York, 1982; 1-66.

5. Cammack, R. Iron-Sulfur Clusters in Enzymes: Pathways of Electron Transfer. In *Iron-Sulfur Protein Research;* Matsubara, H., Katsube, Y., and Wada, K., Eds.; Japan Scientific Societies Press: Tokyo, 1987; 40.

6. Poulos, T. L.; Kraut, J. (1980) *J. Biol. Chem.* **255**, 10322.

7. Salemme, F. R. (1976) *J. Mol. Biol.* **102**, 563.

8. Curry, W. B.; Grabe, M. D.; Kurnikov, I. V., Skourtis, S. S., Beratan, D. N., Regan, J. J., Aquino, A., Beroza. P.; Onuchic, J. N. (1995) *J. Bioenergetics and Biomembranes.* **27**, 285.

9. Tollin. G. (1995) *J. Bioenergetics and Biomembranes.* **27**, 303.

10. Durham, B.; Fairris, J. L.; McLean, M.; Millett, F.; Scott, J. R.; Sligar, S. G.; Willie, A. (1995) *J. Bioenergetics and Biomembranes.* **27**, 331.

11. Moser, C. C.; Page, C. C.; Farid, R.; Dutton, P. L. (1995) *J. Bioenergetics and Biomembranes.* **27**, 263.

21

12. Mauk, A. G.; Mauk, M. R.; Moore, G. R.; Northrup, S. H. (1995) *J. Bioenergetics and Biomembranes.* **27**, 311.

13. Armstrong, F. A.; Hill, H. A. O.; Walton, N. J. (1988) *Acc. Chem. Res.* **21**, 407.

14. Bowden, E. F. (1997) *The Electrochemical Society Interface*, 40.

15. Rusling, J. F. (1997) *The Electrochemical Society Interface*, 26.

16. Taniguchi, I. (1997) *The Electrochemical Society Interface*, 34.

17. Betso, S. R.; Klapper, M. H.; Anderson, L. B. (1972) *J. Am. Chem. Soc.* **94**, 8197.

18. Eddowes, M. J.; Hill, H. A. O. (1979) *J. Am Chem. Soc.* **101**, 4461.

19. Eddowes, M. J.; Hill, H. A. O (1977) *J. Am.Chem. Soc. Chem. Comm.* 771.

20. Emr, S. A.; Yacynych, A. M. (1995) *Electroanalysis.* **7**, 913.

21. Frew, J. E.; Hill, H. A. O. (1988) *J. Biochem.* **172**, 261.

22. Hill, H. A. O. (1987) *Pure & Appl. Chem.* **59**, 743.

23. Yeh, P.; Kuwana, T. (1977) *Chemistry Letters.* 1145.

24. Schultz, F. A. (1997) *The Electrochemical Society Interface*, 44.

25. Lemberg, R.; Barret, J., *CYTOCHROMES*, Academic Press: New York, 1973, 8.

26. Harrison, P. M., Structure and Function of Small Blue Copper Proteins *Metalloproteins, Part 1: Metal Proteins with Redox Roles*, Adman, E. T., Ed. Verlag Chemie: New York, 1985.

27. Bowden, E. F.; Hawkridge, M. F. (1984) *J. Electroanal. Chem.*, **161**, 355.

28. Albery, W. J.; Eddowes, M. J.; Hill, H. A. O.; Hillman, A. R., (1981) *J. AM. Chem. Soc.*, **103**, 310.

29. Taniguchi, I.; Toyosawa, K.; Yamaguchi, H.; Yasukouchi, K. (1982) *J. Chem. Soc., Chem. Commun.*, 1032.

30.   Rivera, M.; Wells, M. A.; Walker, F. A. (1994) *Biochemistry* **33**, 2161.

31.   Uosaki, K.; Hill, H. A. O. (1981) *J. Electroanl. Chem.*, **122**, 321.

32.   Eddowes, M. J.; Hill, H. A. O.; Uosaki, K. (1979) *J. Am.Chem. Soc.* **101**, 7113.

33.   Eddowes, M. J., Hill, H. A. O., Uosaki, K. (1980) *Bioelect. and Bioener.*, **7**, 527.

34.   Armstrong, F. A.; Hill, H. A. O.; Walton, N. J. (1986) *Quart. Review. Biophy.* **18**, 261.

35.   Noguera, C. (1996) *Physics and Chemistry at Oxide Surfaces*, Cambridge University Press, Ch. 6, 160.

36.   Armstrong, F. A.; Hill, H. A. O.; Oliver, B. N. (1984) *J. Chem. Soc., Chem. Commun.*, 976.

37.   Armstrong, F. A.; Hill, H. A. O.; Oliver, B. N.; Walton, N. J., (1984) *J. Am Chem. Soc.* **106**, 921

38.   Armstrong, F. A.; Cox, P. A.; Hill, H. A. O.; Lowe, V. J.; Oliver, B. N. (1987) *J. Electroanal. Chem.* **217**, 331.

39.   Armstrong, F. A.; Bond., A. M.; Hill, H. A. O.; Psalti, S. M.; Zoski, C. G. (1989) *J. Phys. Chem.* **93**, 6485.

40.   Armstrong, F. A. (1990) *Struc. Bond.* **72**, 137.

41.   Hawkridge, F. M.; Taniguchi, I. (1995) *Comments Inorg. Chem.*, **17**, 163.

42.   Bond., A. M. (1994) *Inorg. Chim. Acta*, **226**, 293.

CHAPTER II

SURFACE MODIFIERS THAT PROMOTE THE

ELECTROCHEMICAL RESPONSE OF

OUTER MITOCHONDRIAL

CYTOCHROME b_5

Introduction

Biomembranes are composed of lipid bilayers, where the concentration is approximately 40% lipid and 60% protein [1]. These natural bilayers are described by the fluid mosaic model [1], which describes the dynamic state of proteins and lipids in these fluid structures. Many biologically important redox systems are imbedded in membranes, e.g. the mitochondrial electron transport chain, as well as the light harvesting photosystems of photosynthesis. It is therefore important for researchers to try and mimic this lipid environment in order to understand physiological redox systems. Salamon *et al.* [2,3], were some of the first researchers to utilize lipids for modifying electrode surfaces. These researchers utilized phosphatidylcholine (a neutral lipid) to promote the electrochemical response of cytochrome c. They noted that by adding dihexadecylphosphate, a negatively charged molecule, they were able to increase the magnitude of the faradaic current and obtain a more reversible electrochemical response for the positively charged cytochrome c. Consequently, even in a lipidic environment, the electrostatic compatibility between

protein and electrode surface is crucial in obtaining a faradaic electrochemical response.

This electrostatic involvement in the lipid environment has been confirmed by other researchers [4] who observed no electrochemistry of cytochrome c at neutrally charged lipids (a mixture of phosphatidylcholine and cholesterol), but only observed a response in the presence of a negatively charged lipid (lauric acid). The versatility of utilizing lipids to modify the electrode surface was demonstrated by Cullison et al., [6] who utilized a lipid environment to obtain the direct electrochemistry of the enzyme cytochrome c oxidase. This enzyme has a molecular weight of approximately 200,000, is composed of 12 subunits, and contains four prosthetic groups [1]. The shear size of this enzyme makes the direct electrochemistry a significant accomplishment. An interesting lipid that has been utilized to promote the electrochemistry of hemoglobin [5], myoglobin [8-11], chlorella ferredoxin[7], and cytochrome P450$_{cam}$ [5] is the cationic lipid, DDAB (didodecyldimethylammonium bromide). (Fig. 1)
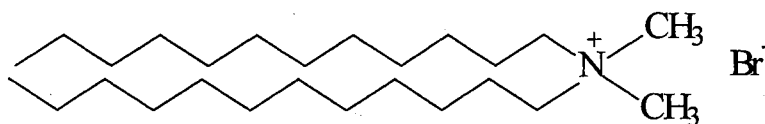
Figure 1. DDAB

Along with lipids, researchers have employed a different type of promoter, such as large polymers that selectively adsorb onto the surface of the electrode to promote the electrochemistry of proteins. Lvov et al., [12] utilized an alternate layer by layer adsorption technique using large polymers like polystyrenesulfonate (MW 50,000) and polyethyleneimine (MW 70,000) to selectively immobilize cytochome c, myoglobin,

hemoglobin, and glucose oxidase. There was no electrochemistry demonstrated, but the adsorbed proteins were shown to be nondenatured. In a later study by Lvov *et al.*, [13] alternate layer by layer adsorption was used to obtain the direct electrochemisty of myoglobin and cytochrome $P450_{cam}$.

We have utilized films of the positively charged lipid DDAB in order to promote the reversible electrochemistry of outer mitochondrial (OM) cytochrome b_5 [14], its dimethyl ester derivative, and a V45L/V61L double mutant of OM cytochrome b_5, with the aim of measuring their redox potentials.

As a novel surface modifier, a mixture of poly(2-methacryloxyethyltrimethyl ammonium bromide), referred to as PMAT, and nafion [15] have also been utilized to promote the electrochemical response of OM cytochrome b_5. The structures of nafion and PMAT are shown in Figures 2 and 3, respectively. In addition, we have used both types of electrode modifiers, DDAB layers and the nafion/ PMAT mixture, to study the interaction between cytochrome c an OM cytochrome b_5.

$$-(CF_2CF_2)_m-CF\,CF_2- $$
$$| $$
$$O $$
$$| $$
$$(CF_2CF\,O)_n-CF_2CF_2SO_3^- \; Na $$
$$| $$
$$CF_3 $$
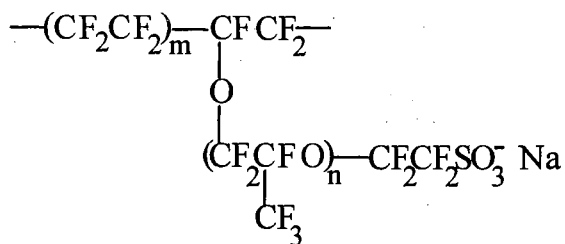
Figure 2. Nafion, m=5-12, n=1
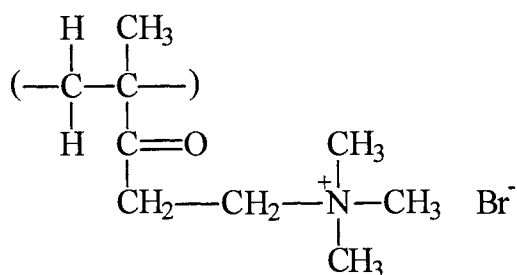
Figure 3. poly(2-methacryloxyethyltrimethyl ammonium bromide) PMAT

Experimental Procedures

Protein Expression and Purification

Recombinant rat liver OM cytochrome b_5 was expressed in *E.Coli* and purified as described below [14]: Culture tubes containing 5 ml of LB broth containing 100 µg/ml ampicillin were inoculated with one colony of the *E. coli* strain Bl 21 (DE3) harboring the rat liver OM cytochrome b_5 recombinant plasmid MRL2 [14]. The tubes were incubated (37°C) at 220 rpm for 12-16 hours. The inoculum was then added to four Fernbach flasks containing 1 liter of LB broth and 100 µg/ml ampicillin and incubated at 37 °C while shaking at 220 rpm. When the optical density at 600 nm reached 1, protein expression was induced by the addition of 1 ml 1 M isopropyl-β-D-thiogalactoside (IPTG), 1 ml of 17 mg/ml of 5-aminolevulinic acid (ALA), and 1 ml of 50 mg/ml of $FeSO_4$. The medium was incubated at 37 °C at 220 rpm for 4 additional hours. The culture was then cooled to 4 °C for a period of one hour. The cells culture was transferred to centrifuge bottles and centrifuged at 4500 rpm for 10 min. The supernatant was decanted, and the centrifuge bottles with the cells pellets were stored at -20 °C.

Purification consisted of the following procedure: Lysis buffer (50 mM Tris HCl, 1 mM EDTA, 100 mM NaCl, pH 7.5) was added and the cells resuspended at 4 °C. Cells were lysed with lysozyme (10 mg/ml) , 160 µl of lysozyme per gram of *E. coli*, 32 µl of 50 mM phenylmethylsulfonyl (PMSF) per gram of *E. coli*, and 4 mg of deoxycolic acid per gram of *E. coli*. The mixture was then stirred every 5 minutes for 20 minutes followed by equilibration at 37 °C for 20 minutes. The mixture was subsequently stirred for 1 hour at room temperature. The resulting solution was sonicated and ultracentrifuged at 45000 rpm for 1 hour in order to remove cell debris. The supernatant was decanted and placed inside a dialysis membrane and dialyzed against ion exchange buffer (10 mM EDTA, 50 mM Tris, pH 7.4). The buffer was changed several times in a 24 hour period. The dialyzed solution was applied to a DE-52 (Whatman) anion exchange column equilibrated with buffer. The protein was eluted with a linear salt gradient, 0-500 mM NaCl, in ion exchange buffer. The red fractions containing the cytochrome were collected and concentrated to approximately 1 ml by ultafiltration using a membrane with a 3 kD molecular weight cutoff. This concentrated solution was passed through a Sephadex G-50 column equilibrated with 100 mM KCl, 20 mM Tris, pH 7.4. The protein purity was determined by monitoring the ratio of absorbances A_{280}/A_{412} by electronic spectroscopy; only those chromatographic fractions exhibiting a ratio $A_{280}/A_{412} < 0.2$ were used in order to obtain homogeneous protein. Purified rat liver OM cytochrome was exchanged into 100.0 mM MOPS, pH 7.0 by dialysis, concentrated to approximately 0.80 mM by ultrafiltration (Y30 Diaflo ultrafiltration membranes, Amicon), aliquoted, and then frozen at −20 °C. Horse heart cytochrome c was purchased from Sigma and used without further purification. Didodecyldimethyl ammonium bromide (DDAB) was purchased from Aldrich. Nafion 5% solution in ethanol

was purchased from Aldrich, and poly(methacryloxyethy trimethyl ammonium bromide) 20% solution and average MW = 50,000 was purchased from Polysciences, Inc.

Cyclic Voltammetry

Cyclic Voltammetry was carried out with a BAS-CV50W potentiostat (Bioanalytical Systems, West Lafayette, IN). A miniature 1 mm or a 3 mm diameter glassy carbon working electrode was used along with a platinum wire counter-electrode, and an Ag/AgCl reference electrode equipped with a fiber junction purchased from Cypress systems. All electrodes were placed in a single-compartment glass cell of approximately 700 μl.

Electrode Modification with DDAB Layers

Modification of a mini glassy carbon electrode consisted of the following procedure: The electrode was polished with an alumina polish (BAS, 1 micron particle size) and rinsed with nanopure water in between polishing steps. The electrode was then sonicated for 2 minutes in nanopure water and rinsed with water. The electrode was allowed to dry at room temperature until all water was evaporated, appproximately 5 minutes. Modification of the electrode consisted of dipping the electrode for 10 seconds in a 0.05 M solution of DDAB in chloroform at 4°C [7]. The electrode was dried at room temperature for 30 minutes and then immersed in the electrochemical cell containing 250 μL of protein. The electrochemical cell used for cyclic voltammetry was bathed in water kept at a constant temperature of 22 °C with the aid of a Isotemp Refrigerator Circular model 910 (Fischer Scientific). The cyclic voltammograms were performed in a 100 mM MOPS buffer (pH 7.2).

Electrode Modification with Nafion/PMAT Mixtures

The electrode was polished with an alumina polish (BAS) and rinsed with nanopure water in between polishing steps. The electrode was then sonicated for 2 minutes in

29

nanopure water, rinsed with water, and allowed to dry at room temperature (for approximately 5 minutes). Modification of the electrode consisted of applying 1 μl of a mixture, consisting of 0.02% nafion and 0.02% PMAT in ethanol, to the electrode surface with the aid of a microsyringe. The electrode was allowed to dry, on average, 4-5 hours. All electrochemical measurements were carried out in 100 mM MOPS.

Electrochemical Measurements

The appropriately modified electrode was immersed in a dearated protein solution, and a stream of nitrogen was blown gently across the surface of the protein solution in order to maintain the solution anarobic. Protein concentrations were typically 100 μM, and their concentrations were measured by UV-vis spectrophotometry using the Soret band corresponding to their oxidized state. The extinction coefficient used for OM cytochrome b_5 (6), its dimethyl ester derivative, and the V45L/V61L mutant of OM cytochrome b_5 is 130 mM^{-1} cm^{-1}. An extinction coefficient of 109.5 mM^{-1} cm^{-1} was used for oxidized cytochrome c (7). All reduction potentials were measured with respect to the Ag/AgCl electrode, but the values have been converted to the normal hydrogen electrode.

Results and Discussion

Figure 4 shows the electrochemical response of OM cytochrome b_5 at a DDAB coated glassy carbon electrode. The electrochemical response is generated by repeated cycling of the potential until the magnitude of the current remains constant. In this case, shown in Fig. 3, the potential was cycled more than 15 times to reach a steady state current. This cycling of the current was necessary in order for the protein to be incorporated into the lipid film [7]. This incorporation of the negatively charged protein into the positively charged lipid layer
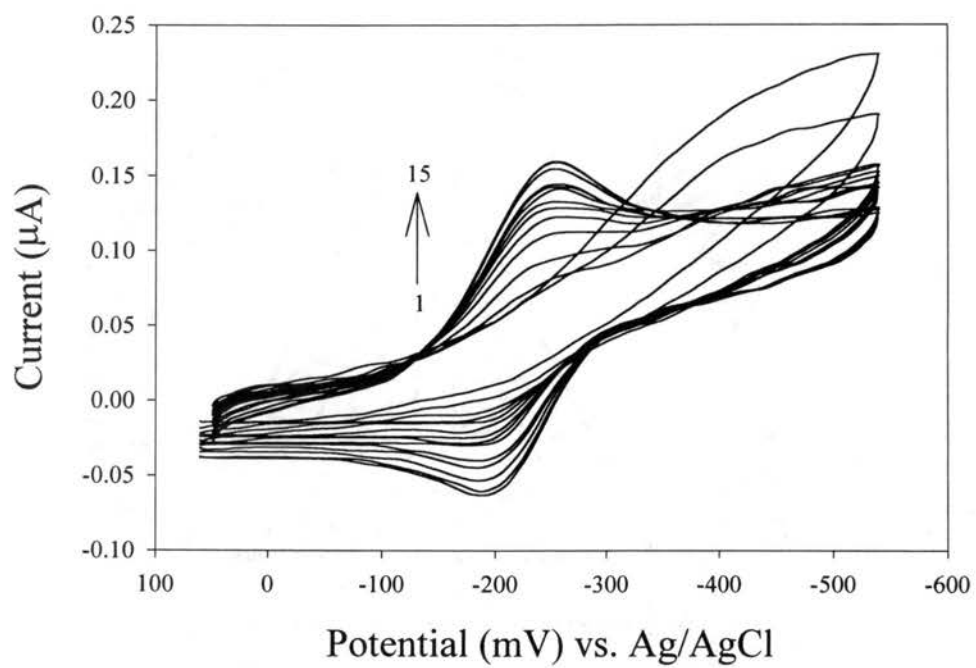
Figure 4. Cyclic voltammetric response of 100 μM OM cytochrome b_5 at a DDAB modified glassy carbon electrode.
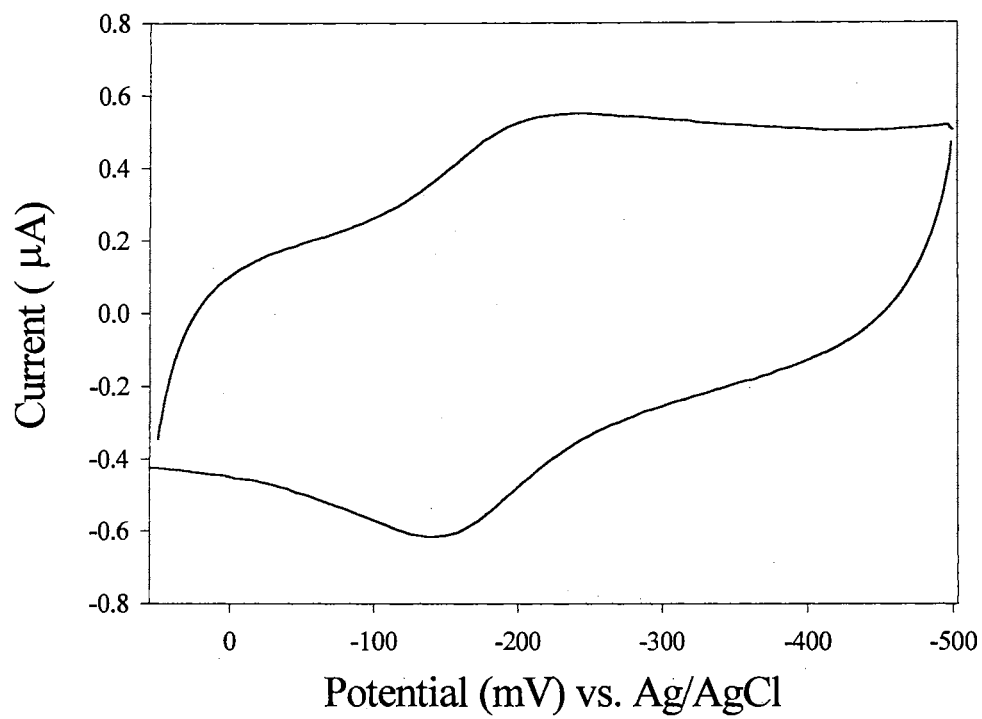
Figure 5. Cyclic voltammetric response of 100 μM solution of OM cytochrome b_5 dimethyl ester at a DDAB modified glassy carbon electrode.

demonstrates the importance of electrostatics in electrochemical communication between protein and electrode modifier. The reduction potential measured for OM cytochrome b_5 at this modified electrode is -27 mV vs NHE. The sweep rate corresponded to 3 mV/s, the peak to peak separation is 59 mV, and the ratio of the peak currents is unity. These electrochemical characteristics correspond to a reversible nernstian response. Figure 5 shows the cyclic voltammetric response obtained with the dimethyl ester derivative of OM cytochrome b_5 at a DDAB modified glassy carbon electrode. This response was obtained at a glassy carbon electrode with a 3 mm diameter. This larger electrode displays a significantly larger charging current (Fig. 5) than the 1 mm glassy carbon electrode (Fig.4). This makes a noteworthy difference in the appearance of the cyclic voltammograms. The sweep rate corresponds to 10 mV/s and the peak to peak separation is 56 mV. The reduction potential of the dimethyl ester derivative measured at these surfaces is 20 mV vs NHE. Figure 6 shows the cyclic voltammetric response of V45L/V61L mutant of OM cytochrome b_5 on a DDAB modified glassy carbon electrode. The sweep rate corresponds to 10 mV/s and the peak to peak separation is 56 mV. The reduction potential of the V45L/V61L mutant at these electrodes is -13 mV vs NHE. The significance of the reduction potentials will be elaborated upon in Chapter V.

Interaction Between OM Cytochrome b_5 and Cytochrome c at DDAB Modified Electrodes

Figure 7 displays two cyclic voltammograms, both obtained at DDAB modified glassy carbon electrode surfaces. One corresponds to the cyclic voltammetric response obtained for OM cytochrome b_5 (100μM), and the other corresponds to the next consecutive cyclic
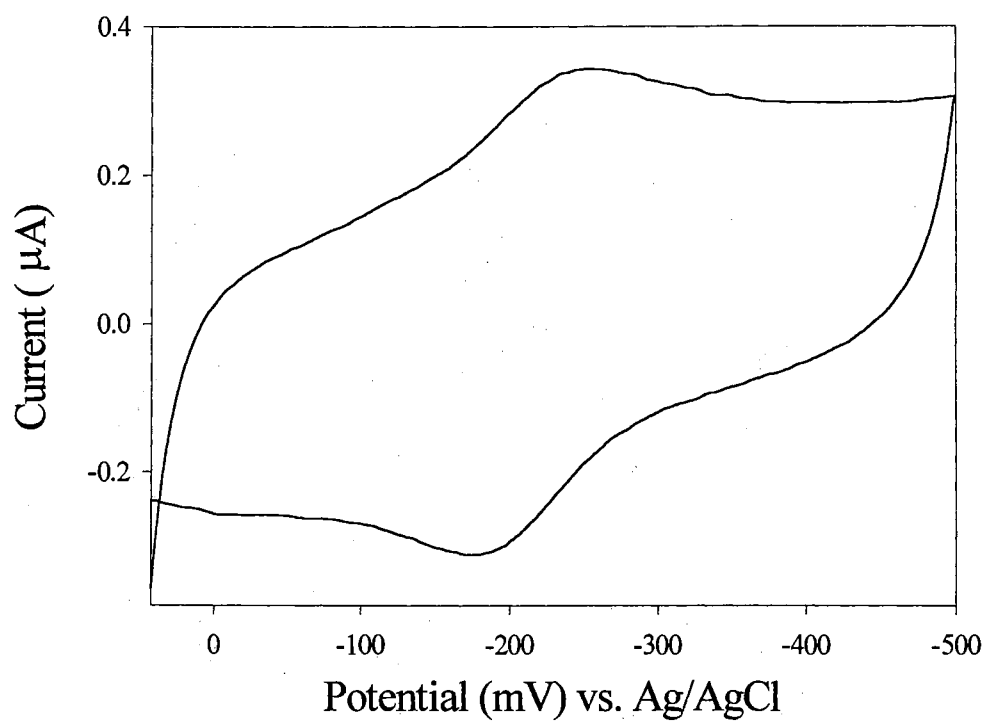
Figure 6. Cyclic voltammetric response of 100 μM solution containing V45L/V61L mutant at the DDAB electrode.
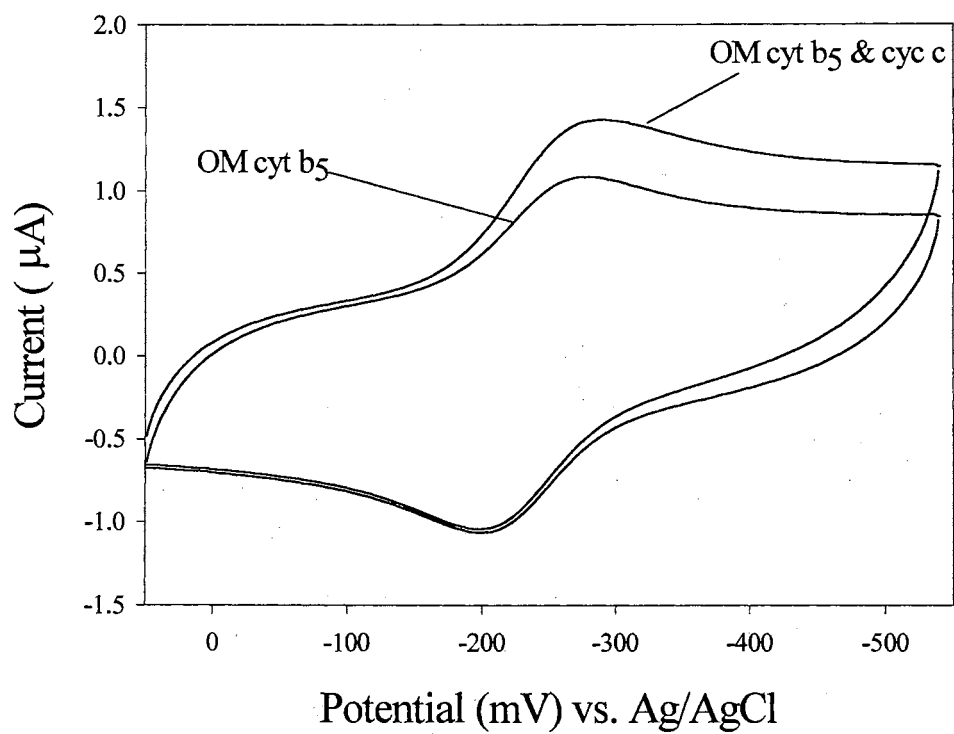
Figure 7. Cyclic voltammetric response of 100 μM OM cytochrome b_5 and 100 μM cytochrome c.

35

voltammogram upon the addition of 100 μM of cytochrome c. It is evident from the superposition of the two cyclic voltammograms that the cathodic current increases with the addition of cytochrome c to a solution of OM cytochrome b_5. This is attributed to a catalytic process [17], whereby reduced OM cytochrome b_5 is reoxidized by transferring electrons to cytochrome c. It is interesting to note that the shape of the cyclic voltammogram does not display two cathodic waves as demonstrated previously by Seetharaman *et al.*, [16]. These investigators demonstrated that at a gold electrode modified with β-mercaptopropionate and in the presence of polylysine, the electrode surface selectively transfers electrons to OM cytochrome b_5, even in the presence of cytochrome c. The selective reduction of OM cytochrome b_5 is followed by a homogeneous electron transfer reaction between the two redox proteins in solution (OM cytochrome b_5 and cytochrome c). This generates a typical cyclic voltammetric response characterized by two cathodic waves, a prepeak, and a mainpeak. The authors concluded that the prepeak was due to the depletion of cytochrome c in the diffusion layer. The absence of two cathodic waves in the voltammogram shown in Fig. 7 indicates that the lipid environment lowers the diffusion coefficient of the proteins within the films, thereby not allowing a prepeak to separate from the mainpeak. Consequently, the homogeneous second order electron transfer reaction between reduced OM cytochrome b_5 and oxidized cytochrome c is slowed down. In addition, the films on the electrode surface consist of multilayers determined to be several μm thick [5]. Since the lipid films are positively charged, the negatively charged cytochrome c would not be expected to penetrate easily into the films. Therefore, OM cytochrome b_5 is reduced at the electrode surface and then must move back through the lipid film to transfer the electron to cytochrome c. Even though there is electron transfer

occurring between the physiological partner proteins (OM cytochrome b_5 and cytochrome c), the electrode architecture prevents fast electron transfer from occurring between the proteins. If the films were one layer thick it may be possible to achieve a fast homogeneous electron transfer reaction between the two proteins. This was not pursued further because other surfaces and surface modifiers were found to accomplish this task with relatively limited technical difficulty.

Nafion and PMAT Mixtures

Figure 8 shows a cyclic voltammogram of 100 μM OM cytochrome b_5 at a glassy carbon electrode modified with 0.02% nafion and 0.02% PMAT. The sweep rate is 25 mV/s, peak to peak separation is 15 mV, and the ratio of the peak currents (i_{pc}/i_{pa}) is unity. The almost complete superposition of the cathodic and anodic waves indicates that the protein is adsorbed at the surface [17]. The midpoint potential for the wild type protein at this electrode is -4.5 mV vs NHE. Figure 9 shows the cyclic voltammetric responses of OM cytochorme b_5 at this modified electrode from scan rates 10 mV/s to 100 mV/s. A plot of the peak cathodic currents (from Figure 9) vs the scan rate is shown in Figure 10. This linear relationship indicates that the protein is adsorbed at the electrode surface. To further substantiate the adsorbed nature of the protein, the following experiment was performed: A modified glassy carbon electrode was placed in a concentrated solution of OM cytochrome b_5 for five minutes and then rinsed with water. The electrode was subsequently immersed in a solution containing only buffer and the cyclic voltammogram, shown in Figure 11, was obtained. The faradaic response of Fig. 11 provides obvious experimental evidence demonstrating that OM cytochrome b_5 is adsorbed at the electrode surface.
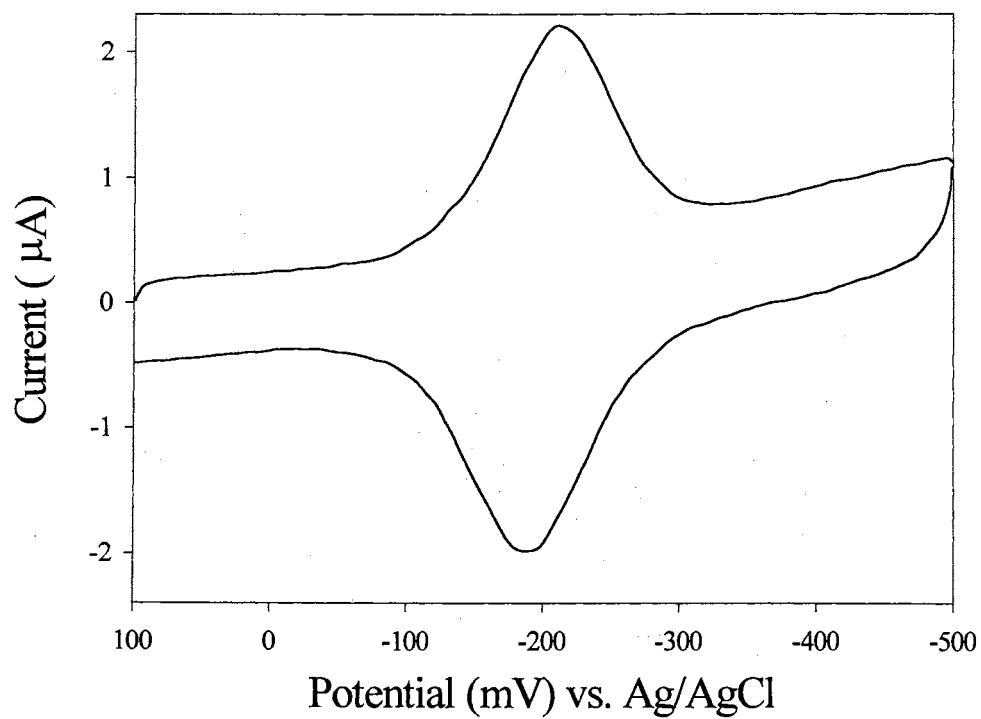
Figure 8. Cyclic voltammetric response of OM cytochrome b_5 and 0.02% nafion and 0.02% PMAT modified glassy carbon electrode.
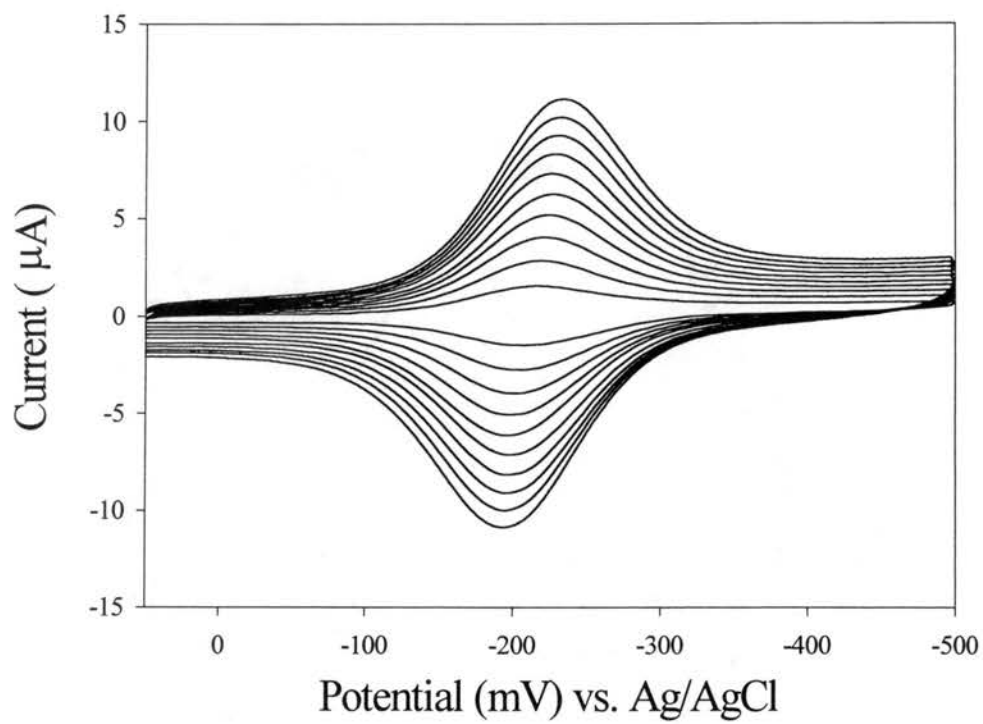
Figure 9. Cyclic voltammograms from 10 mV/s to 100 mV/s for OM cytochrome b$_5$ at a 0.02% nafion and 0.02% PMAT modified electrode.
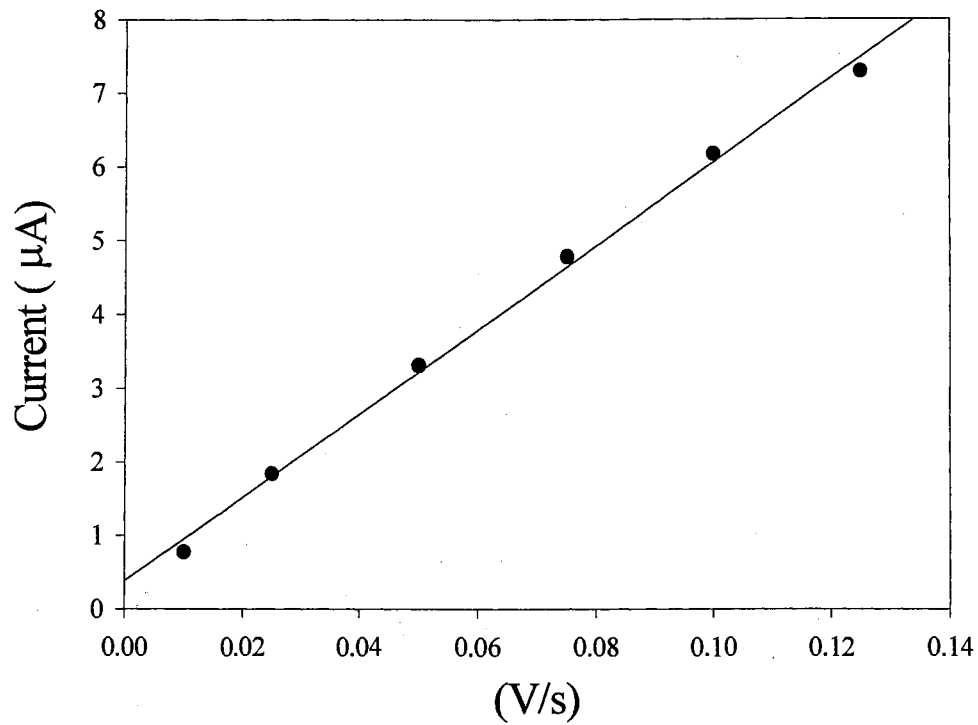
Figure 10. Peak cathodic current *vs* scan rate obtained with OM cytochrome b_5 at a 0.02% nafion and 0.02% PMAT modified glassy carbon electrode
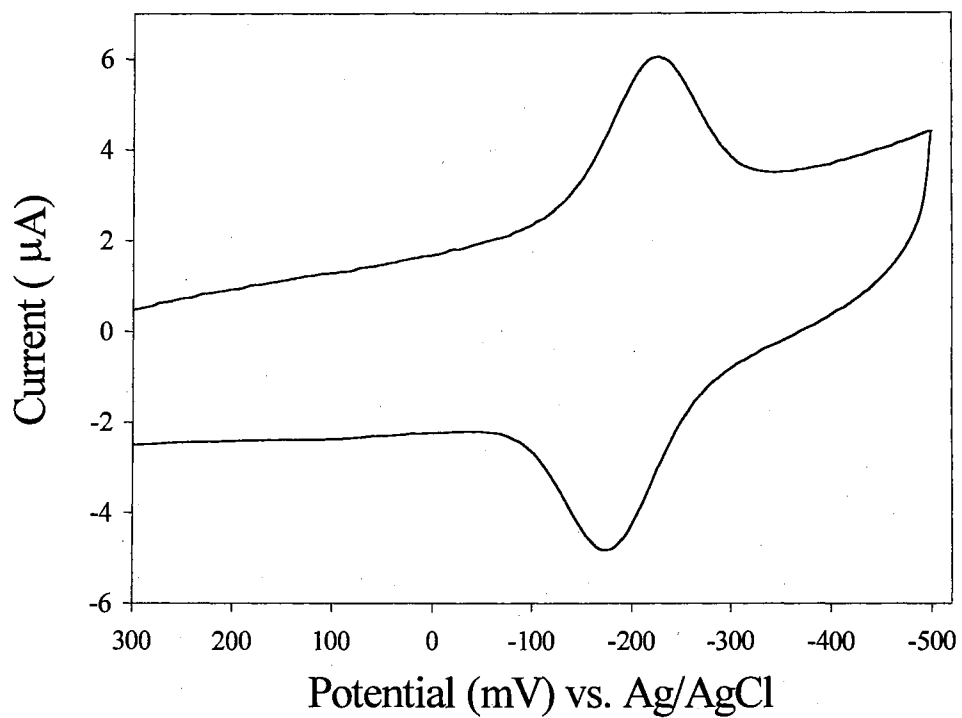
Figure 11. Faradaic response obtained for OM cytochrome b$_5$ immersed in a solution containing only 100 mM MOPS. Previous to the cyclic voltammetric experiment the protein was adsorbed onto the modified electrode surface.
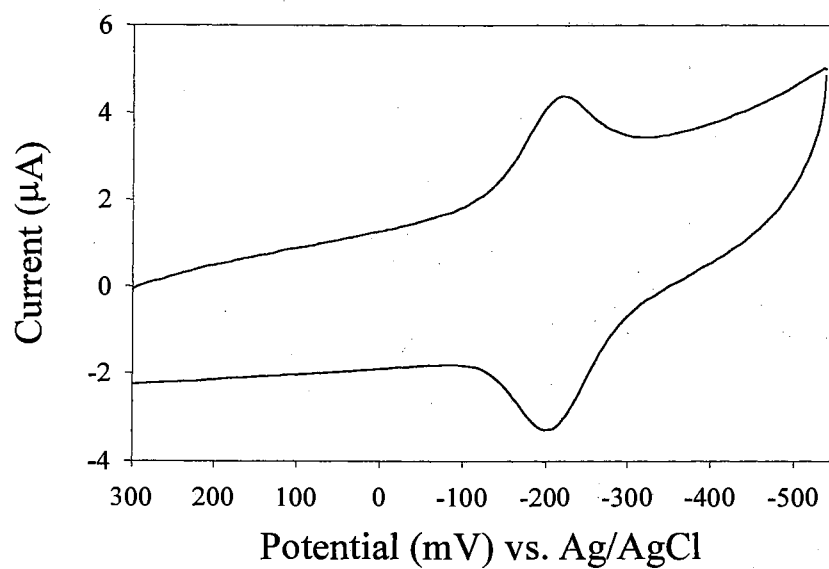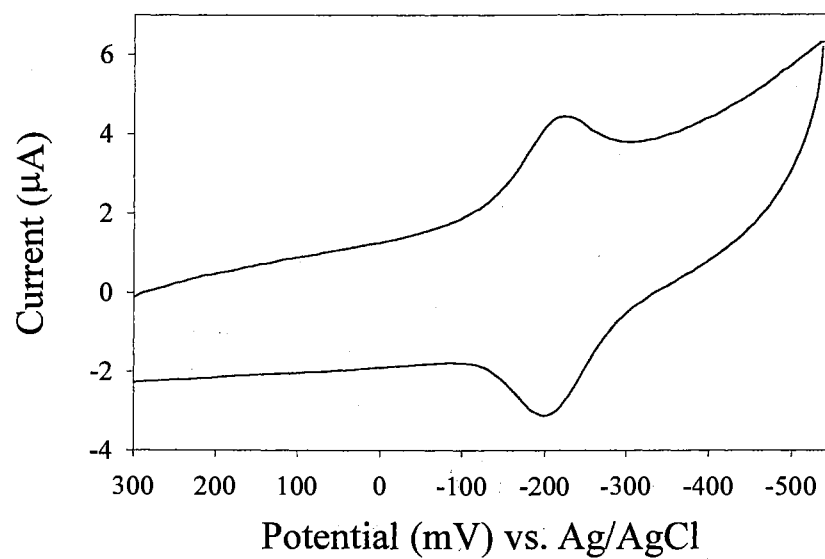
Figure 12. Top: cyclic voltammogram taken in a solution of 100 μM OM cytochrome b_5. Bottom: cyclic voltammogram taken in a solution containing 100 μM OM cytochrome b_5 and 100 μM cytochrome c.

Interaction Between OM Cytochrome b₅ and Cytochrome c at a Nafion/PMAT Modified Electrode

The effect that cytochrome c would have on the cyclic voltammetric response of OM cytochrome b_5 was explored. This is shown in Figure 12. The cyclic voltammogram in the top panel of Figure 12 was obtained from OM cytochrome b_5 at the modified glassy carbon electrode. The cyclic voltammogram in the bottom panel is the next consecutive cyclic voltammogram upon the addition of 100 μM of cytochrome c. There is no difference in the magnitude of cathodic current indicating that there is negligible electron transfer occurring between reduced OM cytochrome b_5 and oxidized cytochrome c. It is more probable that OM b_5 is so strongly attached to the electrode surface that in the time scale of the experiment it is unable to transfer an electron to cytochrome c.

Nafion/PMAT Modified Glassy Carbon Electrode for other Proteins: Spinach Ferredoxin

To explore the versatility of the nafion and PMAT mixture in promoting the electrochemical response of other proteins, spinach ferredoxin, a negatively charged protein, was examined. Figure 13 is the cyclic voltammetric response of a solution consisting of 100 μM of spinach ferredoxin at a 0.02% nafion and 0.02 % PMAT modified glassy carbon electrode. The peak to peak separation of 64 mV and peak current (i_{pc}/i_{pa}) ratio of 1.1 indicates a reversible process. The midpoint potential for spinach ferredoxin at this electrode is -387 mV vs NHE. The peak separation of 64 mV is close to the ideal peak separation of 59 mV for a one electron transfer diffusion controlled process. Further substantiating the diffusion controlled electrochemical response of spinach ferredoxin at these modified electrodes, is the lack of Faradaic response obtained at this surface if
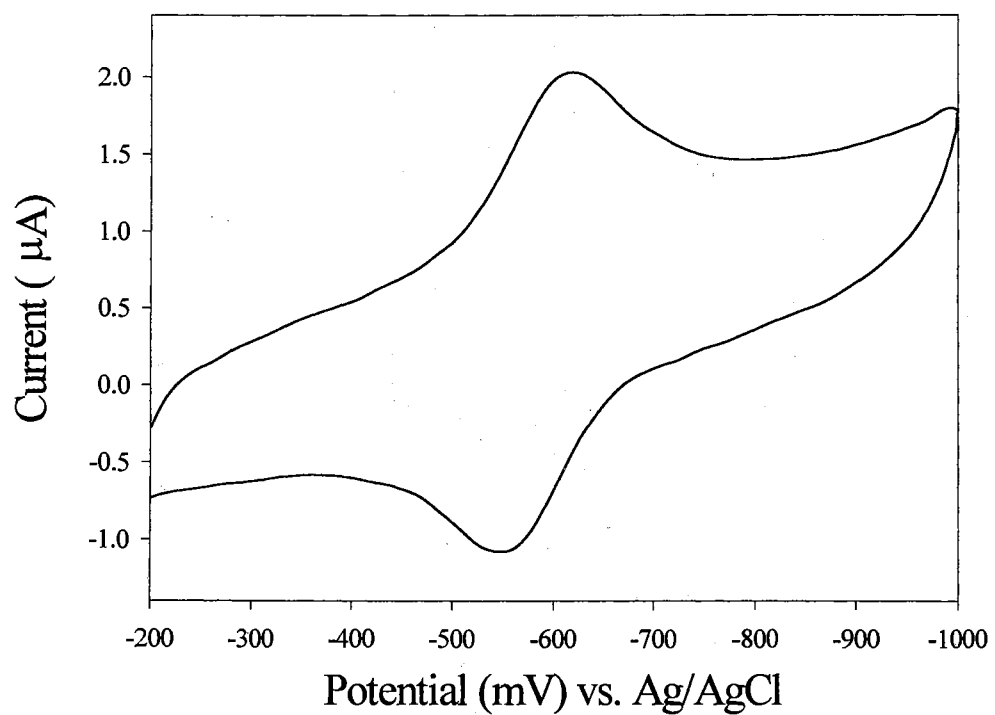
Figure 13. Cyclic voltammogram (scan rate 25 mV/s) of 100 μM spinach ferredoxin at 0.02% nafion and 0.02% PMAT modified glassy carbon electrode.

one repeats the experiments that generated Figure 11. These experiments show that the combination of nafion and PMAT is a surface modifier. The PMAT polymer was chosen because of the quaternary ammonium ions which would give the necessary complementary charge to the electrode surface, hence promoting the electrochemistry of negatively charged proteins. It is noteworthy that by modifying the glassy carbon surface with PMAT alone, the electrochemical response is transient. This was attributed to the polymer dissolving off the electrode surface. Nafion has been utilized extensively as a cation exchange membrane [20-22] and as a modifier for electrode surfaces [19, 23, 24]. As seen in Figure 2, nafion is a copolymer composed of tetrafluoroethylene and vinyl sulphonic acid [22]. One of the inherent properties of this material is its insolubility in water. Due to the hydrophobic nature of this polymer, there should be a favorable interaction with the glassy carbon surface. The exact nature of the surface remains unknown, but it is the authors belief that nafion acts as glue, thereby immobilizing the PMAT polymer at the electrode surface via electrostatic interactions. This immobilization of the polymer could be accomplished by forming salt bridges with the sulfonate groups on the nafion, and the quarternary ammonium ions on the polymer. In agreement with this idea, the electrochemical response is significantly more stable in the presence of nafion.

The electrochemical response of OM cytochrome b_5 is characteristic of an adsorbed species, whereas the electrochemical response displayed by spinach ferredoxin is diffusion controlled. Even though both proteins are negatively charged, their interaction at the electrode surface is quite different. This difference in the interaction of proteins at the electrode surface has been noted previously by Armstrong *et al.,* [18]. They also noticed that magnesium ions were ineffective in promoting the electrochemistry of spinach

ferredoxin at an edge plane pyrolytic graphite electrode. Magnesium ions promoted the electrochemical response of *Clostridium Pasteurianum* ferredoxin and rubredoxin, both negatively charged proteins. Therefore, the interaction of each protein with the electrode surface is more complicated than simple electrostatics. This difference, in the interaction of OM cytochrome b_5 and spinach ferredoxin with the electrode surface, displays the difficulty in obtaining the electrochemical response of a large number of proteins at one surface.

Conclusion

DDAB is capable of promoting the reversible electrochemisty of OM cytochrome b_5, its dimethyl ester derivative, and the V45L/V61L mutant. This lipid modifier is very versatile and offers a simple method for surface modification that is suitable for communicating with negatively charged proteins [5]. The lipid modifiers operate like other promoters in offering a favorable environment for the protein to communicate with the electrode, and prevent denaturing of the protein at the electrode surface. The thickness of the films hinders the movement of the proteins inside the films, making it difficult to observe and measure coupled protein reactions.

A novel surface capable of promoting the electrochemisty of OM cytochrome b_5 and spinach ferredoxin is the nafion/ PMAT mixture. At this surface, OM cytochrome b_5 is strongly adsorbed, whereas spinach ferredoxin displays the characteristics of a diffusion controlled process. This difference in the interaction underscores the need to continue to explore the interaction of proteins with solid surfaces. The knowledge acquired will aid in understanding the complex interaction of proteins in vivo, and may generate the technology necessary to utilize redox proteins in bioreactors.

References

1. Horton, R. H.; Moran, L. A.; Ochs, R. S.; Rawn, J. D.; Scrimgeour, K. G. *Principles of Biochemistry;* 1993 Prentice-Hall: New Jersey.

2. Salamon, Z.; Tollin, G. (1991) *J. Bioelect. Bioener.*, **26**, 321.

3. Salamon, Z.; Tollin, G., (1992) *J. Bioelect. Bioener.*, **27**, 381.

4. Bianco, P.; Halakjian, J. (1994) *Electrochim. Acta*, **39**, 911.

5. Rusling, J. F., (1997) *The Electrochemical Society Interface*, 26.

6. Cullison, J. K.; Hawkridge, F. M.; Nakashima, N.; Yoshikawa, S. (1994) *Langmuir*, **10**, 877.

7. Nassar, A.-EF.; Rusling, J. F.; Tominaga, M.; Yanagimoto, J.; Nakashima, N. (1996) *J. Electroanal.Chem.*, **416**, 183.

8. Nassar, A.-EF.; Willis, W. S.; Rusling, J. F. (1995) *Anal. Chem.*, **67**,2386.

9. Nassar, A.-EF.; Zhang, Z.; Chynwat, V.; Frank, H. A.; Rusling, J. F. (1995) *J. Phys. Chem*, **99**, 11013.

10. Nassar, A.-EF.; Zhang, Z.; Hu, N.; Rusling, J. F.; Kumosinski, T. F. (1997) *J. Phys. Chem*, **101**, 2224.

11. Nassar, A.-EF.; Bobbitt, J. M.; Stuart, J. D.; Rusling, J. F. (1995) *J. Am. Chem. Soc.*, **117**,10986.

12. Lvov, Y.; Ariga, K.; Ichinose, I.; Kunitake, T. (1995) *J. Am. Chem. Soc.*, **117**, 6117.

13. Lvov, Y.; Lu, Z.; Schenkman, J. B.; Zu, X.; Rusling, J. F. (1998) *J. Am. Chem. Soc.*, **120**, 4073.

14. Rivera, M.; Barillas-Mury, C.; Christensen, K. A.; Little, J. W.; Wells, M.A. ; Walker, F. A. (1992) *Biochemistry*, **31**, 12233.

15. Martin, C. R.; Rhoades, T. A.; Ferguson, J. A. (1982) *Anal. Chem.*, **54**, 1641.

16. Seetharaman, R.; White, S. P.; Rivera, M. (1996) *Biochem.*, **35,**. 12455.

17. Bard, A. J.; Faulkner, L. R., *Electrochemical Methods Fundamentals and Applications.*1980, New York: John Wiley & Sons.

18. Armstrong, F. A.; Cox, P. A.; Hill, H. A. O.; Lowe, V. J.; Oliver, B. N. (1987) *J. Electroanal.Chem.* **217**, 331.

19. Shi, M.; Anson, F. C. (1996) *J. Electroanal. Chem.*, 41.

20. Hsu, W. Y.; Gierke, T. D. (1983) *J. Mem. Scie.* **13**, 306.

21. Steck, A.; Yeager, H. L. (1980) *Anal. Chem.* **52**, 1215.

22. Yeo, R. S. (1980) *Polymer*, **21**, 432.

23. Szentirmay, N. N.; Martin, C. R. (1984) *Anal. Chem.*, **56** 1898.

24. Martin, C.R.; Dollard, K. A. (1983) *J. Electroanal. Chem.*, **159**, 127.

CHAPTER III

ELECTROCHEMICAL MEASUREMENT OF SECOND ORDER

HOMOGENEOUS ELECTRON TRANSFER RATE

CONSTANTS BETWEEN OM CYTOCHROME

b_5 AND CYTOCHROME c AT GLASSY

CARBON AND INDIUM TIN

OXIDE SURFACES

Introduction

Important biological processes such as photosynthesis and cellular respiration involve the controlled vectorial flow of electrons. How this flow of electrons occurs, how the proteins recognize each other, and how intermolecular electron transfer occurs is of considerable interest. Researchers have made great strides toward understanding these fundamental processes. The use of electrochemical techniques has contributed to our current understanding of intermolecular electron transfer and some of the factors controlling these processes. The modified electrode solution interface, in some regards, mimics the interaction of physiological partner proteins, thereby contributing to our understanding of these fundamental processes in vivo.

The use of the indium oxide surface, initially reported by Yeh and Kuwana [15], in order to obtain the direct electrochemistry of cytochrome c, has prompted other researchers

to exploit the intrinsic nature of the metal oxide surface with the aim of promoting the electrochemistry of other proteins. For example, Harmer et al., [12] utilized ruthenium dioxide, iridium dioxide, and tungsten oxide electrodes to obtain the reversible electrochemistry of cytochrome c, azurin, ferredoxin, rubredoxin, and plastocyanin. Electrochemical responses of myoglobin and spinach ferredoxin have also been obtained at indium oxide electrodes [13,14]. The great appeal of the metal oxide electrodes stems form their high charge density [31] and the limited amount of surface preparation that is involved, in order to obtain protein-compatible surfaces.

An exceptional material that has been utilized extensively to obtain the direct electrochemistry of numerous proteins and enzymes is pyrolytic graphite [16-19]. Unfortunately, pyrolytic graphite electrodes are not commerically available and the electrodes must be fabricated in house. In contrast, glassy carbon electrodes are commercially available and therefore these electrodes have been utilized extensively by electrochemists interested in the study of small molecules. Glassy carbon electrodes are also attractive because of the large potential window that is available in aqueous environments [2], (positive one volt to minus one volt). Glassy carbon is produced by high temperature heating of polymers such as polyacrylonitrile [1]. The material can be described as a compact mass of tangled graphitic fibers [1]. Glassy carbon has been shown to have a great deal of surface functional groups [20-25], and therefore should exhibit a favorable electrode surface for communicating directly with proteins. There have been several reports describing the use of glassy carbon electrodes in obtaining the direct electrochemistry of proteins and enzymes. For example, Hagen et al.[3] activated a glassy carbon electrode by utilizing hot nitric acid to obtain the direct electrochemistry of

cytochrome c. Heering, *et al.,*[4] utilized a methane flame to activate glassy carbon with the aim of obtaining the direct electrochemistry of a flavodoxin from *Desulfovibrio vulgaris,* and the direct electrochemistry of several high-potential iron-sulfur proteins [5]. Butt *et al.*[6], utilized a glassy carbon electrode that was strictly polished to obtain the direct electrochemistry of the enzyme hydrogenase. The direct electrochemistry, has been reported, of several blue copper proteins, (stellacyanin, plantacyanin, plastocyanin, and zurin) at glassy carbon electrodes [7-9]. The glassy carbon electrode utilized in these studies was activated by polishing in air and sonicating, the authors made no elaboration on surface activation. In an intriguing report, the direct electrochemistry of cytochrome c was reported at a bare glassy carbon electrode [10]. The authors utilized polishing to activate the electrode, but stressed the importance of utilizing new polishing cloth in between polishing steps in order to avoid contamination of the electrode surface. The surface cleanliness of glassy carbon has been stressed by numerous researchers [1, 26-28]. Hu *et al.,*[11] utilized glass plates for polishing glassy carbon, instead of the conventional polishing pads and extensive sonication, to produce a highly activated surface. The glassy carbon surface seems prone to contamination from the polishing pads, polishing agents, and laboratory air [11].

The studies described herein describe the effects of sonication on glassy carbon with the aim of obtaining the direct electrochemistry of redox proteins. The glassy carbon electrode has been utilized to obtain the reversible electrochemistry of cytochrome c and OM cytochrome b_5, and was also employed to measure the second order homogeneous electron transfer rate constant between OM cytochrome b_5 and cytochrome c. Indium tin oxide (ITO) electrodes have also been utilized to measure the reduction potential of OM cytochrome b_5 and the second order homogeneous electron transfer rate between OM

cytochrome b_5 and cytochrome c.

Experimental Procedure

Recombinant rat liver Outer Mitochondrial (OM) cytochrome b_5 was expressed as described in Chapter II. Horse heart cytochrome c was purchased from Sigma and used as received. Polylysine MW = 3400 was purchased from Sigma and used without further purification. All other reagents were from Aldrich or Sigma and were used as received.

Cyclic voltammetry was carried out with a Bioanalytical Systems (BAS) 50 W computer-controlled potentiostat using a three electrode configuration. The working electrode was either a 3 mm glassy carbon electrode or an indium tin oxide electrode, a platinum wire counter-electrode, and a silver/silver chloride miniature reference (Cypress Systems). Surface activation of the working electrodes is described below.

Electrode Modification-Sonochemical Activation of Glassy Carbon

The electrodes (3 mm diameter)(BAS) were polished for 10 minutes with alumina polishing slurry on texmat pads (BAS), and rinsed in between with deionized water. The electrodes were partially submerged in a ultrasonic cleaning bath containing deionized water and sonicated for 30 minutes. The ultrasonic cleaning bath was a Bransonic ultrasonic cleaner model 2210 operating at a frequency of 47 KHz and input power of 125 watts. The electrodes were then rinsed with deionized water and used immediately. The solution in the electrochemical cell typically consisted of 100 μM of OM cytochrome b_5, 300 μM of polylysine (M W = 3400), and 100 mM MOPS, pH 7.0, or 100 μM of cytochrome c and 100 mM MOPS, pH 7.0. The maximum volume utilized for these experiments was 300 μl.

Electrochemical Cell

The electrochemical cell used with the glassy carbon electrode (3 mm, BAS) is shown

Teflon Stopcoc

Septum

Reference
Electrode

ACE Thread

Solution

Vacuum
Attachment

Counter
Electrode

Working
Electrode
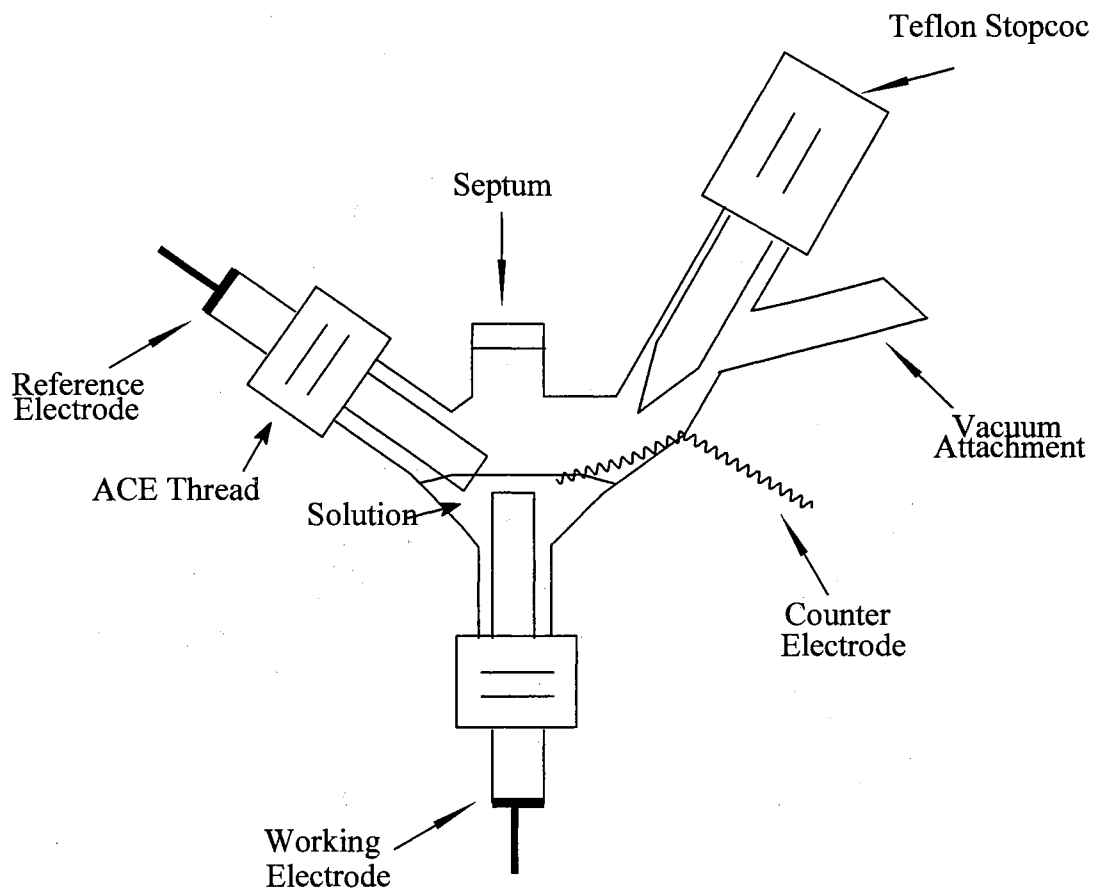
Figure 1. Electrochemical cell used with glassy carbon electrodes.

in Figure 1. The electrochemical cell consisted of a modified version of a cell previously reported (3). Modifications were as follows: a platinum wire was permanently attached and sealed through the side of the glass cell. The positioning of the vacuum line was directly off of the glass extension with an ace threaded top and a stopcock attached. The working electrodes were maintained in the inverted configuration. Before each cyclic voltammetric experiment, the contents of the cell were evacuated and then filled with high purity nitrogen. This procedure was repeated five times in order to minimize the concentration of oxygen in the electrochemical cell. After the last vacuum application, high purity nitrogen was allowed to continually flush the system, while maintaining positive pressure inside the electrochemical cell.

Preparation and Conditions for Indium Tin Oxide Electrodes

Glass-slides (2.50 cm x 2.50 cm) coated on one side with indium-doped tin oxide (ITO) semiconductor films exhibiting a typical resistance of less than 10 ohms were purchased from Delta Technologies (Stillwater, MN). The ITO working electrode was conditioned by sonicating for 30 min in each of the following solutions: 1% alconox in deionized water, ethanol, and deionized water. The clean electrodes were subsequently dried with a stream of nitrogen and used immediately. The solution in the electrochemical cell was degassed by bubbling high-purity nitrogen for 30 minutes and subsequently blanketed with nitrogen in order to maintain anaerobicity. The solution in the electrochemical cell typically consisted of 100 μM of OM cytochrome b_5, 300 μM of polylysine (M W = 3400), and 100 mM MOPS, pH 7.0, or 100 μM of cytochrome c and 100 mM MOPS, pH 7.0. The maximum volume utilized for these experiments was 250 μl.
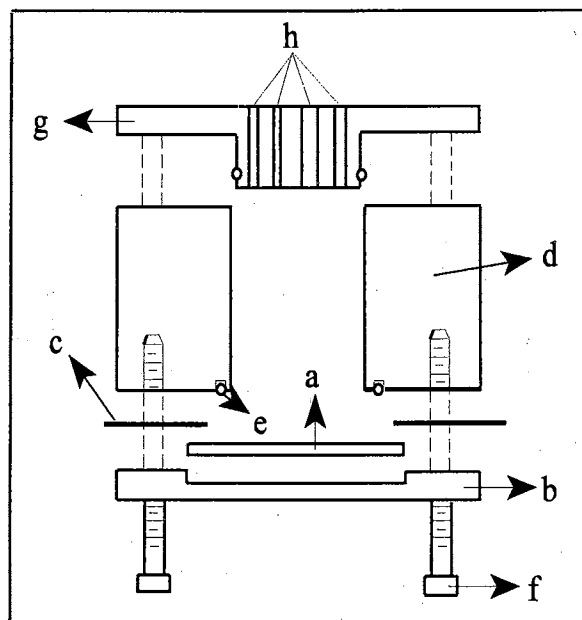
Figure 2. Schematic cross-section representation of the electrochemical cell utilized in this investigation. (a) ITO electrode, (b) base assembly, (c) aluminum foil electrical contact, (d) plexiglass cell body (e) o-ring, (f) four screws for cell assembly, (g) cell cap, (h) ports for reference and auxiliary electrodes and for nitrogen inlet and outlet.

55

schematically in Fig.2) was constructed out of plexiglass. In order to assemble the electrochemical cell, the ITO electrode (a) was fitted into the indentation of the cell assembly (b) and electrical contact with the semiconductor surface was achieved with the aid of an aluminum foil (c). The main body of the electrochemical cell (d), 3.80 cm in diameter, was placed on top of the base assembly so that the o-ring (e) made contact with the semiconductor surface, hence defining an electrode-diameter of 9.3 mm. Finally, the assembled cell was tightened with four screws (f). The solution to be analyzed, typically 300 μL, was placed on the exposed semiconductor surface and the electrochemical cell is capped with cell-cap (g). The latter was outfitted with four holes (h) utilized to insert the reference and auxiliary electrodes, and nitrogen inlet and outlet lines.

Results and Discussion

A glassy carbon electrode was polished with alumina and then briefly sonicated for two minutes. The electrode was placed in a solution consisting of 100 μM of horse heart cytochrome c and 100 mM MOPS pH 7.0. Figure 3B shows the cyclic voltammetric response obtained at this freshly polished glassy carbon electrode. The background cyclic voltammetric response is shown for comparison. As is noted from the cyclic voltammogram in Fig. 3B, the electrochemical response is non reversible, indicating that the interaction between cytochrome c with the glassy carbon surface is not favorable for fast electron exchange. In subsequent experiments the polishing procedure was modified in order to include extensive sonication of the polished glassy carbon electrode with the aim of producing a surface that was more amenable to interaction with proteins. The sonication step was extended to thirty minutes. Figure 4 shows the background subtracted cyclic

voltammetric response obtained with horse heart cytochrome c at a glassy carbon electrode treated with ultrasound for 30 minutes. The scan rate was to 15 mV/s, and the voltammogram displays ΔE_p = 68-70 mV, a midpoint potential of 273 mV (vs NHE) and the ratio of the peak currents (i_{pc}/i_{pa}) is unity; these parameters are typical of reversible heterogeneous electron transfer reactions. The background subtracted cyclic voltammogram in Fig. 4 was digitally simulated (Digisim 2.0, BAS). The parameters utilized to simulate the response are given in Table 1. The heterogeneous electron transfer rate constant and diffusion coefficient were obtained from the digital simulation and were determined to be 1.5 x 10^{-3} cm/s and 1.2 x 10^{-6} cm^2/s, respectively. The diffusion coefficient was also determined by utilizing the Randles-Sevcik relationship [32], which is given by equation 1:

$$i_p = 2.69 \; x \; 10^5 \; n^{3/2} \; A \; D^{1/2} \; C \; \upsilon^{1/2} \qquad (1)$$

The Randles-Sevcik equation relates the peak current (i_p) to number of electrons transferred (n), electrode area (A), diffusion coefficient of the species (D), concentration of electroactive species (c), and the scan rate (υ). By utilizing the Randles-Sevcik equation, the diffusion coefficient was determined to be 1.0 x 10^{-6} cm^2/s. The heterogeneous electron transfer rate constant was also determined by the method of Nicholson and Shain [33] which involves solving equation 2 for the heterogeneous electron transfer rate constant.

$$k^o = \psi \left[D_o \pi v \left(\frac{nF}{RT} \right) \right]^{1/2} \left(\frac{D_r}{D_o} \right)^{\alpha/2} \qquad (2)$$
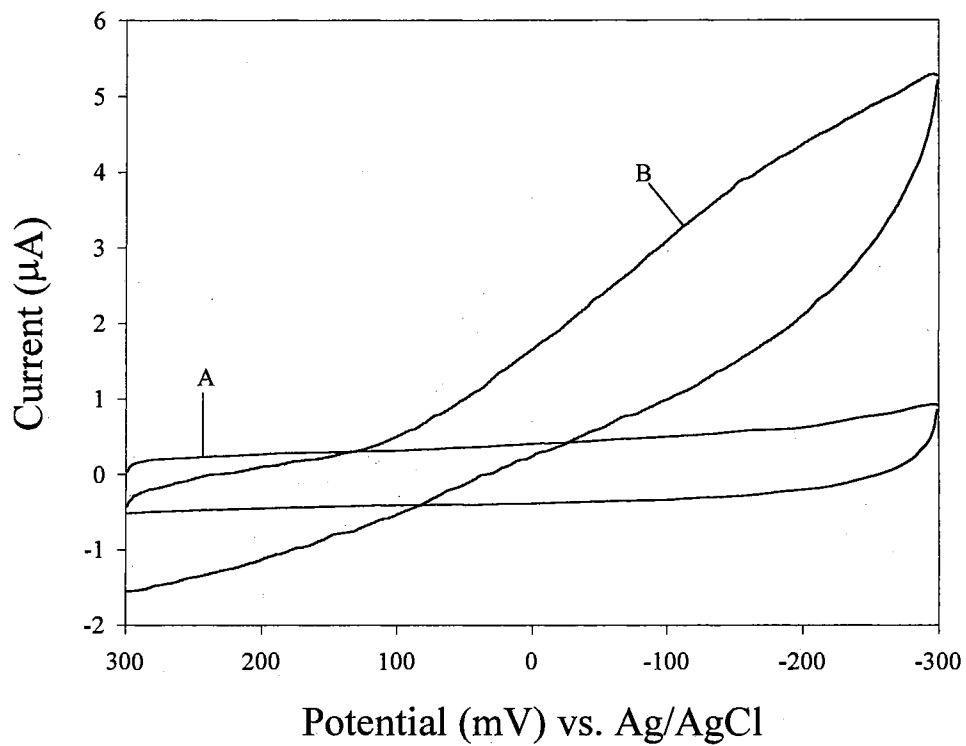
Figure 3. (A) Background; (B) Cyclic voltammetric response of 100 μM cytochrome c in 100 mM MOPS at a freshly polished glassy carbon electrode.
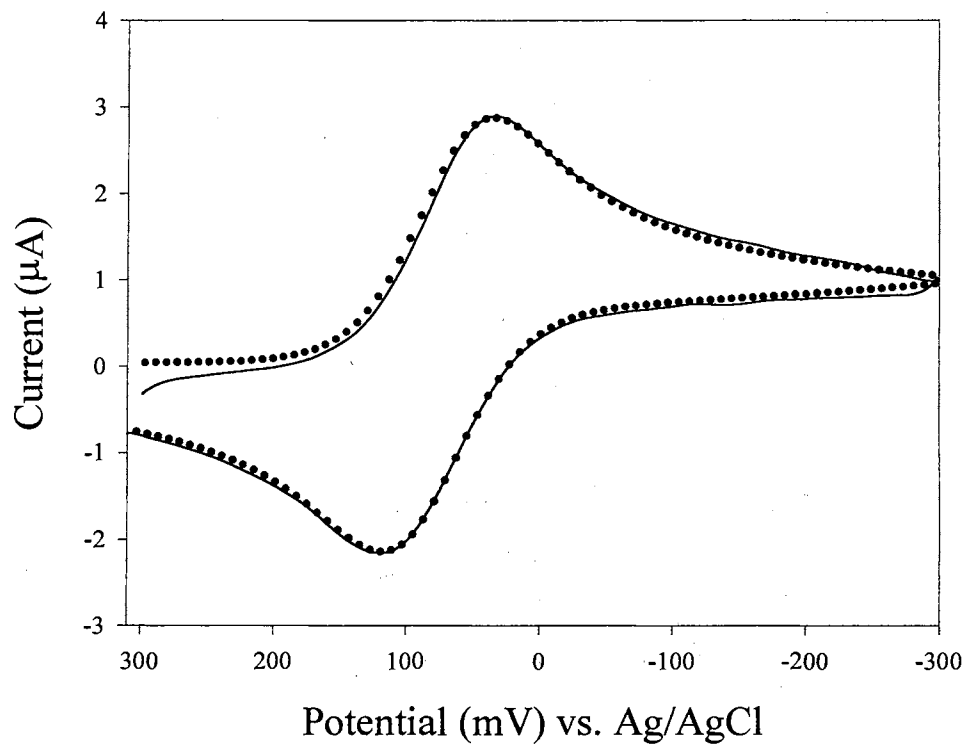
Figure 4. (_____) Background subtracted cyclic voltammetric response obtained at a glassy carbon electrode treated with ultrasound for 30 minutes. The solution contained 100 μM cytochrome c in 100 mM MOPS, pH 7.0. (•) Digital simulation of the experimental response with the following parameters: k_s = 0.0015 cm/s, D_o cyc c^{ox} = D_o cyc c ^{red} = 1.2 x 10^{-6} cm^2/s, scan rate = 15 mV/s, α = 0.50.

59

The parameters in equation 2 have previously been defined, with the exception of ψ, which is a kinetic parameter [35]. The value determined for the heterogeneous electron transfer rate constant is 1.4×10^{-3} cm/s. Consequently, the values for the diffusion coefficient and the heterogeneous electron transfer rate constant obtained by digital simulation are in good agreement with the values obtained by classical methods. Furthermore, both values are in good agreement with those determined for cytochrome c at different electrode surfaces [29,31].

The improved electrochemical response seems to originate from the removal of contaminants from the electrode surface. It has been previously established that polishing in air can produce functional groups on the glassy carbon surface [20], and that most carbon electrodes have a variety of functional groups on the surface, including carboxyl and hydroxyl groups [11,20,36]. It has also been determined that roughly 20 percent of the carbon surface contains functionalities [26]. These groups would be expected to interact favorably with the positively charged cytochrome c. It is important to note however, that a large portion of the surface may adsorb hydrophobic contaminants. These contaminants, in turn, may block most of the surface or act as nucleation sites for the denaturation of cytochrome c. Therefore it is likely that ultrasound aids with the removal of contaminants from the electrode surface and in the process exposes functionalities (i.e. carboxyl and hydroxyl groups) that promote the reversible electrochemistry of the protein.

In order to gain additional insight into the interactions between glassy carbon electrodes and proteins, the direct electrochemistry of OM cytochrome b_5, a negatively charged protein, was explored. Figure 5 displays the background subtracted cyclic voltammetric response of a solution consisting of 100 μM of OM cytochrome b_5, 300 μM in polylysine

and 100 mM MOPS. The sweep rate corresponds to 15 mV/s. The midpoint potential, as determined from the cyclic voltammetric response, is -18 mV vs NHE. The simulated cyclic voltammetric response is also shown also in Figure 5, and parameters used to simulate the response are listed in Table 1. The heterogeneous electron transfer rate constant, along with the diffusion coefficient, were obtained from the simulation and were determined to be 3.0 x 10^{-3} cm/s and 1.3 x10^{-6} cm^2/s, respectively. The value of the diffusion coefficient determined by equation one is 1.3 x 10^{-6} cm^2/sec. Utilizing the method of Nicholson and Shain [33] the heterogeneous electron transfer rate constant was determined to be 2.5 x 10^{-3} cm/s. At the glassy carbon electrode, OM b$_5$ displays reversible electrochemical characteristics; i.e. ΔE_p = 63-68 mV and a ratio of the peak currents (i_{pc}/i_{pa}) of unity. In the absence of polylysine, OM cytochrome b$_5$ does not interact with the electrode surface (Fig. 6a). It is only with the addition of polylysine that a faradaic response is obtained (Fig. 6b) Polylysine, acts as a promoter, allowing the negatively charged protein to approach the negatively charged surface. The diffusion controlled electrochemistry is demonstrated by the linear plot of the peak cathodic current versus the square root of the scan rate (Fig.7).

Homogeneous Electron Transfer Between Cytochrome b$_5$ and Cytochrome c at Glassy Carbon Electrodes.

Seetharaman $et\ al.$[30], performed an interesting series of experiments, whereby a gold electrode modified with β-mercaptopropionate was shown to be selective for the positively charged cytochrome c. On the other hand, the addition of polylysine to the system resulted in the selective reduction of the negatively charged cytochrome b$_5$ ($E^{o'}$ = -100 mV vs NHE), in the presence of cytochrome c ($E^{o'}$ = 260 mV vs NHE). The selectively reduction of cytochrome b$_5$ was followed by a second order homogeneous electron transfer reaction,
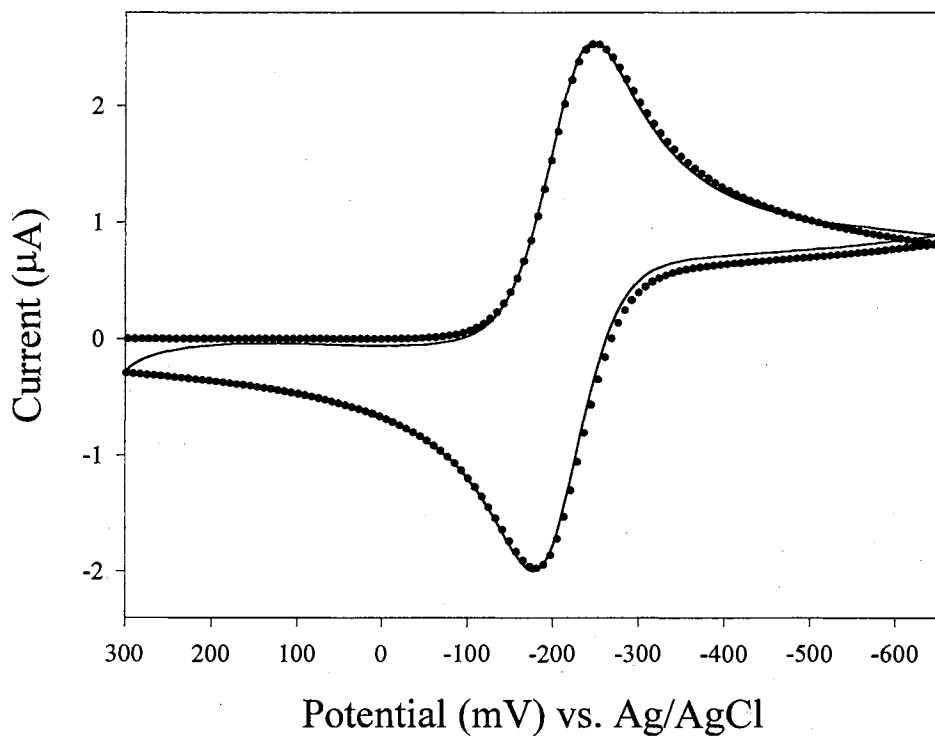
Figure 5. (——) Background subtracted cyclic voltammograms obtained at a glassy carbon electrode from solutions containing 100 µM OM cytochrome b_5 and 300 µM polylysine in 100 mM MOPS, pH 7.0. (•) Digital simulation of the experimental response with the following parameters: k_s = 0.003 cm/s, D_o cyc b_5^{ox} = D_o cyc b_5^{red} = 1.3 x 10^{-6} cm^2/s, scan rate = 15 mV/s, α = 0.50.

Table 1

Parameters for digital simulation of charge transfer rate constants and second order homogeneous electron transfer rate constant.

	cytochrome c	OM cyt b_5	cyt b_5 + cyt c
$E^{o'}$ (Ag/AgCl) (V)	0.077	-0.215	-0.214
Transfer Coefficient, α	0.5	0.5	0.5
k_s (cm/s)	$1.5 \times 10^{-3} \pm 1.0 \times 10^{-4}$	$3.0 \times 10^{-3} \pm 1.5 \times 10^{-4}$	3.0×10^{-3}
k_f (M^{-1}s^{-1})			4.5×10^{6}
k_b (M^{-1}s^{-1})			11.25
Anal. Conc. cyc. c (μM)	100.0		100.0
D_o cyt c ^{ox} (cm^2 s^{-1})	$1.2 \times 10^{-6} \pm 2.0 \times 10^{-7}$		1.3×10^{-6}
D_o cyt c ^{red} (cm^2 s^{-1})	1.2×10^{-6}		1.3×10^{-6}
Anal. Conc. cyt b_5 (μM)		100.0	100.0
D_o cyt b_5 ^{ox} (cm^2 s^{-1})		$1.29 \times 10^{-6} \pm 2.0 \times 10^{-7}$	1.27×10^{-6}
D_o cyt b_5 ^{red} (cm^2 s^{-1})		1.29×10^{-6}	1.27×10^{-6}
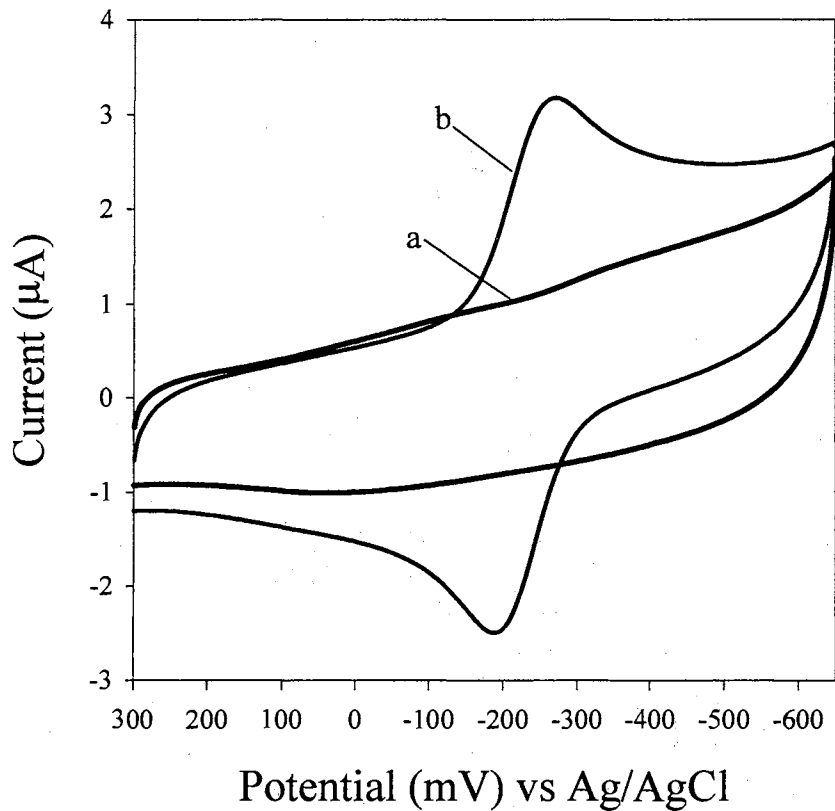
Figure 6. a) Cyclic voltammetric response obtained at a glassy carbon electrode from a solution containing 100 μM cytochrome b_5 in 100 mM MOPS, pH 7.0. b) Cyclic voltammetric response obtained at a glassy carbon electrode from a solution containing 100 μM cytochrome b_5 and 300 μM polylysine in 100 mM MOPS, pH 7.0.

Figure 7. Graph illustrating the linear correlation between the cathodic peak current (i_{pc}) and square root of scan rate ($v^{1/2}$).
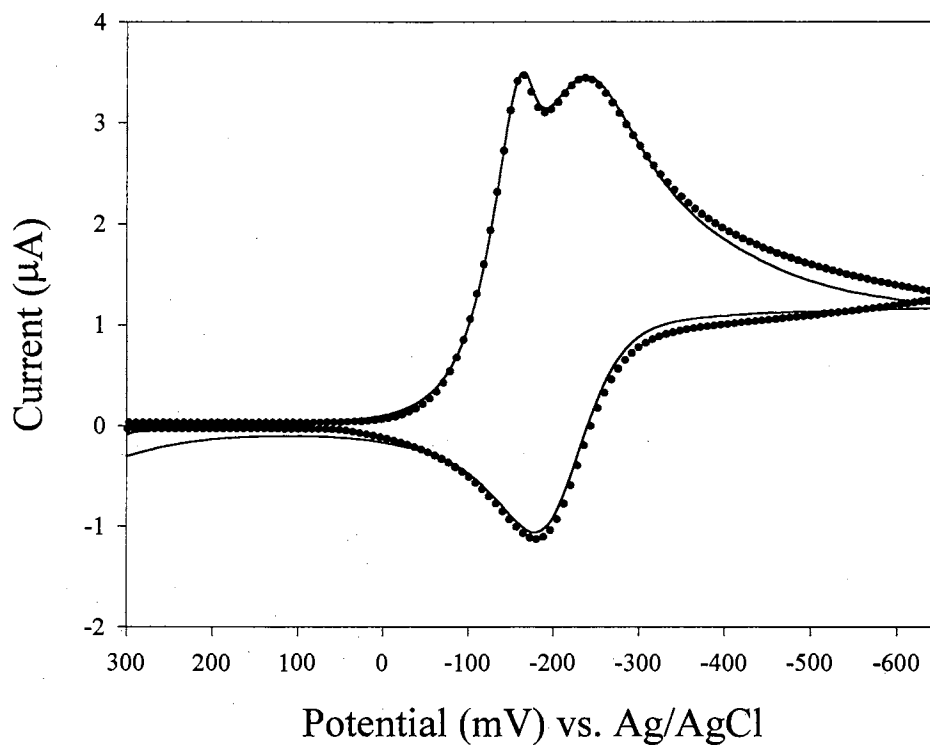
Figure 8. (____) Cyclic voltammogram obtained from a solution containing 100 μM OM cytochrome b₅, 100 μM cytochrome c, 300 μM polylysine. Scan rate = 10 mV/s. (●) Simulated cyclic voltammogram invoking the mechanism shown by equations 1 and 2. Parameters for simulation are shown in Table 1.

where electroreduced cytochrome b_5 was reoxidized by oxidized cytochrome c. This homogeneous electron transfer had a profound effect on the shape of the cyclic voltammetric response, which is characterized by two cathodic peaks, a main peak and a prepeak, and only one anodic peak. These authors also simulated the above described electrochemical response and obtained a second order homogeneous electron transfer rate constant, for the oxidation of ferrocytochrome b_5 by ferricytochrome c. This selective reduction of OM cytochrome b_5 in the presence of cytochome c mimicked the natural electron flow between these two physiological partner proteins.

In accordance with the above experiment, Figure 8 represents the electrochemical response of a solution containing 100 μM of cytochrome c, 100 μM of OM cytochrome b_5, and 300 μM polylysine in 100 mM MOPS. The cyclic voltammetric response is characterized by exhibiting a pre-peak and a reversible wave. Consequently, it can be concluded that in the presence of polylysine, the ultrasound-activated glassy carbon electrode discriminates against cytochrome c. The electrochemical response was simulated using the following EC mechanism [30];

$$\text{cyt } b_5(\text{III}) + e^- \overset{k_s}{\rightleftharpoons} \text{cyt } b_5(\text{II}) \tag{3}$$

$$\text{cyt } b_5(\text{II}) + \text{cyt c (III)} \underset{k_b}{\overset{k_f}{\rightleftharpoons}} \text{cyt } b_5(\text{III}) + \text{cyt c(II)} \tag{4}$$
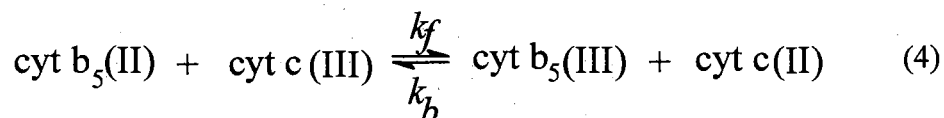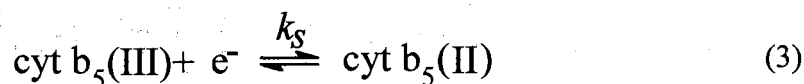
where cyt b_5 (III) represents the oxidized form of OM cytochrome b_5 and cyt b_5 (II) represents the reduced form of OM cytochrome b_5. Cyt c (III) and cyt c (II) represent the oxidized and reduced forms of cytochrome c, respectively. In equations 3 and 4, k_s

represents the heterogeneous electron transfer rate constant, and k_f represents the second order homogeneous electron transfer rate constant, respectively. The parameters utilized for the simulation are listed in Table 1. The second order homogeneous electron transfer rate constant was determined to be $4.5 \times 10^6 \text{ M}^{-1} \text{ s}^{-1}$.

The electrochemical response in Figure 8 is interesting in light of the response obtained by Bagby et al.[31]. These authors obtained two independent electrochemical responses from a mixture of cytochrome c and OM cytochrome b_5 at an edge plane pyrolytic graphite electrode. The electrochemical response of OM cytochrome b_5 was thought to be promoted by cytochrome c, since no other promoters were present. The key to the electrochemical response obtained above is the promoter polylysine, which makes the electrode positively charged, and allows electrostatic discrimination of cytochrome c to occur.

Indium Tin Oxide

Figure 9 displays the cyclic voltammetic response from a solution containing 100 μM OM cytochrome b_5 and 24 μM polylysine in 100 mM MOPS pH 7.0 at an indium tin oxide electrode. The midpoint potential corresponds to -56.5 mV vs NHE, and the electrochemical response is characterized by ΔE_p = 60-63 mV and peak current ratio (i_{pc}/i_{pa}) of unity. In the absence of polylysine there is a complete absence of Faradaic response from solutions containing only OM cytochrome b_5. This is likely to originate from the electrostatic repulsion of the negatively charged protein and the negatively charged electrode. The addition of the promoter, therefore, allows this coulombic repulsion to be overcome, thereby allowing the protein to communicate with the electrode. The heterogeneous electron transfer rate constant and the diffusion coefficient of OM cytochrome b_5 were determined by
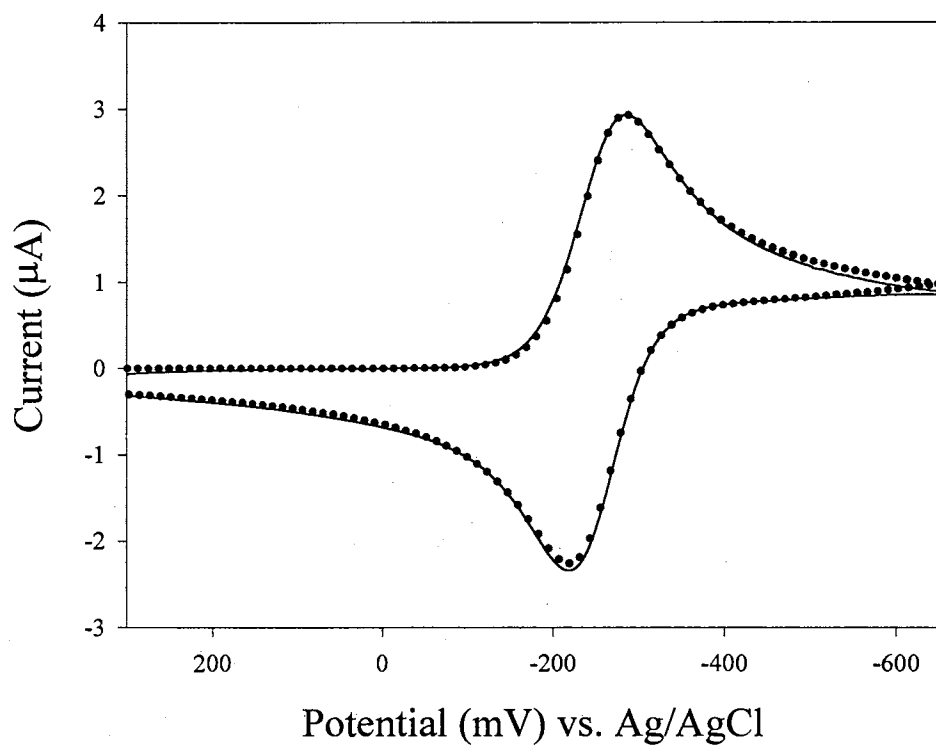
Figure 9. (——) Background subtracted cyclic voltammograms obtained at an indium tin oxide electrode from a solution containing 100 μM cytochrome b_5 and 24 μM polylysine in 100 mM MOPS, pH 7.0. (•) Digital simulation of the experimental response with the following parameters: k_s = 0.0047 cm/s, D_o cytochrome b_5^{ox} = D_o cytochrome b_5^{red} = 1.35 x 10^{-6} cm²/s, scan rate = 20 mV/s, α = 0.50.

digital simulation to be 4.7×10^{-3} cm/s and 1.35×10^{-6} cm^2/s, respectively (Table 2). Figure 10 shows the linear plot of the peak cathodic current (i_{pc}) vs the square root of the scan rate. This linear relationship indicates a diffusion controlled process.

It was noticed that the electrochemical response of OM cytochrome b$_5$ is more persistent at the metal oxide electrode than at the glassy carbon surface. This could be attributed to the higher charge density [31] of the metal oxide surface. The extensive oxide network would be expected to make a more hydrophilic surface, thereby preventing adsorption and denaturation of the protein at the electrode surface [34]. A contributing factor could be that organic contaminants do not tend to adsorb as readily on metal oxide surfaces [31], thereby poisoning of the electrode is slower to occur at these surfaces.

Homogeneous Electron Transfer Between Cytochrome b$_5$ and Cytochrome c at Indium Tin Oxide Electrodes.

The cyclic voltammetric response of a solution consisting of 100 μM OM cytochrome b$_5$, 100 μM cytochrome c and 24 μM polylysine is shown in Figure 11. The characteristic electrochemical response exhibiting a pre-peak and a main peak is obtained, indicating that the selective reduction of OM cytochrome b$_5$ is occurring in the presence of cytochrome c, followed by a homogeneous electron transfer reaction between the two proteins. Simulating the electrochemical response by the mechanism described in equations 3 and 4 leads to a second order homogeneous electron transfer rate constant of 9.8×10^8 M^{-1} s^{-1}, μ = 0.024 M (Table 2). The magnitude of the rate constant measured is in agreement with those previously reported by Meyer $et\ al.$[39] using flash photolysis techniques (1.3×10^9 M^{-1} s^{-1}, μ = 0.035 M). The difference in the second order homogeneous electron transfer rate
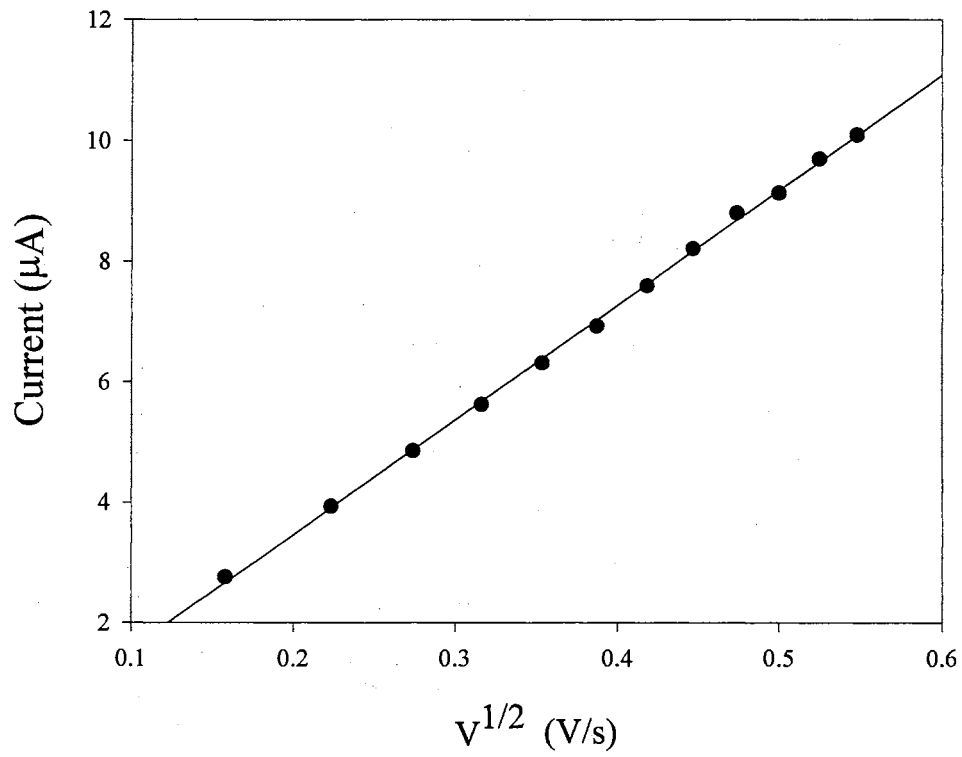
Figure 10. Graph illustrating the linear correlation between the cathodic peak current (i_{pc}) and square root of scan rate ($v^{1/2}$).
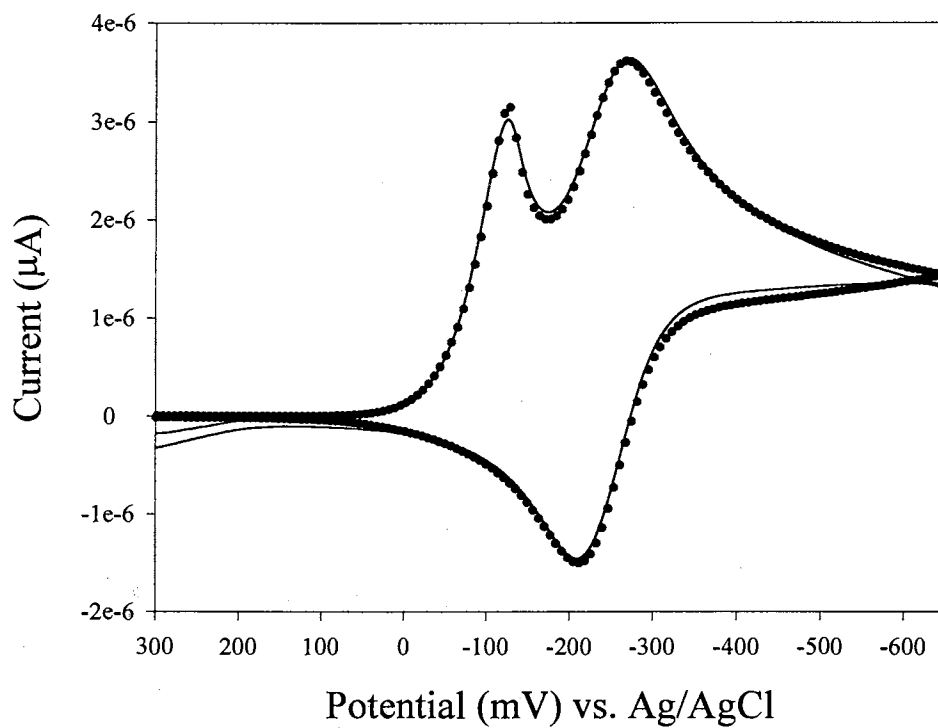
Figure 11. (____) Cyclic voltammogram obtained from a solution containing 100 μM cytochrome c, 100 μM cytochrome b5, and 24 μM polylysine at an indium tin oxide electrode. Scan rate = 20 mV/s. (•) Simulated cyclic voltammogram invoking the mechanism shown by equations 1 and 2. Parameters for simulation are shown in Table 2.

Table 2

Parameters for digital simulation of charge transfer rate constants and second order homogeneous electron transfer rate constant at ITO electrode

	OM cyt b_5	cyt b_5 +cyt c
$E^{o'}$ (Ag/AgCl) (V)	-0.252	-0.214
Transfer Coefficient, α	0.5	0.5
k_s (cm/s)	4.7×10^{-3}	5.0×10^{-3}
k_f ($M^{-1} s^{-1}$)		9.8×10^8
k_b ($M^{-1} s^{-1}$)		2182
Anal. Conc. cyt. c (μM)		100.0
D_o cyt c ^{ox} ($cm^2 s^{-1}$)		1.1×10^{-6}
D_o cyt c ^{red} ($cm^2 s^{-1}$)		1.1×10^{-6}
Anal. Con. cyt b_5 (μM)	100.0	100.0
D_o cyt b_5 ^{ox} ($cm^2 s^{-1}$)	1.35×10^{-6}	1.2×10^{-6}
D_o cyt b_5 ^{red} ($cm^2 s^{-1}$)	1.35×10^{-6}	1.2×10^{-6}

constant measured at the glassy carbon electrode (4.5×10^6 M^{-1} s^{-1}), and the rate constant

measured at the indium tin oxide electrode is due to the higher ionic strength of the solution

used for the glassy carbon experiment ($\mu = 0.300$ M). The rate of electron transfer between

these physiological partner proteins is known to be ionic strength dependent [30].

Seetharaman et al. [30], determined the second order homogeneous electron transfer rate

constants to be 2.9×10^8 $M^{-1}s^{-1}$ at $\mu = 0.078$ M, and 1.6×10^7 $M^{-1}s^{-1}$ at $\mu = 0.230$ M.

Mediated Approach to Selectively Reduce Other Proteins

The selective electro-reduction of OM cytochrome b_5 at the above mentioned surfaces

allows the second order homogeneous electron transfer rate constant between

ferrocytochrome b_5 and ferricytochrome c to be measured, as described previously by

Seetharaman et al. [30]. Could this approach be applicable to measuring the second order

homogeneous electron transfer rate constant between other proteins? This was explored by

trying to selectively reduce spinach ferredoxin [37] in the presence of cytochrome $P450_{cam}$.

Figure 12 displays the cyclic voltammetric response of 100 μM of spinach ferredoxin,

(a negatively charged protein), and 250 μM of polylysine in 100 mM MOPS at the activated

glassy carbon electrode. The electrochemical response is quasireversible with a ΔE_p of 75-

90 mV. The midpoint potential was determined to be -406 mV vs. NHE. The glassy

carbon electrode, in the presence of the promoter polylysine, is able to communicate with

the negatively charged protein. It was hoped that spinach ferredoxin could be selectively

reduced at the glassy carbon electrode in the presence of cytochrome $P450_{cam}$, and be

reoxidized by the enzyme. Figure 13 shows the cyclic voltammetric response of a solution

consisting of 100 μM of cytochrome $P450_{cam}$, 100 μM spinach ferredoxin, and 300 μM
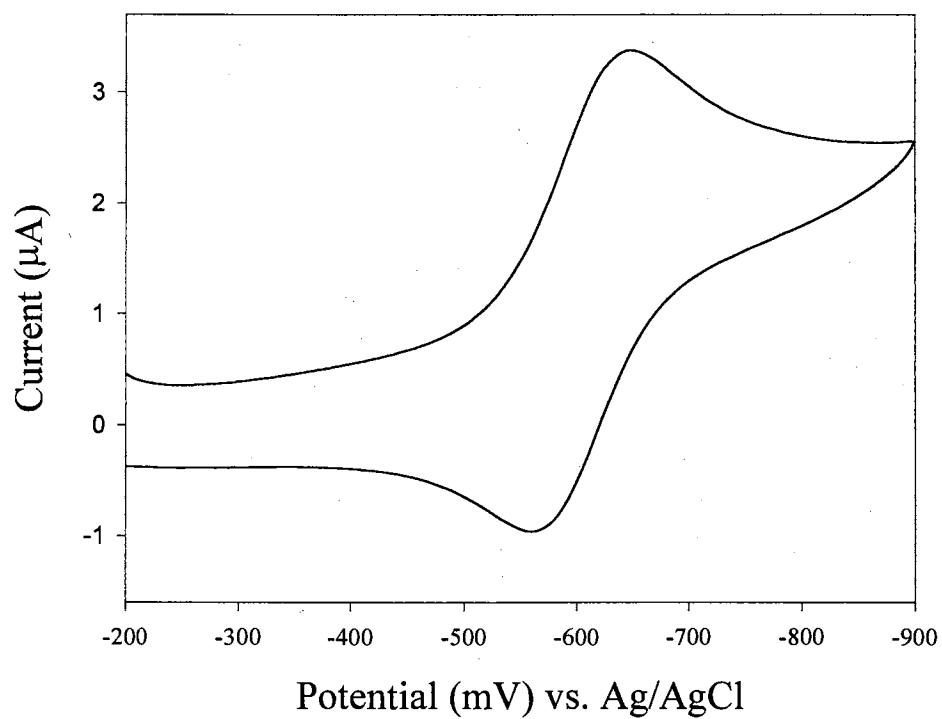
Figure 12. Background subtracted cyclic voltammogram obtained at a glassy carbon a electrode from a solution containing 100 μM spinach ferredoxin and 300 μM polylysine in 100 mM MOPS, pH 7.0.
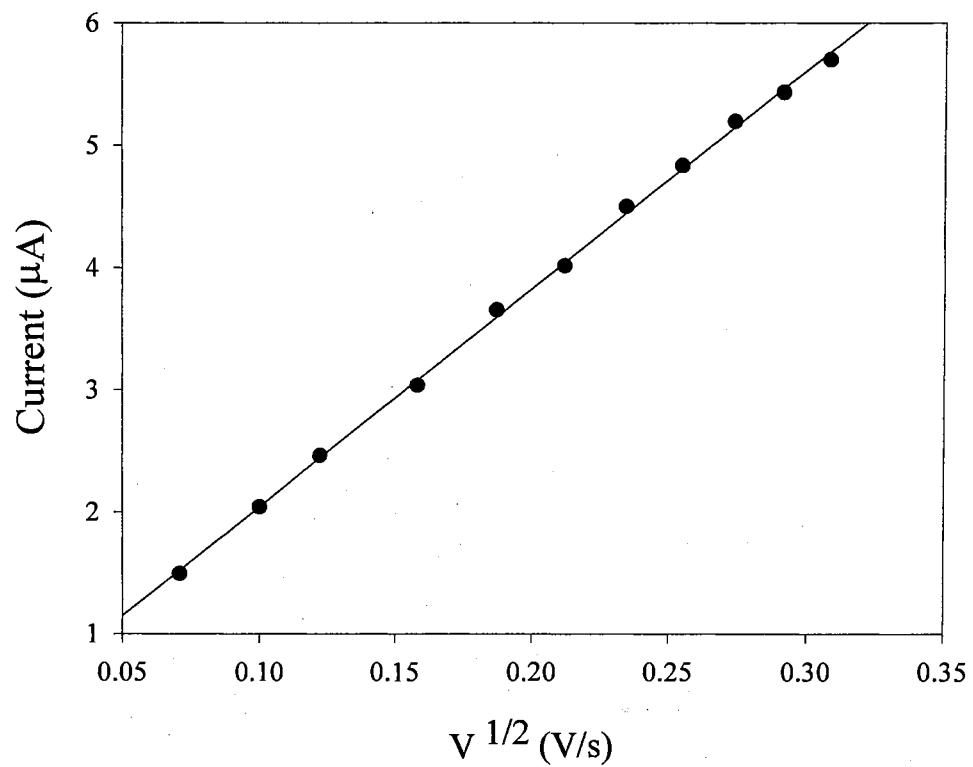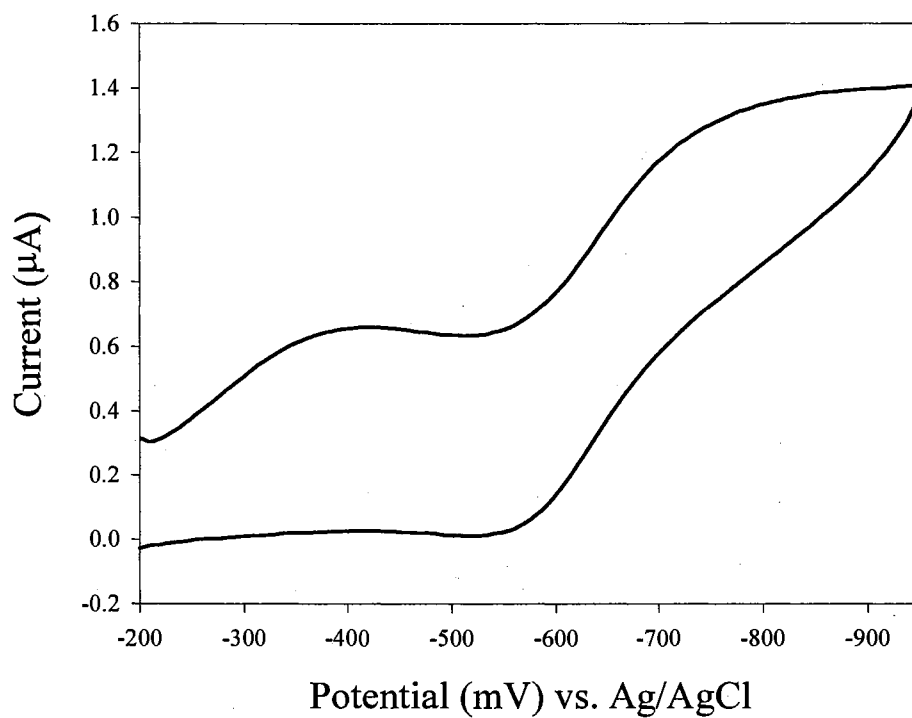
Figure 13. Cyclic voltammogram obtained from a solution containing 100 μM spinach ferredoxin, 100 μM cytochrome P450$_{cam}$, 300 μM polylysine. Scan rate = 1 mV/s.

polylysine in 100 mM MOPS. As can be seen from the cyclic voltammogram, the electrode surface is not selective only for spinach ferredoxin, but apparently also interacts with cytochrome P450$_{cam}$. The direct response of the enzyme is irreversible at the ultrasound activated glassy carbon electrode. The enzyme seems to adsorb at the glassy carbon surface, probably due to hydrophobic interactions between the electrode and the surface of the enzyme. Either way, the electrochemical wave due to the enzyme is inactive toward substrate turnover. By comparison, the direct electrochemistry of cytochrome P450$_{cam}$ at a pyrolytic graphite surface at 4 °C has been previously reported [38], but direct turnover of the enzyme was not obtained. Furthermore, the electrochemical response was shown to depend on enzyme purity, such that reversible voltammetry could only be observed with freshly purified enzyme [38]. The pyrolytic graphite surface has approximately 33% functionalities [30], whereas glassy carbon contains 20% [26]; therefore, one can speculate that the larger number of appropriate sites on pyrolytic graphite surfaces may contribute to the transient reversible electrochemistry of cytochrome P450$_{cam}$ at these electrodes. Both surfaces have a high degree of hydrophobic character, which makes it easy for a protein to denature.

Similar experiments carried out with spinach ferredoxin and cytochrome P450$_{cam}$ at indium oxide electrodes do not show the same trend as the glassy carbon electrode (this is discussed in Chapter IV). This is attributed to the higher charge density of the metal oxide electrode, which prevents the enzyme from readily adsorbing onto the electrode surface.

Conclusion

The surface-solution interface is crucial in obtaining electrochemical communication of proteins. In order for electrochemical communication to take place, it is necessary for the

77

protein to bind to the electrode transiently in order for electron transfer to occur. The characteristics of the surface, i.e. functionalities, hydrophilicity, help to 1) steer the protein toward the electrode surface in an optimum orientation for facile electron transfer, and 2) prevent the irreversible adsorption and denaturation of the protein at the electrode surface. Even if the electrode surface has functional groups that are favorable for the protein to bind, these may not be readily accessible to the protein due to surface contamination. This is believed to be the cause of inactivation of the freshly polished glassy carbon electrode. The use of extensive sonication thoroughly cleans (removes contaminants from) the surface, thereby activating it for electrochemistry. In this context, it is noteworthy that Bowden *et al.* [31] obtained the direct electrochemistry of cytochrome c at unmodified gold and platinum electrodes. This unpromoted electrochemistry was attributed to a clean electrode surface. These researchers also noted that by exposing a gold electrode to laboratory air for five minutes, the electrochemical response of cytochrome c was obliterated [31]. This seems to be the case with glassy carbon electrode as well, because its surface appears to have a high affinity for organic contaminants that block the functionalities or act as nucleation sites for protein adsorption and denaturation at the electrode surface.

Once the glassy carbon electrode is properly cleaned, it is quite versatile since the electrochemistry of a number of proteins, including cytochrome c, OM cytochrome b_5, and spinach ferredoxin can be readily obtained. In the presence of polylysine, the surface was preferentially selective toward OM cytochrome b_5 even in the presence of cytochrome c, a protein with a more positive reduction potential and an opposite surface charge. As was shown previously [30], the electrostatic interactions at the electrode surface can be used to create vectorial electron transfer, which in turn, can be utilized to measure rate constants for

protein-protein electron transfer reactions. The electrochemical response of OM cytochrome b_5 was also explored at an indium tin oxide electrode and the homogeneous second order electron transfer rate constant was measured. Even though both types of electrodes (the glassy carbon and indium tin oxide), are active toward small electron transfer proteins, the surface presented to the proteins is considerably different. The metal oxide electrodes have a higher charge density and are less prone to contamination. Researchers interested in exploring protein electrochemistry and coupled protein reactions have to pay special attention to the solution-electrode interface in obtaining the desired results.

References

1. Kissinger, P. T.; Heineman, R. W., Laboratory Techniques in Electroanalytical Chemistry, 1996, New York: Marcel Dekker.

2. Bard, A. J.; Faulkner, L. R., *Electrochemical Methods Fundamentals and Applications*. 1980, New York: John Wiley & Sons.

3. Hagen, W. R. (1989) *Eur. J. Biochem.* **182**, 523.

4. Heering, H. A.; Hagen, W. R. (1996) *J. Electroanal. Chem.*, **404**, 249.

5. Heering, H. A.; Bulsink, B. M.; Hagen, W. R.; Meyer, T. E. (1995) *Biochemistry*, **34**, 14675.

6. Butt, J. N., Filipiak, M., Hagen, W. R., (1997), *Eur. J. Biochem.* 245, pp 116-122.

7. Ikeda, O.; Sakurai, T. (1994) *Eur. J. Biochem*, **219**, 813.

8. Sakurai, T.; Ikeda, O.; Suzuki, S. (1990) *Inorg. Chem*, **29**, 4715.

9. Sakurai, T.; Nose, F.; Fujiki, T.; Suzuki, S. (1996) *Bull. Chem. Soc. Jpn*, **69**, 2855.

10. Dong, S. J.; Chi, Q. (1992) *J. Chin. Chem. Lett.*, **3**, 857.

11. Hu, I.; Karweik, D. H.; Kuwana, T. (1985) J. Electroanal. Chem. **188**, 59.

12. Harmer, M. A.; Hill, H. A. O. (1985) *J. Electroanal. Chem.* **189**, 229.

13. Tominaga, M.; Kumangai, T.; Takita, S.; Taniguchi, I. (1993) Chem. Lett. 177

14. Taniguchi, I.; Hirakawa, Y.; Iwakiri, K.; Tominaga, M.; Nishiyama, K. (1994) *J. Chem. Soc., Chem. Commun.*, 953.

15. Yeh, P.; Kuwana, T. (1977) *Chemistry Letters.*, 1145.

16. Armstrong, F. A.; Hill, H. A. O.; Oliver, B. N. (1984) *J. Chem. Soc., Chem. Commun.*, 976.

17. Armstrong, F. A.; Hill, H. A. O.; Oliver, B. N.; Walton, N. J. (1984) *J. Am Chem.*

80

Soc. **106**, 921.

18.   Armstrong, F. A.; Cox, P. A.; Hill, H. A. O.; Lowe, V. J.; Oliver, B. N. (1987) *J. Electroanal. Chem.* **217**, 331.

19.   Armstrong, F. A.; Bond. A. M.; Hill, H. A. O.; Psalti, S. M.; Zoski, C. G. (1989) *J. Phys. Chem.* **93**, 6485.

20.   Kamau, G. N.; Willis, W. S.; Rusling, J. F. (1985) *Anal. Chem.* **57**, 545.

21.   Kuo, T.; McCreery, R. L. (1999) *Anal. Chem*, **71**, 1553.

22.   Fagan, D.T.; Hu, I.; Kuwana, T. *Anal. Chem.* **57**, 2759.

23.   Collier, W. G.; Tougas, T. P. (1987) *Anal. Chem.* **59**, 396.

24.   Evans, J. F.; Kuwana, T. (1979) *Anal. Chem.* **51**, 358.

25.   Panzer, R. E.; Elving, P. J. (1975) *Electrochimica Acta*, **20**, 635.

26.   Chen, P.; McCreery, R. L. (1996) *Anal. Chem.* **68**, 3958.

27.   Zak, J.; Kuwana, T. (1982) *J. Am. Chem. Soc.,* **104**, 5514.

28.   Engstrom, R. C.; Strasser, V. A. (1984) *Anal. Chem.* **56**, 136.

29.   Eddowes, M. J.; Hill, H. A. O. (1979) *J. Am Chem. Soc.* **101**, 4461.

30.   Seetharaman, R.; White, S. P.; Rivera, M. (1996) *Biochemistry* , **35**, 12455.

31.   Bowden, E. F.; Hawkridge, M. F. (1984) *J. Electroanal. Chem.,* **161** 355.

32.   Bard, A. J.; Faulkner, L. R., *Electrochemical Methods Fundamentals and Applications.* 1980, New York: John Wiley & Sons.

33.   Nicholson, R. S.; Shain, I. (1964) *Anal. Chem*, **36**, 706.

34.   Taniguchi, I. (1997) *The Electrochemical Society Interface*, 34.

35.   Nicholson, R. S. (1965) *Anal. Chem.,* **37**, 1351.

36.   Deakin, M. R.; Stutts, K. J.; Wightman, R. M. (1985) *J. Electroanal. Chem.* **182**

113.

37.   Berg, J. A.; Holm, R. H. Structure and Reactions of Iron-Sulfur Protein Clusters and Their Synthetic Analogs. In *Iron-Sulfur Proteins;* Spiro, T. G., Ed.; John-Wiley & Sons, Inc.: New York 1982; 1-66.

38.   Kazlauskaite, J.; Westlake, A. C. G.; Wong, L.-L.; Hill, H. A. O. (1996) *Chem. Commun*, 2189.

39.   Meyer, T. E.; Rivera, M.; Walker, F. A.; Mauk, M. R.; Mauk, A. G.; Cusanovich, M. A.; Tollin, G. (1993) *Biochemistry* **32**, 622.

CHAPTER IV

FERREDOXIN-MEDIATED ELECTROCATALYTIC

DEHALOGENATION OF HALOALKANES

BY CYTOCHROME P450$_{cam}$

Introduction

The cytochrome P450 family of enzymes is involved in a variety of biological

oxidation reactions, including hydroxylations, epoxidations, and heteroatom oxidations.

Cytochrome P450$_{cam}$, originally isolated from the bacterium *Pseudomonas putida*, catalyzes

the regio- and stereospecific hydroxylation of *d*-camphor to produce 5-*exo*-hydroxycamphor

[1,2]. The monooxygenation reaction requires, in addition to *d*-camphor and molecular

oxygen, two reducing equivalents which originate from NADH and are sequentially

transferred via the flavin group of NADH-putidaredoxin reductase to the 2Fe-2S-Cys$_4$ cluster

of putidaredoxin and in turn to the heme iron in cytochrome P450$_{cam}$. Consequently, reduced

putidaredoxin acts as a direct electron donor to oxidized cytochrome P450$_{cam}$. The reaction

cycle is shown in Figure 1.

Although cytochrome P450$_{cam}$ was initially considered to be substrate specific, it

was later shown to oxidize molecules closely related to its natural substrate (*e.g.*

adamantanone, adamantane, norcamphor) [3-5], and molecules not related to camphor such
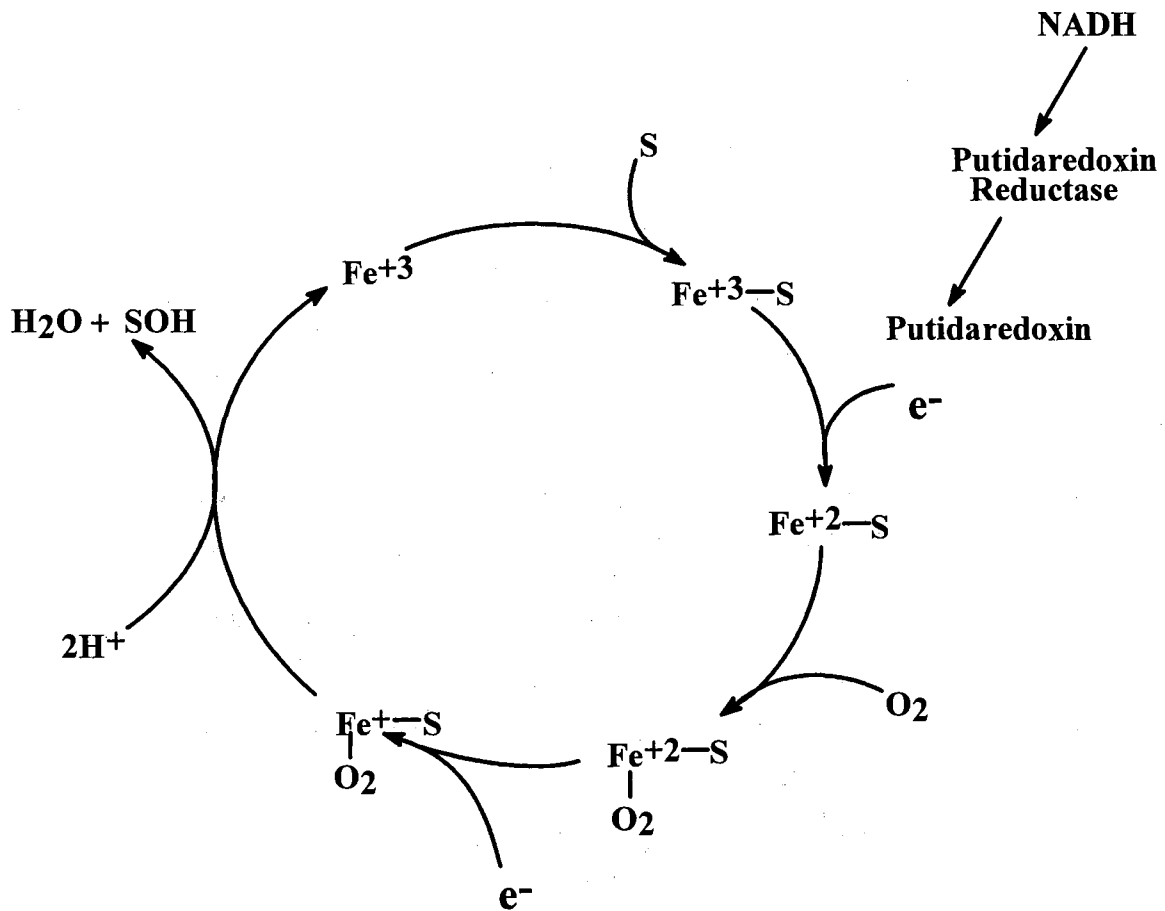
Figure 1. Schematic representation of cytochrome P450$_{cam}$ reaction cycle. The substrate is represented by S.

as cys-β-methylstyrene [6], and thioanisole [7]. It has also been shown that cytochrome

P450$_{cam}$ can perform non-physiological reductive dehalogenation reactions [8] and

accordingly, it has been extensively studied for potential applications in the bioremediation

of halogenated hydrocarbons [9-11]. These findings have led to the postulation that

cytochrome P450$_{cam}$ may find useful applications in the regio- and stereo-selective synthesis

of commodity chemicals as well as in bioremediation schemes. One possible way of

achieving these goals may be to electrochemically address cytochrome P450$_{cam}$ at an

electrode surface in order to supply the enzyme with the reducing equivalents needed to carry

out its catalytic cycle, hence avoiding the use of NADH, NADH-putidaredoxin reductase

and putidaredoxin.

Significant progress has been achieved toward the electrochemical activation of

cytochrome P450$_{cam}$. For example, the cyclic voltammetry of cytochrome P450$_{cam}$ has been

observed at low temperatures (4°C) with an edge-plane pyrolytic graphite electrode by

utilizing highly pure and freshly purified enzyme [12]. The reversible cyclic voltammetry

of cytochrome P450$_{cam}$ incorporated in lipid films has also been reported [13]. It was shown

that cytochrome P450$_{cam}$ trapped in these films is capable of catalyzing the electrochemically

driven reduction of trichloroacetic acid under anaerobic conditions. It is interesting that the

formal potential corresponding to the one-electron reduction of substrate-free cytochrome

P450$_{cam}$ trapped in the lipid films is approximately 180 mV more positive than the formal

potential measured for the substrate-free enzyme in solution (-303 mV *vs* NHE) [13].

Although the origin of this large shift in the reduction potential is not clear, the lipid

environment and double layer effects at the electrode surface have been implicated [13].

The direct electrochemistry of cytochrome P450$_{cam}$ has also been obtained with alternate

layer-by layer films deposited on electrode surfaces [14]; these films were also used to electrochemically drive the epoxidation of styrene.

In a different approach to harvest the catalytic power of cytochrome $P450_{cam}$, the mediator cobalt sephulcrate was used to electrolyze the fusion protein containing the heme domain of cytochrome P450 4A1 linked to the flavin domain of NADPH cytochrome P450 reductase [15]. This system was used to perform the electrocatalytically driven T-hydroxylation of lauric acid. In a different study, a solution containing putidaredoxin and cytochrome $P450_{cam}$ was electrolyzed at an antimony-doped tin oxide electrode in the presence of oxygen and d-camphor [16]. It was reported that putidaredoxin is reduced at the semiconductor electrode surface and subsequently transfers the reducing equivalents to cytochrome $P450_{cam}$. It is interesting to note, however, that the hydroxylation of camphor to produce 5-exo-hydroxycamphor required the concentration of putidaredoxin in the electrolytic cell to be at least five hundred-fold larger than that of cytochrome $P450_{cam}$. Although the need for such a large excess of putidaredoxin is not clear, it was postulated to originate from a slow rate of heterogeneous electron transfer (k_s) between the electrode and putidaredoxin. In agreement with this idea, the value of k_s measured for putidaredoxin at the antimony doped tin oxide electrode was reported to be 1.0×10^{-4} cm/sec [16].

An alternative to the use of putidaredoxin as an electron donor to cytochrome $P450_{cam}$ is the utilization of spinach ferredoxin. The active site of this electron transfer protein also consists of a 2Fe-2S-Cys_4 cluster [17] that exhibits a reduction potential (- 430 mV vs NHE) [18,19] sufficiently negative to reduce cytochrome $P450_{cam}$, even in the absence of substrate. It is also known that spinach ferredoxin cannot substitute the effector role that putidaredoxin plays in the monooxygenation reactions performed by cytochrome

P450$_{cam}$ [20]. However, it has been reported that spinach ferredoxin can transfer the two electrons needed by cytochrome P450$_{cam}$ in order to carry out the reductive dehalogenation of halogenated hydrocarbons [21]. Accomplishing the electrocatalytic reductive dehalogenation of haloalkanes is highly desirable since recent work has demonstrated the capabilities of naturally occurring cytochromes P450 to reductively degrade compounds such as haloalkanes [9, 11, 22] and other recalcitrant xenobiotics such as atrazine and thiocarbamate herbicides [23]. Consequently, we explored the possibility of utilizing spinach ferredoxin to mediate the electrochemical activation of cytochrome P450$_{cam}$. The results of this investigation clearly demonstrate that spinach ferredoxin is a suitable electron transfer protein for shuttling electrons between an electrode surface and cytochrome P450$_{cam}$ in order to activate cytochrome P450$_{cam}$ toward reductive dehalogenation reactions. The usefulness of this approach resides in abolishing the need for fragile chemicals and enzymes such as NADH and cytochrome P450 reductase. Furthermore, the voltammetric experiments aimed at demonstrating the catalytic activity have also produced important insights into the factors controlling the turnover of reductive dehalogenation reactions.

Experimental Procedures

Protein Expression and Purification

The recombinant plasmid harboring the cytochrome P450$_{cam}$ gene was a generous gift of Professor Stephen Sligar [24].

Cytochrome P450$_{cam}$ was expressed in *E. coli* as described previously by Unger *et al.* [24]. Expression of the protein consisted of the following: Culture tubes containing 4 ml of LB broth containing (100 µg/ml ampicillin) were inoculated with one colony of the *E. coli* strain containing the recombinant plasmid. The tubes were incubated at 37°C, at 220

87

rpm for 12 hours. The inoculate was then added to four Fernbach flasks containing 1 liter of LB broth (100µg/ml ampicillin) and incubated at 37 °C while shaking at 220 rpm. When the absorbance of the medium reached 0.7, protein expression was induced by the addition of D(+) Camphor to a final concentration of 70 µM. The medium was further incubated at 37 °C at 220 rpm for 5 hours. The culture was cooled to 4 °C for a period of one hour. The medium with cells was transferred to centrifuge bottles and centrifuged at 4500 rpm for 10 min. The supernatant was decanted, and centrifuge bottles with the cells stored in the freezer at -20 °C.

Recombinant cytochrome P450$_{cam}$ expressed in *E. coli* was purified to homogeneity by the method reported previously by Gunsalus and Wagner [2]. Purification consisted of the following procedure: at 4° C, lysis buffer (50 mM Tris HCl, 1 mM EDTA, 100 mM NaCl pH 7.5) is added and the cells resuspended. Cells are lysed with lysozyme (10 mg/ml) , 160 µl of lysozyme per gram of *E. coli*, 32 µl of 50 mM phenylmethylsulfonyl (PMSF) per gram of *E. coli* and 4 mg of deoxycolic acid per gram of *E. coli*. The mixture is then stirred every 5 minutes for 20 minutes, followed by equilibration at 37 °C for 20 minutes. The mixture was additionally stirred for 1 hour at room temperature. The resulting solution was sonicated and ultracentrifuged at 45000 rpm for 1 hour. The supernatant was decanted and placed inside a dialysis membrane and dialyzed against ion exchange buffer (10 mM EDTA, 50 mM Tris, pH 7.4, 1 mM Camphor). The buffer was changed several times in a 24 hour period. The dialyzed solution was applied to a DE-52 (Whatman) anion exchange column equilibrated with buffer and camphor. The protein was eluted with a linear salt gradient, 0-500 mM KCl in buffer. The brown fractions containing the cytochrome were collected and concentrated. This concentrated solution was passed through a Sephadex G-

100 column equilibrated with 100 mM KCl, 20 mM Tris, pH=7.4, and 1 mM Camphor. Camphor was separated from the protein by passing the solution through a Sephadex G-10 column equilibrated with 100 mM MOPS, pH 7.0 neutralized with Tris base. The Protein purity was determined by monitoring the ratio of absorbances A_{418}/A_{280} by electronic spectroscopy; only those chromatographic fractions exhibiting a ratio $A_{418}/A_{280} \geq 1.50$ were used in order to obtain homogeneous protein. Purified cytochrome $P450_{cam}$ was exchanged into 100.0 mM MOPS, pH 7.0 by dialysis, concentrated to approximately 0.80 mM by ultrafiltration (Y30 Diaflo ultrafiltration membranes, Amicon), aliquoted and then frozen at –20 °C. Spinach ferredoxin was purchased from Sigma and subsequently exchanged into 100 mM MOPS buffer, pH 7.0 utilizing a 10 DG disposable chromatography column (Bio-Rad Laboratories), concentrated to 1.0 mM, aliquoted and frozen at –20 °C. Polylysine with average molecular weight 3400 was purchased from Sigma and used as received.

Cyclic Voltammetry

Cyclic Voltammetry was carried out with a BAS-CV50W potentiostat (Bioanalytical Systems, West Lafayette, IN). Glass-slides (2.50 cm x 2.50 cm) coated on one side with indium-doped tin oxide (ITO) semiconductor films exhibiting a typical resistance of less than 10 ohms were purchased from Delta Technologies (Stillwater, MN) and used as working electrodes. A platinum wire auxiliary electrode and a Ag/AgCl reference electrode containing a fiber junction were purchased from Cypress Systems (Lawrence, KS). The electrochemical cell was described in the previous chapter.

The solution in the electrochemical cell was deaerated by bubbling high-purity nitrogen for 30 minutes and subsequently blanketed with nitrogen in order to maintain anaerobicity. Solutions used in the electrochemical studies were typically prepared in 100

mM MOPS, pH 7.0, and contained 100 μM spinach ferredoxin, 300 μM polylysine, and 100 to 200 μM cytochrome P450$_{cam}$ The ITO working electrode was conditioned by sonicating for 30 min in each of the following solutions: 1% alconox in deionized water, ethanol, and deionized water. The clean electrodes were subsequently dried with a stream of nitrogen and used immediately.

Gas Chromatography-Mass Spectrometry

The identity of the products generated by the catalytic activity of cytochrome P450$_{cam}$ in the electrochemical cell was determined by gas chromatography-mass spectrometry (GC-MS). To this end, the solution in the electrochemical cell was sampled with a 100 μm polydimethylsiloxane solid phase microextraction (SPME) fiber. The fiber was subsequently placed into the injection port of a Hewlett Packard (HPG 1800A) GC-MS in order to desorb the extracted material into the GC column [25].

Results and Discussion

Reversible Electrochemistry of Spinach Ferredoxin

Spinach ferredoxin is an electron transfer protein whose active site is a 2Fe-2S-Cys$_4$ cluster. Its molecular surface possesses an asymmetric distribution of acidic residues that impart a highly localized negative charge to the area on the protein surface surrounding the active site. It is well established that this highly localized negative electrostatic field on the surface of spinach ferredoxin is used for molecular recognition and electrostatic binding with physiological protein partners such as nitrite oxidoreductase, sulfite oxidoreductase and thioredoxin [17]. This type of electrostatic recognition among electron-transfer proteins has been successfully utilized in order to promote their direct electrochemistry at electrodes bearing a charge complementary to that surrounding the active site of the protein

90

[26-33] (see introductory chapter). The negative charge [34] on the surface of indium oxide electrodes was initially exploited by Yeh and Kuwana [35] in order to obtain the unmediated electrochemistry of cytochrome c, a positively charged protein. In subsequent studies, the voltammetry of negatively charged proteins has been obtained at indium oxide electrodes by addition of a polycation in order to overcome the electrostatic repulsion between the negatively charged electrode and protein surfaces [26, 36].

Typical cyclic voltammograms obtained at an indium-doped tin oxide electrode from solutions containing spinach ferredoxin and polylysine are shown in Fig. 2. By comparison, omission of polylysine or ferredoxin results in the absence of a Faradaic response, observations that are in agreement with previous reports demonstrating that the direct electrochemistry of plant ferredoxins at indium oxide electrodes is promoted by polylysine [36, 37]. Consequently, the role of polylysine as a promoter is consistent with the negative charge of the ITO electrode-surface and the highly localized negative electrostatic field surrounding the active site of spinach ferredoxin [17]. The ratio of the cathodic to anodic peak currents (i_{pc}/i_{pa}) is unity and the peak to peak separation (ΔE_p) is 60 mV. The heterogeneous electron transfer rate constant (k_s) and the diffusion coefficient (D_o) for spinach ferredoxin were obtained by simulating the cyclic voltammograms with the aid of the program Digisim (Bioanalytical Sytems), a simulator for cyclic voltammetric responses [38]. These values are 2.5×10^{-3} cm/s and 1.6×10^{-6} cm^2/s, respectively. Utilizing the Randles-Sevcik equation [42] and the method of Nicholson and Shain [53], the diffusion coefficient and the heterogeneous electron transfer rate constant for spinach ferredoxin were also determined to be 2.7×10^{-6} cm^2/s and 2.5×10^{-3} cm/s, respectively. Both of these measurements are in good agreement with each other and with previously
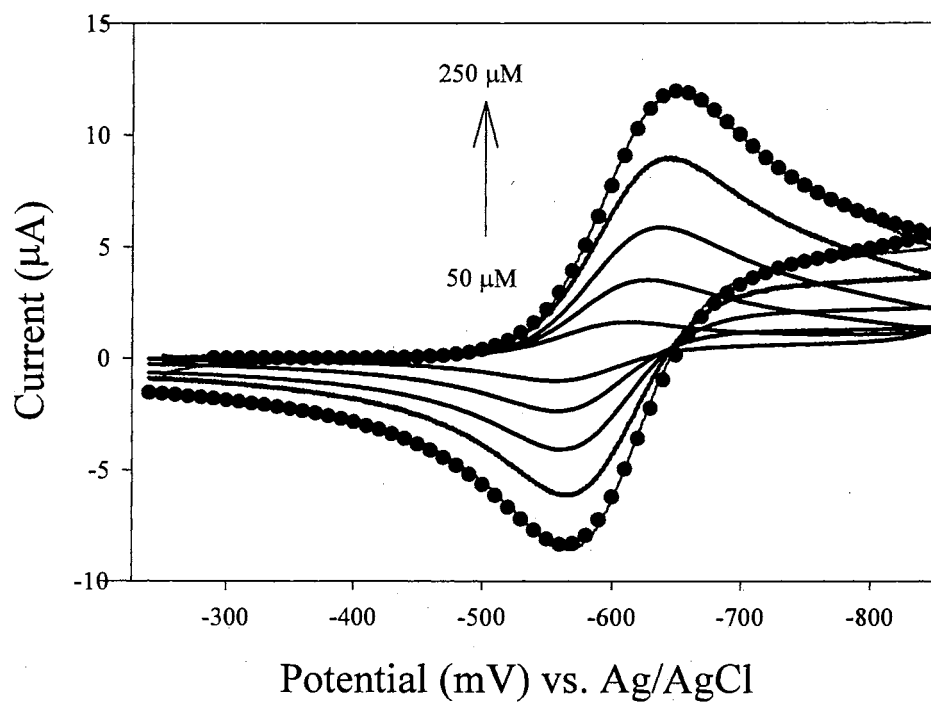
Figure 2. (____) Background subtracted cyclic voltammograms obtained at an ITO electrode from solutions containing different concentrations of spinachferredoxin and polylysine (300 μM) in 100 mM MOPS, pH 7.0. (•) Digital simulation of the experimental response with the following parameters: $k_s = 0.0025$ cm/s, D_o $Fd^{ox} = D_o$ $Fd^{red} = 1.6 \times 10^{-6}$ cm^2/s, scan rate = 20 mV/s, $\alpha = 0.50$.
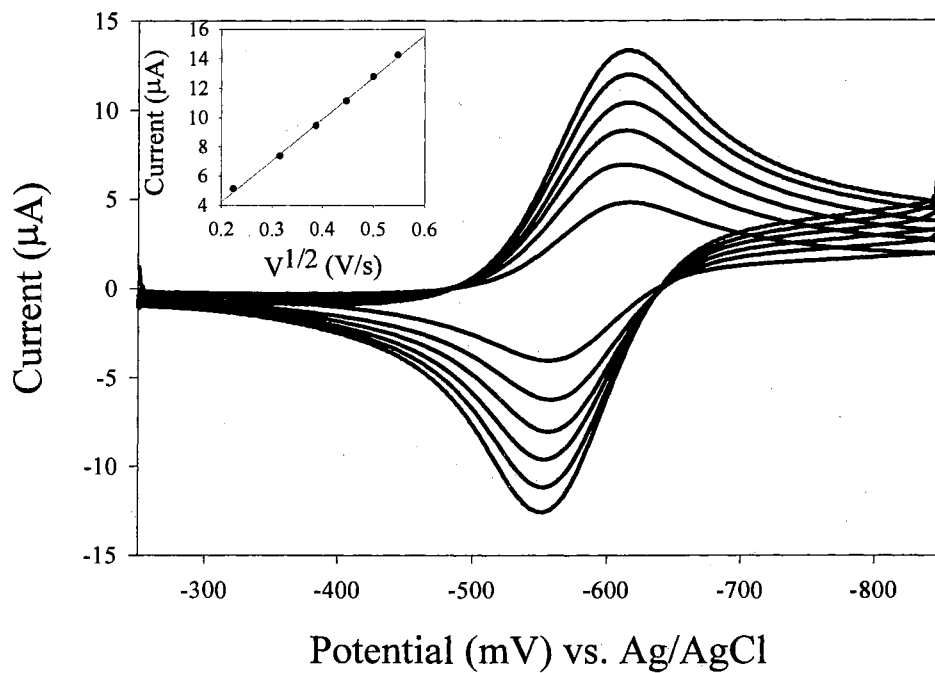
Figure 3. Background subtracted cyclic voltammograms obtained from a solution containing spinach ferredoxin (100 μM) and polylysine (300 μM) at scan rates from 50 mV/s to 300 mV/s in 50 mV/s increments. The inset displays the linear correlation between the square root of scan rate and cathodic peak current.

reported values [36, 39, 40]. The linear correlation between the square root of the scan rate and the cathodic peak current (Fig. 3) demonstrates that the electrochemical process is diffusion controlled. In the region of scan rate explored, 10 mV/s to 300 mV/s, the cathodic to anodic peak separation, ΔE_p, is 60 mV and the cathodic to anodic peak current ratio (i_{pc}/i_{pa}) is unity.

<div align="center">

Ferredoxin-Mediated Electrochemical Reduction
of Camphor-Bound Cytochrome P450$_{cam}$

</div>

The cyclic voltammogram of a solution containing an equimolar mixture of spinach ferredoxin and cytochrome P450$_{cam}$ bound to camphor is shown in Fig. 4. Two reduction peaks (-567 mV and -635 mV) are observed in the cathodic scan, and only one oxidation peak (-570 mV) is observed during the corresponding anodic scan. The peaks at -635 mV and -570 mV correspond to a reversible wave (E$_{1/2}$ = -603 mV) arising from the reduction and subsequent reoxidation of spinach ferredoxin at the electrode surface. The first reduction peak (-567 mV), which is not accompanied by its oxidation counterpart, originates from coupling the electrochemical reduction of spinach ferredoxin to a homogeneous reaction in which an electron is transferred from reduced spinach ferredoxin to camphor-bound ferric cytochrome P450$_{cam}$ [41]. Consequently, the first reduction peak, termed a pre-peak hereafter, originates from the depletion of substrate-bound ferric cytochrome P450$_{cam}$ in the diffusion layer. This sequence of events, summarized by equations 1 and 2, and shown schematically in Fig. 5, is typical of the EC mechanism [42]:

$$Fd^{ox} + e^- \underset{}{\overset{k_s}{\rightleftharpoons}} Fd^{re} \qquad (1)$$

$$Fd^{red} + P450^{ox}\text{-}S \underset{k_b}{\overset{k_f}{\rightleftharpoons}} Fd^{ox} + P450^{red}\text{-}S \qquad (2)$$

<div align="center">

94

</div>
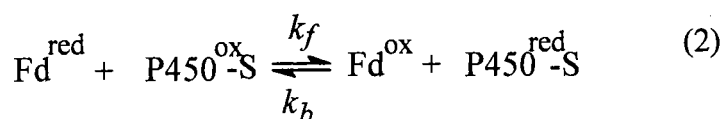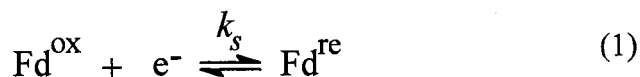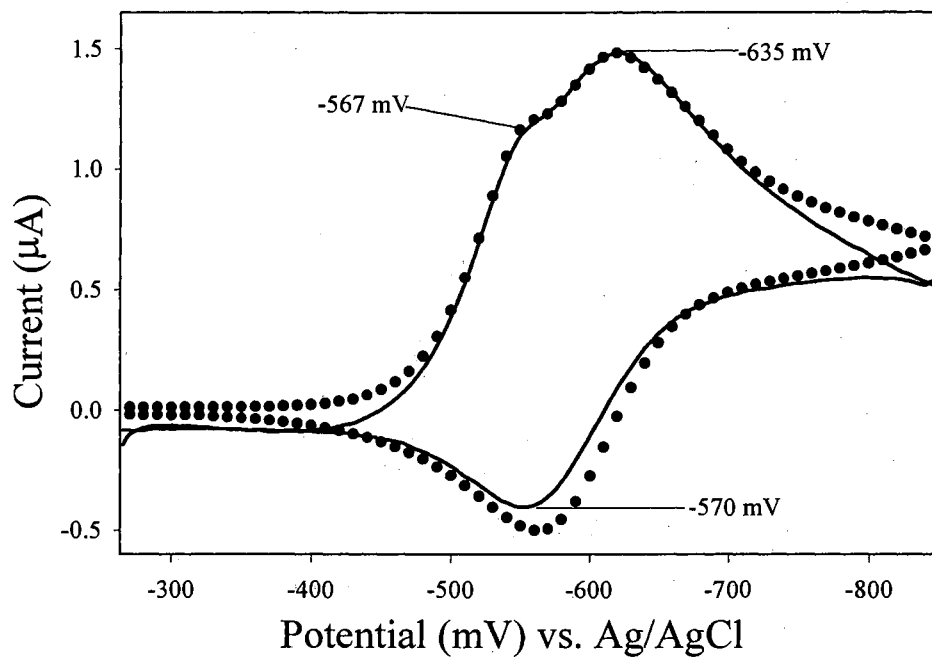
Figure 4. (___) Cyclic voltammogram obtained from a solution containing 100 μM spinach ferredoxin, 100 μM cytochrome P450$_{cam}$, 300 μM polylysine and saturated with camphor. Scan rate = 3 mV/s. (•) Simulated cyclic voltammogram invoking the mechanism shown by equations 1 and 2. Parameters for simulation are shown in Table 1.
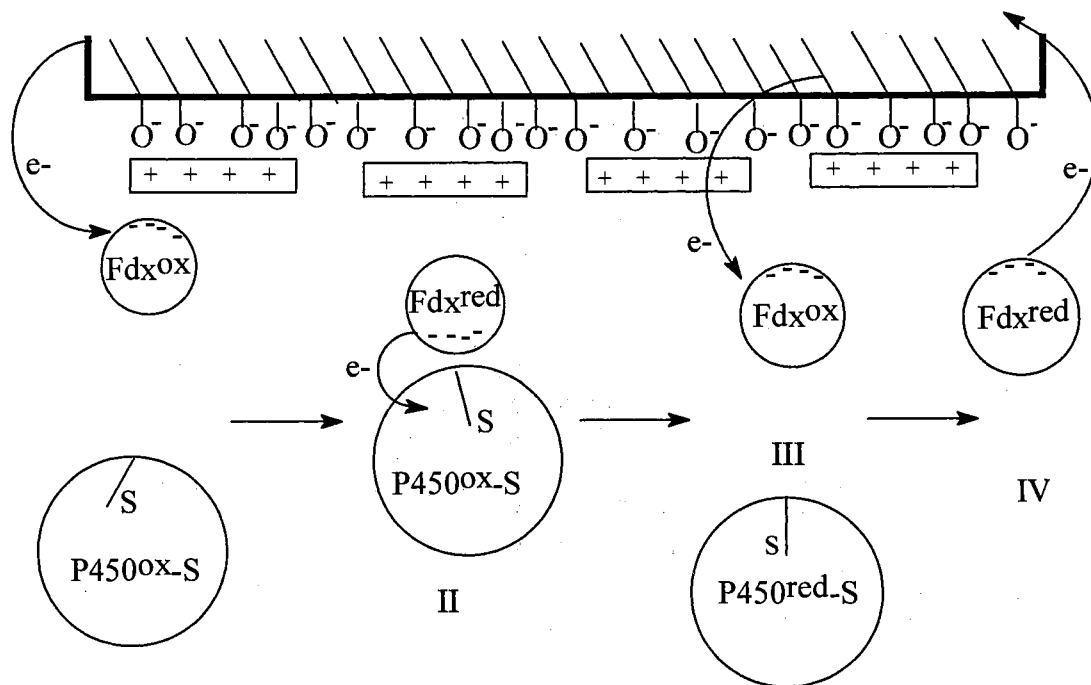
Figure 5. Schematic representation of the sequence of electron transfer reactions that give rise to the electrochemical response shown in Fig. 4. (I) Selective electrochemical reduction of spinach ferredoxin in the presence of cytochrome $P450_{cam}$. (II) Oxidation of spinach ferredoxin by substrate-bound cytochrome $P450_{cam}$. This reaction gives rise to the depletion of camphor-bound ferric cytochrome $P450_{cam}$ in the diffusion layer and consequently to the pre-peak shown in Fig. 4. (III) Electrochemical depletion of oxidized spinach ferredoxin that gives rise to the main cathodic peak seen in the voltammogram shown in Fig. 4. (IV) Electrochemical reoxidation of spinach ferredoxin that results in the anodic peak in Fig. 4.

96

In equation 1, Fd^{ox} and Fd^{red} represent oxidized and one-electron reduced spinach ferredoxin, respectively, and k_s represents the corresponding heterogeneous electron-transfer rate constant. In equation 2, $P450^{ox}$-S and $P450^{red}$-S represent ferric and ferrous substrate-bound cytochrome $P450_{cam}$, respectively; k_f and k_b are the corresponding forward and backward second-order electron transfer rate constants. The mechanism summarized by equations 1 and 2 was digitally simulated using the program Digisim 2.1; the simulated and experimental cyclic voltammograms are depicted in Fig. 4 and the parameters obtained from the simulation are listed in Table 1. The agreement between the experimental and simulated responses indicates that the pre-peak in the voltammogram shown in Fig. 4 originates from the depletion of oxidized camphor-bound cytochrome $P450_{cam}$ in the diffusion layer. The depletion of the latter is a consequence of a homogeneous electron transfer reaction between electro-reduced spinach ferredoxin and oxidized camphor-bound cytochrome $P450_{cam}$, as indicated by equation 2.

The values for the heterogeneous electron transfer rate constant and the diffusion coefficient of spinach ferredoxin utilized in this simulation (Table 1) were obtained experimentally from cyclic voltammograms of solutions containing only spinach ferredoxin and polylysine (see Fig. 2). This strategy permits the evaluation of the second order rate constant (k_f) for the transfer of one electron from reduced spinach ferredoxin to camphor-bound ferric cytochrome $P450_{cam}$ with a higher degree of confidence.

Additional evidence, corroborating that the pre-peak in the voltammogram shown in Fig. 4 originates from a homogeneous second order electron transfer reaction in which reduced spinach ferredoxin (generated at the electrode surface) transfers an electron to camphor-bound cytochrome $P450_{cam}$, was obtained as follows: A solution saturated with

Table 1

Parameters for digital simulation of the catalytic response obtained from a mixture containing spinach ferredoxin, cytochrome $P450_{cam}$ and substrate

Substrate	Camphor	Hexachloroethane
$E^{o'}$ (*vs* Ag/AgCl)	-0.605	-0.605
Transfer Coefficient, α	0.50	0.50
k_s (cm/s)	$2.5 \times 10^{-3} \pm 2 \times 10^{-5}$	2.5×10^{-3}
k_f	$1.5 \times 10^{5} \pm 2 \times 10^{4}$	
k_b	4.5	
k_{f1} (M^{-1} s^{-1})		2.1×10^{7}
k_{b1} (M^{-1} s^{-1})		1.5
k_{f2} (M^{-1} s^{-1})		$1.0 \times 10^{5} \pm 3 \times 10^{4}$
k_{b2} (M^{-1} s^{-1})		13.3
k_{f3} (M^{-1} s^{-1})		$1.2 \times 10^{4} \pm 2 \times 10^{3}$
k_{b3} (M^{-1} s^{-1})		5.5
k_{f4} (s^{-1})		$1.5 \times 10^{-2} \pm 3 \times 10^{-3}$
k_{b4} (s^{-1})		2.0
Anal. Conc. Fd^{ox} (μM)	100.0	130.0
D_o Fd^{ox} ($cm^2 s^{-1}$)	$1.6 \times 10^{-6} \pm 4 \times 10^{-7}$	2.0×10^{-6}
D_o Fd^{red} ($cm^2 s^{-1}$)	$1.6 \times 10^{-6} \pm 4 \times 10^{-7}$	2.0×10^{-6}
Anal Conc. $P450^{ox}$ (μM)	100.0	230.0
D_o $P450^{ox}$ ($cm^2 s^{-1}$)	$5.6 \times 10^{-7} \pm 8 \times 10^{-8}$	6.3×10^{-7}
D_o $P450^{red}$ ($cm^2 s^{-1}$)	$5.6 \times 10^{-7} \pm 8 \times 10^{-8}$	6.3×10^{-7}

camphor and containing spinach ferredoxin and polylysine was titrated with cytochrome P450$_{cam}$. The results of this titration, summarized in Fig. 6, show that in the absence of cytochrome P450$_{cam}$ the voltammogram of spinach ferredoxin is devoid of a pre-peak. Addition of cytochrome P450$_{cam}$ to the original solution, however, results in the presence of a pre-peak whose intensity increases with increasing concentrations of cytochrome P450$_{cam}$. This observation is consistent with the idea that the pre-peak originates from the depletion of oxidized cytochrome P450$_{cam}$ in the diffusion layer, as described by equation 2. In a different experiment, a solution saturated with camphor and containing polylysine and cytochrome P450$_{cam}$ was titrated with spinach ferredoxin. The results of this experiment, summarized in Fig. 7, clearly indicate that in the absence of spinach ferredoxin, the voltammetric response originating from the mixture does not produce a Faradaic current. Addition of spinach ferredoxin to the original mixture results in the characteristic voltammogram consisting of a pre-peak and a reversible wave. Moreover, the magnitude of the current for the cathodic and anodic peaks corresponding to the reversible wave increases as the concentration of ferredoxin is increased, consistent with the idea that the reversible wave originates from the reduction and oxidation of ferredoxin at the electrode surface. By comparison, the magnitude of the current corresponding to the pre-peak does not change, which is consistent with the fixed concentration of cytochrome P450$_{cam}$ during the titration experiment.

In order to satisfy the requirements for the EC mechanism [42-44], the reduction of P450^{ox}-S at the electrode surface has to be much slower than the forward homogeneous second-order reaction in equation 2, therefore resulting in the negligible reduction of P450^{ox}-S at the electrode surface. The discrimination of biomolecules at electrode surfaces

leading to the EC mechanism has been reported for a mixture of cytochrome b_5 and cytochrome c. [45]. In the case of a system containing these two electron transfer proteins, a gold electrode modified with β-mercaptopropionate was shown to be selective for the positively charged cytochrome c. On the other hand, the addition of polylysine to the system resulted in the selective reduction of the negatively charged cytochrome b_5 ($E^{o'} = -100$ mV), in the presence of cytochrome c ($E^{o'} = 250$ mV). This electrostatic discrimination of biomolecules at the electrode surface resulted in a voltammogram exhibiting a pre-peak and a reversible wave [45]. Accordingly, the presence of a pre-peak in the cyclic voltammogram shown in Fig. 4 demonstrates that although camphor-bound $P450^{ox}$ is thermodynamically more easily reducible ($E^{o'} = -176$ mV vs NHE) than spinach ferredoxin ($E^{o'} = -420$ mV vs NHE), the former appears not to interact with the electrode in an orientation that facilitates heterogeneous electron exchange (see above). It is therefore interesting to explore if the discrimination of cytochrome $P450_{cam}$ at the electrode surface may also originate from unfavorable electrostatic interactions with the electrode. To this end, it is useful to visualize the Poisson-Boltzmann (PB) calculations initially reported by Roitberg et al.[46] for cytochrome $P450_{cam}$ (Fig. 8A and B) and from similar calculations performed on spinach ferredoxin (PDB ID: 1A70) [52] for the purposes of this study (Fig. 8C and D). The results of the PB calculation are readily interpreted by representing the negative electrostatic potential in red, and the positive electrostatic potential in blue. The surface on the "front-side" (nearest the active site), the position of the outermost cysteine ligands to the Fe_2S_2 cluster (Cys 44 and Cys 39) has been highlighted in order to show the relative position of the active site, of spinach ferredoxin (Fig. 8C) reveals the presence of a unique contiguous patch of negative electrostatic potential (red contour at −9 kcal/mol e). By comparison, the
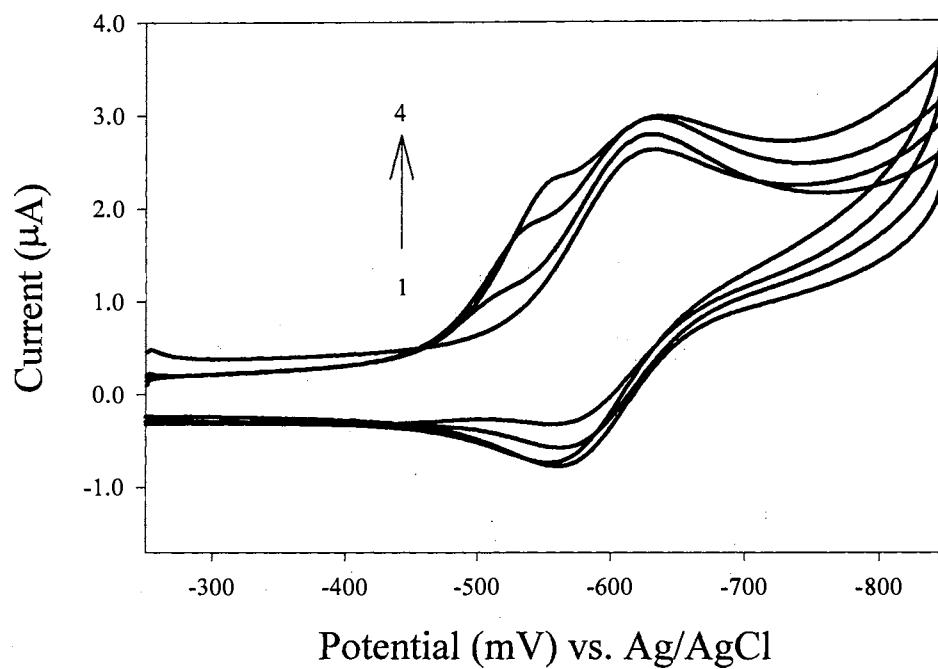
Figure 6. Titration of a solution containing spinach ferredoxin (100 μM) and polylysine (300 μM) in MOPS (100 mM) saturated with camphor (pH 7.0) with cytochrome $P450_{cam}$. (1) Voltammogram obtained in the absence of cytochrome $P450_{cam}$. (2-4) Voltammogram after the addition of cytochrome $P450_{cam}$ to a final concentration of 30 μM, 60 μM and 100 μM, respectively.
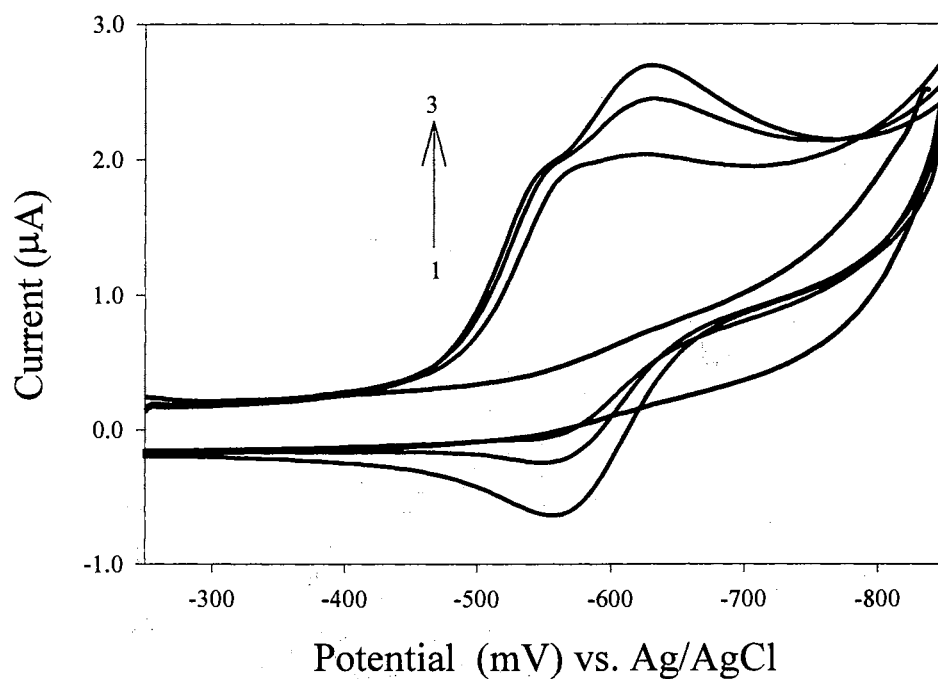
Figure 7. Titration of a solution containing cytochrome $P450_{cam}$ (100 μM) and polylysine (300 μM) in 100 mM MOPS saturated with camphor (pH 7.0) with spinach ferredoxin. (1) Voltammogram obtained in the absence of spinach ferredoxin. (2-4) Voltammograms obtained after the addition of spinach ferredoxin to a final concentration of 50 μM, 75 μM and 100 μM. Scan rates for all voltammograms = 3 mV/s.
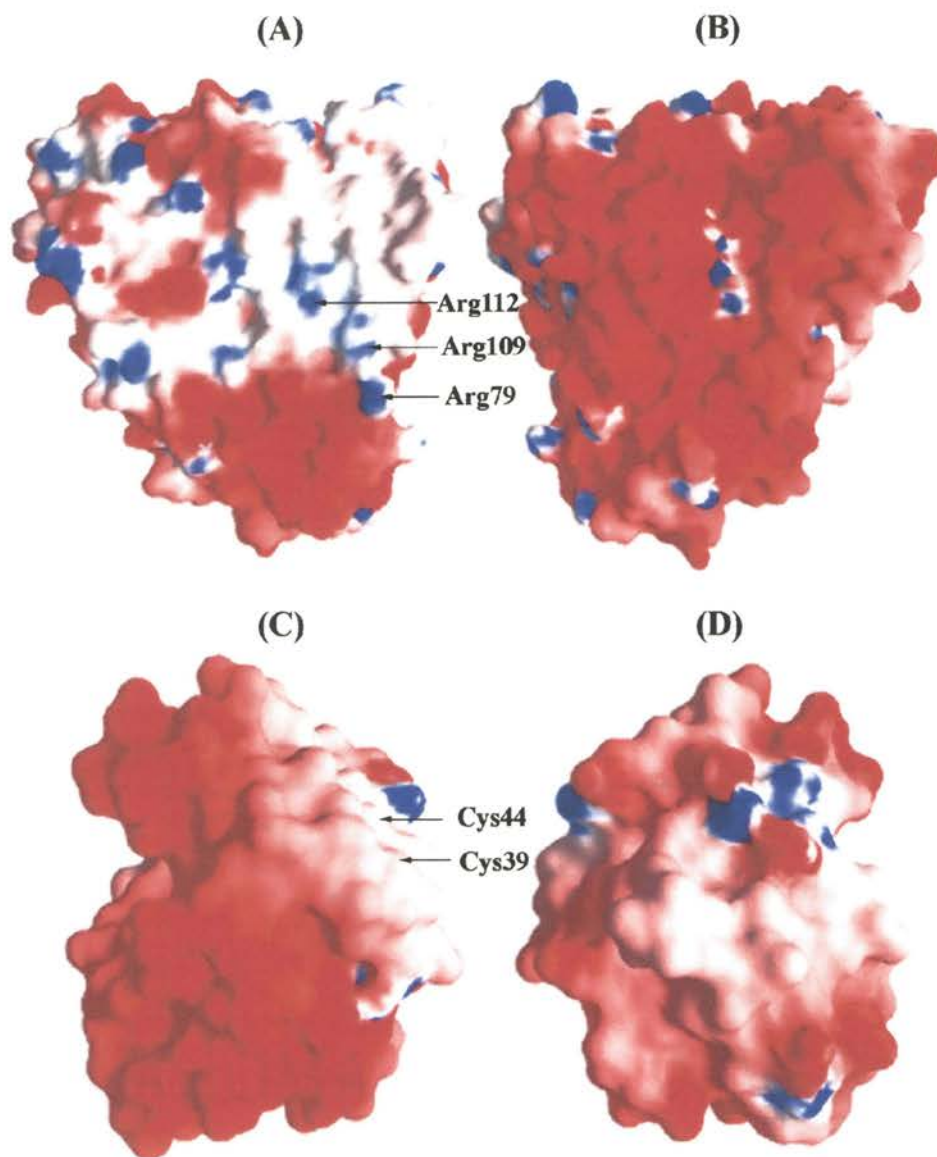
Figure 8. Results of the Poisson Boltzmann electrostatic calculations represented with red contour plots = –9 kcal/mol e and blue contour plots = +9 kcal/mol e. (A). Front side of cytochrome P450$_{cam}$ (B) View obtained by rotating (A) by 180° about the vertical axis of the page. (C) Front side of spinach ferredoxin (D) This view, obtained by rotating (C) 180° degrees about the vertical axis of the page.

protein's "back-side" (Fig. 8 D), which is obtained by rotating the view shown in Fig. 8C by 180° about the vertical axis of the page, shows a surface with a positive to neutral electrostatic potential. It is therefore possible to infer that the negative electrostatic potential on the "front side" of spinach ferredoxin and the positive electrostatic potential imparted by polylysine to the electrode surface, steer the protein towards the electrode with an orientation close to optimum for heterogeneous electron exchange. By comparison, previous work performed with cytochrome $P450_{cam}$ (PDB ID: 1NOO) [51] resulted in the identification of a cluster of positively charged residues (Arg-79, Arg-109, Arg-112) that were postulated to encompass the site on the surface of cytochrome $P450_{cam}$ that is utilized for binding with putidaredoxin [47]. Results obtained from Poisson-Boltzmann calculations have shown that this cluster of amino acids produce discrete patches of positive potential (blue in Fig. 8A) on the "front side" of cytochrome $P450_{cam}$, near its heme active site [46]. Visualization of the surface on the "back-side" of cytochrome $P450_{cam}$ (Fig. 8B) demonstrates the presence of a large contiguous patch of negative electrostatic potential.

The PB calculations performed for cytochrome $P450_{cam}$ (Fig. 8A and B) suggest that in the absence of polylysine the positive potential on the "front side" of cytochrome $P450_{cam}$ may steer the enzyme toward the negatively charged ITO electrode with an orientation appropriate for fast heterogeneous electron exchange. On the other hand, the presence of polylysine in the electrochemical cell may steer the enzyme toward the electrode surface with an orientation that is non-productive for heterogeneous electron exchange. Alternatively, cytochrome $P450_{cam}$ may not interact productively with the electrode even in the absence of polylysine. In order to discern among these alternatives, cyclic voltammetric experiments of solutions containing cytochrome $P450_{cam}$ were carried out in the presence and in the

absence of polylysine. Non Faradaic responses were obtained in both cases. Consequently, it is possible to conclude that in the system consisting of polylysine, spinach ferredoxin and cytochrome $P450_{cam}$, the presence of polylysine in the electrochemical cell guarantees that the protein with the more negative reduction potential (spinach ferredoxin) is readily reduced at the electrode surface. Reduced spinach ferredoxin, in turn, is oxidized by the enzyme possessing a more positive reduction potential (camphor-bound ferric cytochrome $P450_{cam}$) in a homogeneous reaction. The usefulness of this approach to harness the catalytic activity of cytochrome $P450_{cam}$ is described in the next section.

The catalytic cycle (Fig. 1), of cytochrome $P450_{cam}$ requires the stepwise uptake of two electrons by the enzyme [1]. It is also known that carbon monoxide readily binds to the heme iron of reduced camphor-bound cytochrome $P450_{cam}$, therefore inhibiting the uptake of a second electron by the enzyme [48]. This phenomenon was utilized in order to corroborate that the electrochemical response shown in Fig. 4 corresponds exclusively to the transfer of one electron from spinach ferredoxin to ferric camphor-bound cytochrome $P450_{cam}$. To this end, the voltammetric experiments were conducted under an atmosphere of carbon monoxide (CO) instead of an atmosphere of N_2. The voltammogram obtained from an equimolar mixture of spinach ferredoxin and camphor-bound cytochrome $P450_{cam}$ under an atmosphere of CO is identical to the one obtained under an atmosphere of N_2 (Fig. 4). This observation supports the idea that the electrochemical response shown in Fig. 4 corresponds to the transfer of one electron from reduced spinach ferredoxin to oxidized camphor-bound cytochrome $P450_{cam}$, as indicated by equation 2.

Ferredoxin Mediated Electrocatalytic Reductive Dehalogenation Reactions
Performed by Cytochrome P450$_{cam}$

The cyclic voltammogram obtained from a solution containing a mixture of spinach ferredoxin and cytochrome P450$_{cam}$ in the absence of substrate is shown in Fig. 9a. This voltammogram is identical to that obtained from a solution containing only spinach ferredoxin at the same concentration, hence indicating that reduced spinach ferredoxin does not readily reduce substrate-free ferric cytochrome P450$_{cam}$. This observation is interesting in light of the favorable driving force imparted by the relative reduction potentials of spinach ferredoxin (–420 mV *vs* NHE) [18,19] and substrate-free cytochrome P450$_{cam}$ (-300 mV)[1]. In contrast, when the cyclic voltammetric experiments are carried out with a solution containing a mixture of spinach ferredoxin, cytochrome P450$_{cam}$ and the substrate hexachloroethane (1:2:2), under anaerobic conditions, the catalytic response shown in Fig. 9b is obtained. This electrochemical response originates from the ferredoxin mediated electrocatalytic reductive dehalogenation of hexachloroethane to tetrachloroethylene carried out by cytochrome P450$_{cam}$ (see below). This conclusion is in agreement with previous studies carried out with *Pseudomonas putida* G786 , which presented convincing evidence that cytochrome P450$_{cam}$ in *Pseudomonas putida* catalyzes reductive dehalogenation reactions for a variety of halogenated hydrocarbons [8,10]. Subsequent studies performed *in vitro* with isolated cytochrome P450$_{cam}$ reconstituted with NADH, putidaredoxin reductase and putidaredoxin, convincingly demonstrated that cytochrome P450$_{cam}$ is capable of catalyzing the reductive dehalogenation of polychlorinated methanes and ethanes [11,21].

In order to obtain additional information concerning the nature of the catalytic reaction giving rise to the electrochemical response shown in Fig. 9b, the following sequence
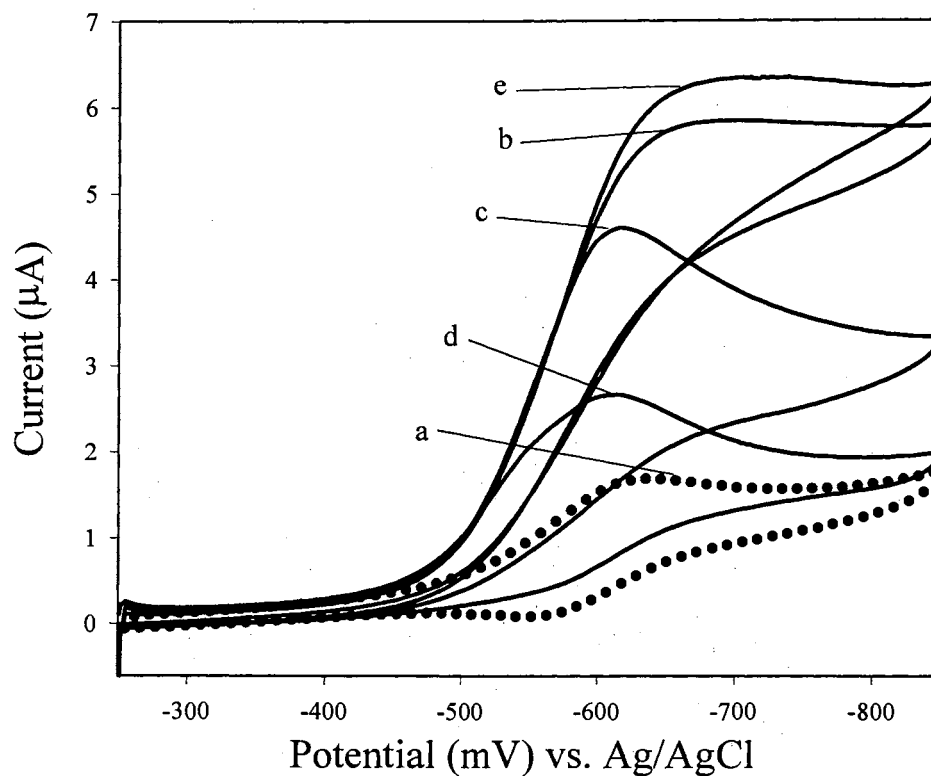
Figure 9. Cyclic voltammograms obtained with a scan rate of 1 mV/s at an ITO electrode: (a) 100 µM spinach ferredoxin, 200 µM cytochrome P450$_{cam}$ and 300 µM polylysine, (b) first scan after the addition of hexachloroethane to the solution in a, (c) second scan after the addition of hexachloroethane, (d) third scan after the addition of hexachloroethane, (e) first scan after the second addition of hexachloroethane to the solution in d.

of experiments was performed: A cyclic voltammogram was initially obtained with a mixture containing only spinach ferredoxin and cytochrome $P450_{cam}$ (Fig. 9a). Addition of hexachloroethane to the electrochemical cell followed by scanning the potential produce the expected catalytic response (Fig. 9b). Subsequent scans give rise to the cyclic voltammograms shown in Fig 9c and d. The progressive decrease in the limiting current with each subsequent potential scan originates from the consumption of substrate (hexachloroethane) by the catalytic action of cytochrome $P450_{cam}$. Addition of more hexachloroethane to the solution contained in the electrochemical cell, followed by scanning the potential gives rise to a voltammogram (Fig. 9e) almost identical to the one obtained after the first addition of substrate (Fig. 9a). Subsequent scanning of the potential after the second addition of substrate result in electrochemical responses similar to those in Fig 9c and d. In fact, the process of adding hexachloroethane in order to perform its electrocatalytic conversion to tetrachloroethylene can be repeated at least four times (approximately 7 h) without deterioration of the electrochemical response, if the temperature of the cell is maintained at 13 °C. If the temperature of the cell is kept above 20 °C the catalytic current gradually shifts cathodically with each subsequent addition of hexachloroethane and is no longer discernible after the third addition of substrate (approximately 3.5 h). It is likely that the decreased stability of the electrochemical response at temperatures above 20 °C is related with the long-term stability of the proteins.

A GC-MS analysis of the solution contained in the electrochemical cell corroborated that the product of the catalytic activity of cytochrome $P450_{cam}$ is tetrachloroethylene. Furthermore, GC-MS analysis of the electrolyzed solution as a function of time demonstrates that as the concentration of hexachloroethane decreases the concentration of

108

tetrachloroethylene increases (Fig. 10). Additional evidence demonstrating the connection between the electrochemical response and the catalytic current is shown in Fig. 11, which shows that the catalytic current is proportional to the concentration of substrate (hexachloroethane) in the electrochemical cell. In this plot, the current measured in the absence of hexachloroethane is due to the reduction of spinach ferredoxin, as discussed above (Fig. 9a). It should also be pointed out that similar results are obtained with pentachloroethane as substrate, except that the product of reductive dehalogenation is trichloroethylene. Figure 12 shows the catalytic response obtained in the presence of pentachloroethane. The following control experiments were carried out in order to provide additional evidence that the catalytic reductive dehalogenation of hexachloroethane in the electrochemical cell is carried out by cytochrome $P450_{cam}$ with electrons provided by the ITO electrode via spinach ferredoxin. Omission of ferredoxin from the electrochemical cell resulted in the absence of a Faradaic response, whereas the omission of cytochrome $P450_{cam}$ resulted in a Faradaic response identical to that seen with experiments containing only spinach ferredoxin (see Fig. 2). Furthermore, GC-MS analysis performed on the solutions utilized for these control experiments after the potential had been cycled three times demonstrated a non-detectable concentration of tetrachloroethylene. Experiments with solutions containing only polylysine and hexachloroethane resulted in the absence of Faradaic response. GC-MS analysis of these solutions after three potential cycles showed the presence of only hexachloroethane. Identical results were obtained when polylysine, spinach ferredoxin and cytochrome $P450_{cam}$ were omitted.

Digital Simulation of The Electrocatalytic Response

The reductive dehalogenation of hexachloroethane to produce tetrachloroethylene and

109
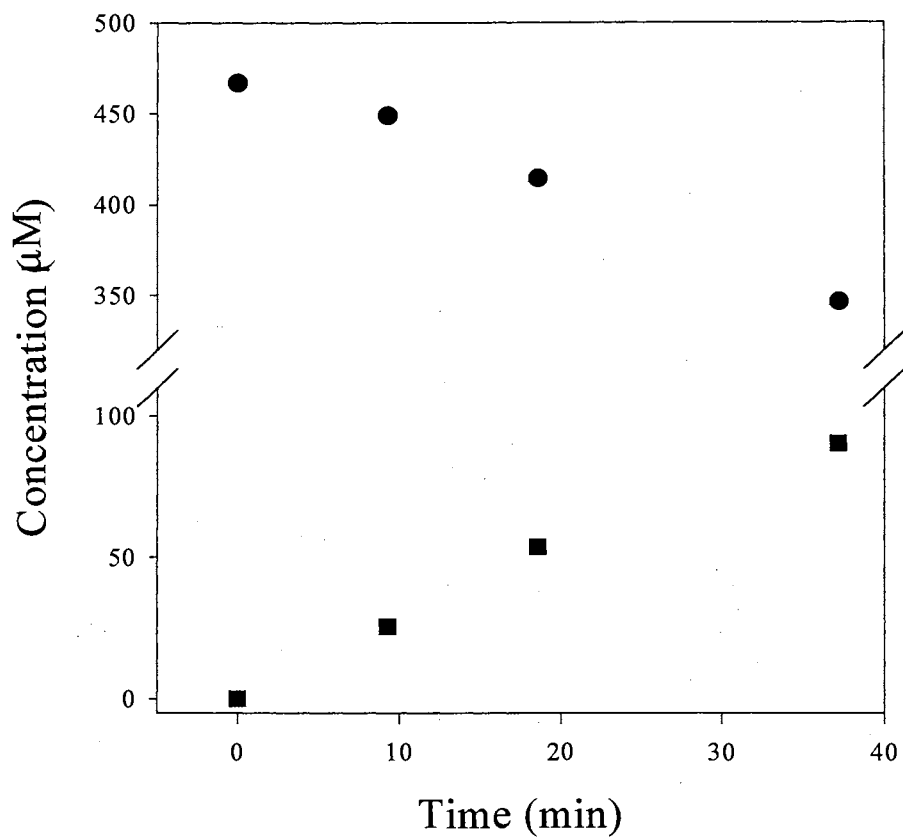
Figure 10. GC-MS analysis of the solution (100 μM spinach ferredoxin, 200 μM cytochrome P450$_{cam}$, 300 μM polylysine and 470 μM hexachloroethane) contained in the electrochemical cell as a function of electrolysis time. (circles) hexachloroethane, (square) tetrachloroethylene.
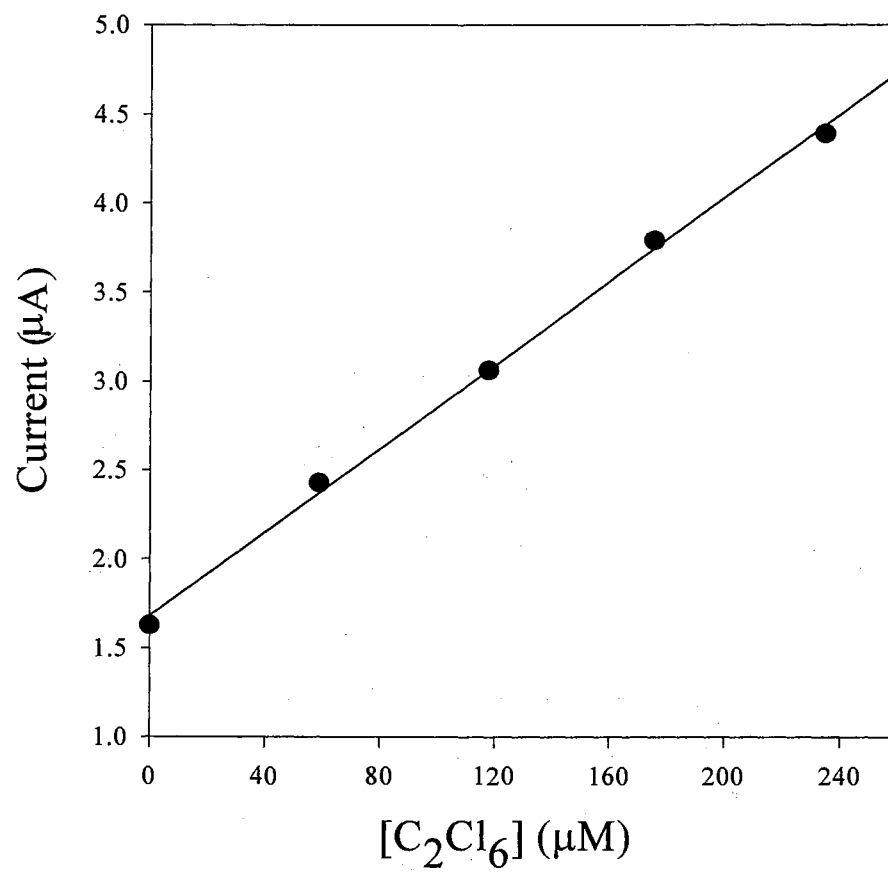
Figure 11. Limiting current as a function of the concentration of substrate (hexachloroethane).
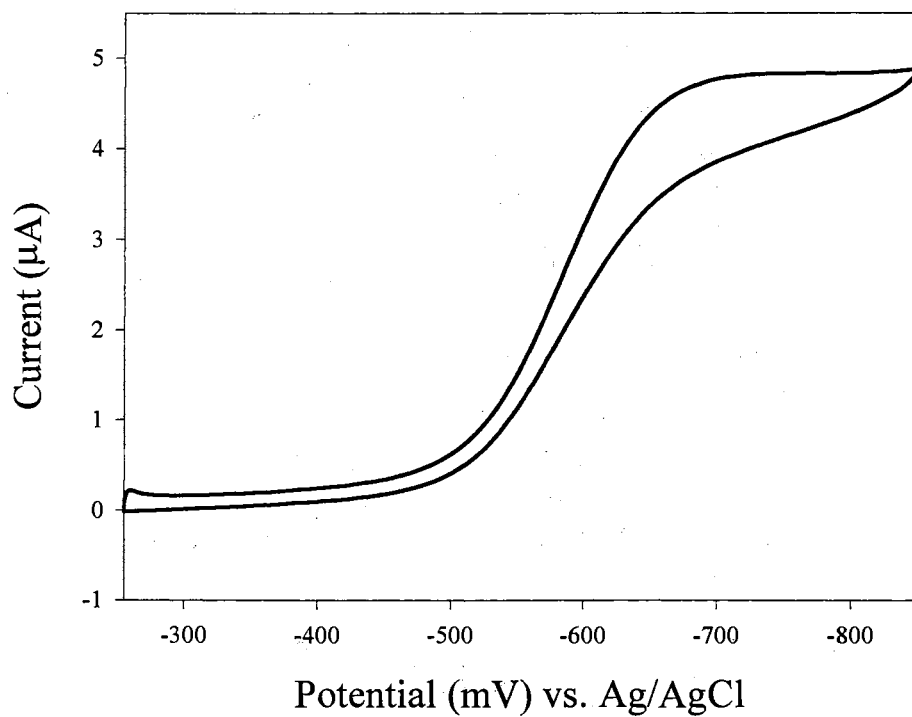
Figure 12. Background subtracted cyclic voltammogram obtained at an ITO electrode with a solution 100 μM in spinach ferredoxin, 200 μM in cytochrome P450$_{cam}$, 300 μM in polylysine and saturated with pentachloroethane.
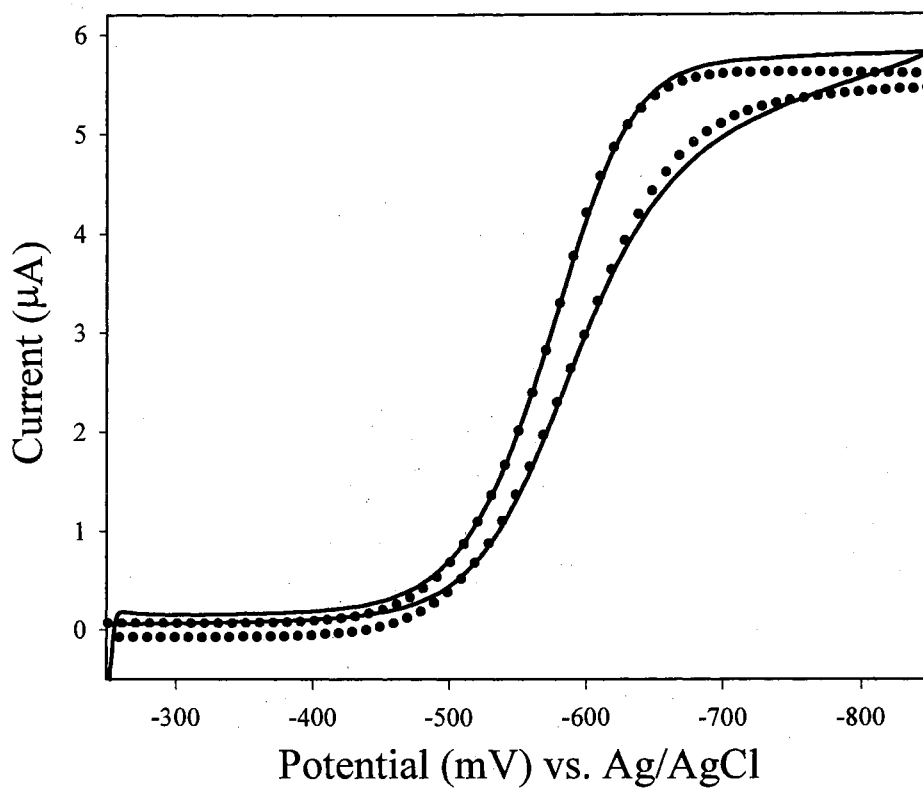
Figure 13. (——) Background subtracted cyclic voltammogram obtained at an ITO electrode with a solution 100 μM in spinach ferredoxin, 200 μM in cytochrome P450$_{cam}$, 300 μM in polylysine and saturated with hexachloroethane. (•) Simulated cyclic voltammogram obtained by invoking the catalytic cycle shown by equations 3-7. Parameters for simulation are shown in Table 1.
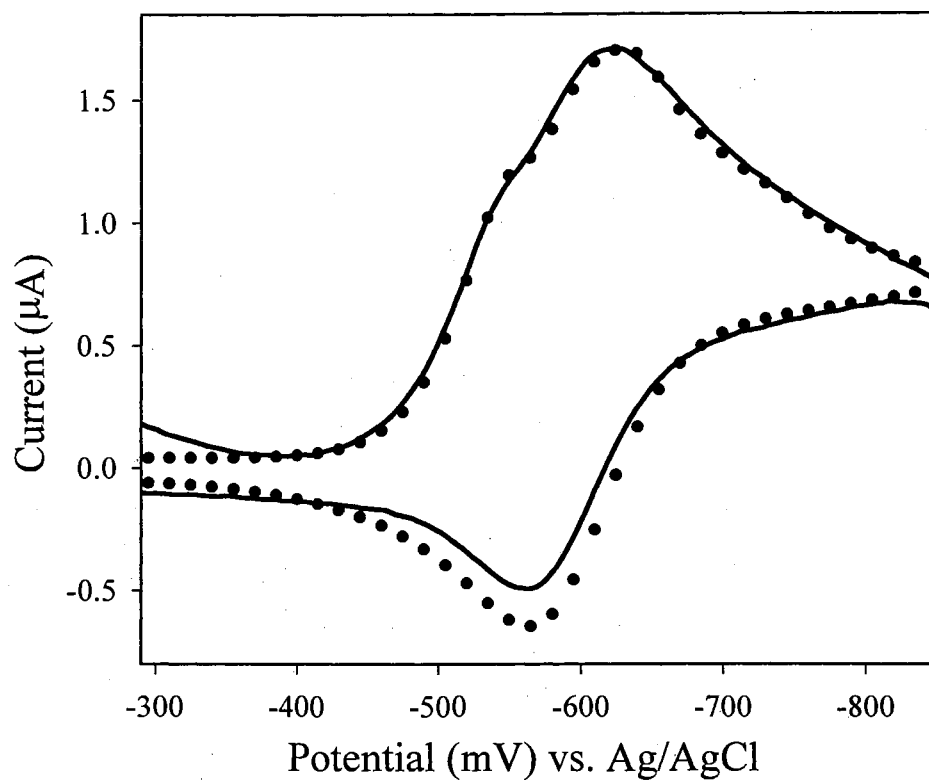
Figure 14. Background subtracted cyclic voltammogram obtained with conditions identical to Figure 12 under an atmosphere of CO. (•) Simulated cyclic voltammogram obtained by invoking the mechanism described by equation 1 and 2.

two chloride ions requires two electrons. In the electrochemical cell, these electrons are shuttled from the ITO electrode to hexachloroethane-bound cytochrome $P450_{cam}$ by spinach ferredoxin in two distinct electron transfer reactions; ferrous substrate-bound cytochrome $P450_{cam}$, in turn, transfers the electrons to hexachloroethane. Assuming that the transfer of an electron from ferrous cytochrome $P450_{cam}$ to its bound substrate is faster than the reduction of substrate-bound ferric cytochrome $P450_{cam}$ by spinach ferredoxin, the minimum mechanism summarized by equations 3-7 was utilized to simulate the catalytic response in Fig. 13. In this mechanism, Fdx^{ox} and Fdx^{red} represent oxidized and reduced spinach ferredoxin, respectively. $P450^{ox}$-S represents ferric cytochrome $P450_{cam}$ bound to substrate, cytochrome $P450^{red}$-S represents ferrous cytochrome P450 bound to substrate, and cytochrome $P450^{ox}$-P represents ferric cytochrome $P450_{cam}$ bound to product.

$$Fd^{ox} + e^- \underset{}{\overset{k_s}{\rightleftharpoons}} Fd^{red} \qquad (3)$$

$$P450^{ox} + S \underset{k_{b1}}{\overset{k_{f1}}{\rightleftharpoons}} P450^{ox}\text{-}S \qquad (4)$$

$$Fd^{red} + P450^{ox}\text{-}S \underset{k_{b2}}{\overset{k_{f2}}{\rightleftharpoons}} Fd^{ox} + P450^{red}\text{-}S \qquad (5)$$

$$Fd^{red} + P450^{red}\text{-}S \underset{k_{b3}}{\overset{k_{f3}}{\rightleftharpoons}} Fd^{ox} + P450^{ox}\text{-}P \qquad (6)$$

$$P450^{ox}\text{-}P \underset{k_{b4}}{\overset{k_{f4}}{\rightleftharpoons}} P450^{ox} + P \qquad (7)$$
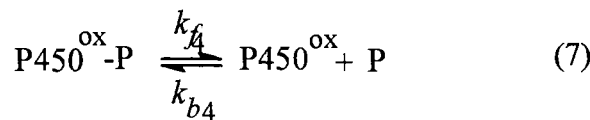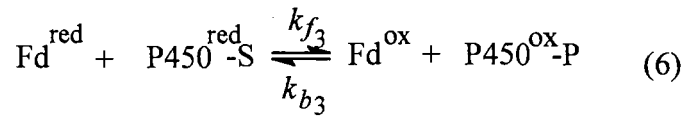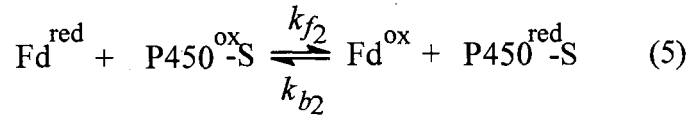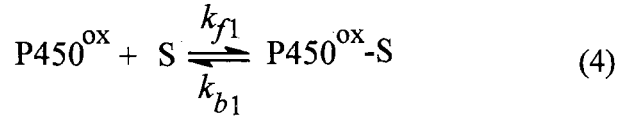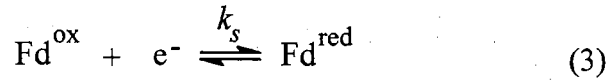
The parameters used to obtain the simulated catalytic response shown in Fig. 9A are summarized in Table 1. Several of these parameters were obtained independently by performing the following experiments: (a) The values corresponding to the heterogeneous electron transfer rate constant (k_s) and to the diffusion coefficient of spinach ferredoxin were obtained from cyclic voltammetric experiments carried out with solutions containing only this protein (see Fig. 2); (b) The values corresponding to the rate constant for the first electron transfer from reduced spinach ferredoxin to hexachloroethane-bound ferric cytochrome $P450_{cam}$ (k_{f2}), and to the diffusion coefficient of cytochrome $P450_{cam}$ were obtained from experiments carried out with solutions containing spinach ferredoxin, cytochrome $P450_{cam}$ and hexachloroethane under an atmosphere of CO. Under these conditions, the electron transfer step from reduced ferredoxin to $P450^{ox}$-S is manifested in the appearance of a pre-peak in the corresponding cyclic voltammogram (Fig 14). By comparison, electron transfer between reduced spinach ferredoxin and $P450^{ox}$ in the absence of substrate does not take place at a discernible rate (see above). Furthermore, the presence of an oxidation peak in the anodic scan shown in Fig. 14 indicates that reduced spinach ferredoxin is oxidized at the electrode surface, thus providing additional evidence for the inhibition of catalytic activity produced by CO. Consequently, the digital simulation of the voltammogram shown in Fig. 13 provides an independent measurement of the second order electron transfer rate constant for the oxidation of spinach ferredoxin by hexachloroethane-bound cytochrome $P450_{cam}$.

Utilizing the independently measured constants, k_s, k_{f2}, and the diffusion coefficient values obtained previously, the digital simulation of the catalytic response (Fig.13) permits evaluation of the constants, k_{f3} and k_{f4}, with a relatively high degree of confidence. The results

of this simulation, summarized in Table 1, indicate that the rate constant for the transfer of the second electron from reduced spinach ferredoxin to hexachloroethane-bound cytochrome P450$_{cam}$ (k_{f3}) is approximately 8 times smaller than the rate constant for the transfer of the first electron (k_{f2}). It is also interesting to note that the analysis described above indicates that the rate-limiting step in the catalytic conversion of hexachloroethane to tetrachloroethylene is the release of the latter from the catalytic site in cytochrome P450$_{cam}$, as indicated by the value of k_{f4}. In support of this idea, it is known that hexachloroethane binds to the catalytic site in cytochrome P450$_{cam}$ with a binding affinity slightly larger than that measured for camphor [21]. Furthermore, the binding of hexachloroethane also results in the concomitant trigger of the well documented [1] spin shift from $S = 1/2$ to $S = 5/2$ that accompanies the dehydration of the distal heme site in cytochrome P450$_{cam}$ [21]. The product of reductive dehalogenation (tetrachloroethylene), therefore, is formed inside the catalytic site of cytochrome P450$_{cam}$ and must egress from it before a new molecule of hexachloroethane is admitted in order to initiate a new catalytic cycle. The insights gained from digital simulation of the catalytic response indicate that tetrachloroethylene egress from the active site appears to proceed relatively more slowly than any of the previous steps in the mechanism, therefore suggesting that this step regulates the overall rate of reductive dehalogenation. Rate-limiting product release in the catalytic activity of cytochrome P450$_{cam}$ has been previously proposed for the oxidation of toluene to benzyl alcohol on the basis of kinetic deuterium isotope effect studies [49]. Finally, it is also interesting to point out that the value of the rate constant for the formation of the hexachloroethane complex of cytochrome P450$_{cam}$ is very similar to that measured for the binding of camphor to cytochrome P450$_{cam}$ (2.5×10^7 M^{-1} s^{-1})[50].

Tetrachloroethylene as Substrate

As mentioned previously, an important early step in the cytochrome P450$_{cam}$ hydroxylation reaction cycle is the binding of substrate, which triggers the consequent conversion of the heme iron from a low-spin to a high-spin state [1]. The change in spin state is thought to result from expelling water, including the water molecule coordinated to the heme iron, from the distal heme cavity in cytochrome P450$_{cam}$. This occurs with an accompanying 150 mV anodic shift in the reduction potential of the enzyme (from – 320 mV to – 170 mV *vs* NHE) [1]. Substrates such as camphor and adamantanone bind in the catalytic site of cytochrome P450$_{cam}$ and expel the coordinated water,[4] with a concomitant > 95% conversion of the spin state and a 130 mV shift in the reduction potential of the enzyme [31]. On the other hand, substrates such as camphane and norcamphor, which allow the coordinated water to remain in the catalytic site, result in lower (-50%) spin state conversion and in considerably smaller shifts in the reduction potential of the enzyme.

In this context, it is interesting to compare the binding affinities and % of spin state conversion that result from the binding of hexachloroethane and tetrachloroethylene to ferric cytochrome P450$_{cam}$. Hexachloroethane binds with K_d = 0.7 μM and results in a > 95% conversion to the high spin state, whereas tetrachloroethylene binds with a K_d = 150 μM resulting in only 40% spin state conversion [11]. By comparison, camphor binds with K_d = 0.84 μM and results in >95% conversion to the high-spin state [3]. It is also important to consider that the more highly chlorinated compounds (e.g. hexachloroethane *vs* tetrachloroethylene) exhibit more positive reduction potentials, thus making them more susceptible to reduction than their less chlorinated counterparts [22]. It is therefore possible to explain the relatively efficient dehalogenation of hexachloroethane by the large

118

anodic shift in the redox potential of the enzyme-substrate complex (*i.e.* increasing the driving force for the oxidation of reduced spinach ferredoxin) and by the positive reduction potential of hexachloroethane. In contrast, although the reasons behind the lack of reactivity toward tetrachloroethylene are not as obvious, it might originate from: (a) A modest anodic shift in the reduction potential of the tetrachloroethylene-bound cytochrome P450$_{cam}$ complex, which is expected to result from a 40% spin state conversion; (b) From the inability of the one-electron reduced P450 complex (P450^{red}-S) to catalyze the reductive dehalogenation of tetrachloroethylene due to the less positive reduction potential of this substrate.

In an attempt to elucidate the reasons underlying the lack of reactivity exhibited by tetrachloroethylene, cyclic voltammetric experiments were carried out with solutions containing ferredoxin, cytochrome P450$_{cam}$ and tetrachloroethylene. The voltammograms obtained from these experiments (Fig. 15) exhibit a pre-peak in addition to the cathodic and anodic waves originating from the electrochemistry of spinach ferredoxin. The presence of a pre-peak in the voltammogram originates from the depletion of ferric tetrachloroethylene-bound cytochrome P450$_{cam}$ that occurs via the selective reduction of spinach ferredoxin at the electrode surface. Furthermore, the separation between the pre-peak and the main peak in the cathodic scan is proportional to the electron transfer rate constant between the electrogenerated species and the species not interacting with the electrode [42, 45]. The presence of a pre-peak almost not separated from the main peak, indicates that reduced spinach ferredoxin is capable of reducing tetrachloroethylene-bound cytochrome P450$_{cam}$, albeit more slowly than when the substrate is hexachloroethane. Simulation of the electrochemical response shown in Fig. 15 with a mechanism identical
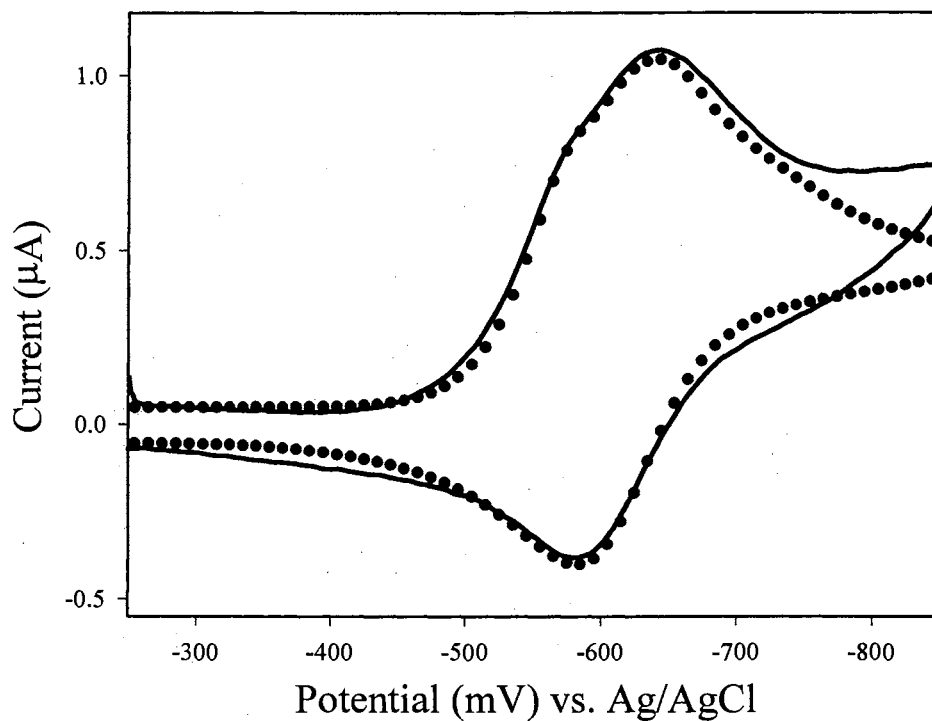
Figure 15. (___) Background subtracted cyclic voltammogram (scan rate = 3 mV/s) obtained at an ITO electrode with a solution 100 µM in spinach ferredoxin, 200 µM in cytochrome P450$_{cam}$, 300 µM in polylysine and saturated with tetrachloroethylene. (•) Simulated cyclic voltammogram invoking the mechanism shown by equations 1 and 2. Parameters for simulation are identical to those listed in Table 1 under camphor, except that the value of the second order rate constant for the reduction of tetrachloroethylene-bound cytochrome P450$_{cam}$ by spinach ferredoxin, k_f, is 2.0 x 10^4 M^{-1} s^{-1}.

to that shown in equations 1 and 2, demonstrates that the electron transfer rate constant for this process is 2.0×10^4 $M^{-1}s^{-1}$. This value is one order of magnitude slower than that measured with hexachloroethane as a substrate. It is therefore possible to conclude that cytochrome P450$_{cam}$ bound to tetrachloroethylene can indeed be reduced by spinach ferredoxin, but that the resultant ferrous heme in the (P450^{red}-S) complex cannot transfer an electron to tetrachloroethylene.

Conclusion

The fortuitous ability of cytochrome P450$_{cam}$ to catalyze reductive dehalogenation reactions attests to its well known catalytic versatility. This lack of specificity for just one substrate has led to an intense effort to harness the catalytic ability of cytochrome P450$_{cam}$ in novel biosynthetic and bioremediation schemes. The catalytic activity of cytochrome P450$_{cam}$, whether involved in oxidative or reductive chemistry, necessitates the input of two reducing equivalents that *in vivo* are typically provided by NADH via the two accessory proteins, putidaredoxin reductase and putidaredoxin. Consequently, most of the *in vitro* studies have been carried out with a reconstituted system consisting of NADH, the two accessory proteins and cytochrome P450$_{cam}$. In this report conclusive evidence has been presented demonstrating that spinach ferredoxin can act as an effective electron shuttle between an electrode surface and cytochrome P450$_{cam}$, hence eliminating the need for expensive and fragile species such as NADH and putidaredoxin reductase, in order to sustain reductive catalysis.

Two important considerations are necessary to make this strategy successful: First, it is important to choose the appropriate electron transfer protein for shuttling electrons between an electrode and cytochrome P450$_{cam}$. Spinach ferredoxin was chosen to play

this role because in addition to being readily accessible, it possesses the appropriate reduction potential and surface electrostatic potential that permits it to transfer electrons to cytochrome P450$_{cam}$. Second, it is necessary to accomplish the selective reduction of the electron transfer protein in the presence of an excess of substrate-bound cytochrome P450$_{cam}$, which by necessity possesses a more positive reduction potential. Cytochrome P450$_{cam}$ does not exchange electrons with the ITO electrode in the presence or in the absence of polylysine, but it is readily reduced by spinach ferredoxin in a homogeneous second order electron transfer reaction.

References

1. Sligar, S. G.; Gunsalus, I. C. (1976) *Proc. Natl. Acad. Sci. USA*, **73**, 1078.

2. Gunsalus, I. C.; Wagner, G. C., *Bacterial P450$_{cam}$ Methylene Monooxygenase Components: Cytochrome m, Putidaredoxin, and Putidaredoxin Reductase*, (1978) in *Methods in Enzymology*, S. Fleisher; L. Packer, Eds., Academic Press: New York, 166.

3. Fisher, M. T.; Sligar, S. G. (1985) *J. Am. Chem. Soc.*, **107**, 5018.

4. Raag, R.; Poulos, T. (1989) *Biochemistry*, **28**, 917.

5. Raag, R.; Poulos, T. L. (1991) *Biochemistry*, **30**, 2674.

6. Fruetel, J. A.; Collins, J. R.; Camper, D. L.; Loew, G. H.; Ortiz de Montellano, P. R. (1992) *J. Am. Chem. Soc.*, **114**, 6987.

7. Fruetel, J.; Chang, Y. T.; Collins, J.; Loew, G.; Ortiz de Montellano, P. R. (1994) *J. Am. Chem. Soc.*, **116**, 11643.

8. Castro, C. E.; Wade, R. S.; Belser, N. O. (1985) *Biochemistry*, **24**, 204.

9. Wackett, L., P.; Sadowsky, M. J.; Newman, L. M.; Hur, H. G. ; Li, S. (1994) *Nature*, **368**, 627.

10. Lam, T.; Vilker, V., L. (1987) *Biotechnol. Bioeng.*, **29**, 151.

11. Logan, M. S. P.; Newman, L. M.; Schanke, C. A.; Wackett, L. P. (1993) *Biodegradation*, **4**, 39.

12. Kazlauskaite, J.; Westlake, A. C. G.; Wong, L.-L.; Hill, H. A. O. (1996) *Chem. Commun*, 2189.

13. Zhang, Z.; Nassar, A.-E. F.; Lu, Z.; Schenkman, J. B.; Rusling, J. F. (1997) *J. Chem. Soc. Faraday Trans.*, **93**, 1769.

14. Lvov, Y. M.; Lu, Z., Schenkman, J. B.; Zu, X.; Rusling, J., F.(1998) *J. Am. Chem. Soc.*, **120**, 4073.

15. Faulkner, K. M.; Shet, M. S.; Fisher, C. W.; Estabrook, R. W. (1995) *Proc. Natl. Acad. Sci. USA*, **92**, 7705.

16. Reipa, V.; Mayhew, M. P.; Vilker, V., L. (1997) *Proc. Natl. Acad. Sci. USA*, **94**, 13554.

17. Knaff, D. B.; Hirasawa, M. (1991) *Biochim. Biophys. Acta*, **93**, 1056.

18. Cammack, R.; Rao, K. K.; Bargeron, C. P.; Hutson, K. G.; Andrew, P. W.; Rogers, L. J. (1977) *Biochem. J.*, **168**, 205.

19. Tagawa, K.; Arnon, D. I. (1968) *Biochim. Biophys. Acta*, **153**, 602.

20. Tyson, C. A.; Lipscomb, J. D.; Gunsalus, I. C.(1972) *J. Biol. Chem.*, **247**, 5777.

21. Li, S.; Wackett, L. P. (1993) *Biochemistry*, **32**, 9355.

22. Vogel, T. M.; Criddle, C. S.; McCArty, P. L. (1987) *Environ. Sci. Technol.*, **21**, 722.

23. Nagy, I.; Compernolle, F.; Ghys, K.; Vanderleyden, J.; Mot, R. (1995) *Appl. Environ. Microbiol.*, **61**, 2056.

24. Unger, B. P.; Gunsalus, I. C.; Sligar, S. G. (1986) *J. Biol. Chem*, **261**, 1158.

25. Rodriguez, J. C.; Rivera, M. (1997) *Chem. Lett.*, 1133.

26. Armstrong, F. A.; Cox, P. A.; Hill, H. A.; Lowe, V. J.; Oliver, B. N. (1987) *Electroanal. Chem.*, **217**, 331.

27. Armstrong, F. A.; Hill, H. A. O.; Walton, N. J. (1988) *Acc. Chem. Res.*, **21**, 407.

28. Bond, A. M. (1994) *Inorg. Chim. Acta*, **226**, 293.

29. Hawkridge, F. M.; Taniguchi, I. (1995) *Comments. Inorg. Chem.*, **17**, 163.

30. Rusling, J. F. (1997) *Interface*, 26.

31. Bowden, E. F.(1997) *Interface*, 40.

32. Taniguchi, I. (1997) *Interface*, 34.

33. Rivera, M.; Wells, M. A.; Walker, F. A. (1994) *Biochemistry*, **33**, 2161.

34. Bowden, E. F.; Hawkridge, F. M.; Blount, H. N. (1984) *J. Electroanal. Chem.*, **161**, 355.

35. Yeh, P.; Kuwana, T. (1977) *Chem. Lett.*, 1145.

36. Taniguchi, I.; Hirakawa, Y.; Iwakiri, K. I.; Tominaga, M.; Nishiyama, K. (1994) *J. Chem. Soc. Chem. Commun.*, 953.

37. Taniguchi, I.; Hayashi, K.; Tominaga, M.; Muraguchi, R.; Hirose, A. (1993) *Denki Kagaku*, **61**, 774.

38. Rudolph, M.; Reddy, D. P.; Feldberg, S. W. (1994) *Anal. Chem.*, **66**, 589A.

39. Taniguchi, I.; Miyahara, A.; Iwakiri, K. I.; Hirakawa, Y.; Hayashi, K.; Nishiyama, K.; Akahashi, T.; Hase, T. (1997) *Chem. Lett.*, 929.

40. Aliverti, A.; Hagen, W. R.; Zanetti, G. (1995) *FEBS Lett.*, **368**, 220.

41. Barker, P. D.; Hill, H. A. O.; Walton, N. J. (1989) *J. Electroanal. Chem.*, **260**, 303.

42. Bard, A. J.; Faulkner, L. R., *Electrochemical Methods Fundamentals and Applications*. 1980, New York: John Wiley & Sons.

43. Reiger, P. H., *Electrochemistry*. 1994, New York: Chapman and Hall.

44. Parker, V. D.; Zheng, G.; Wang, H.(1995) *Acta Chemica Scandinavica*, **49**, 351.

45. Seetharaman, R.; White, S. P.; Rivera, M. (1996), *Biochemistry* **35**, 12455.

46. Roitberg, A. E.; Holden, M. J.; Mayhew, M. P.; Kurnikov, I. V.; Beratan, D. N. ; Vilker, V. L. (1998) *J. Am. Chem. Soc.*, **120**, 8927.

47. Stayton, P. S.; Poulos, T. L.; Sligar, S. G.(1989) *Biochemistry*, **28**, 8201.

48. Hintz, M. J.; Mock, D. M.; Peterson, L. L.; Tuttle, K.; Peterson, J. A. (1982) *J. Biol. Chem.*, **257**, 14324.

49. Ling, K. H.; Hanzlik, R. P. (1989) *Biochem. Biophys. Res. Commun.*, **160**, 844.

50. Mueller, E. J.; Loida, P. J.; Sligar, S. G., *Twenty-five Years of P450$_{cam}$ Research,* in *Cytochrome P450: Structure, Mechanism and Biochemistry*, P.R. Ortiz de Montellano, Ed. 1995, Plenum Press: New York, 83.

51. Poulos, T. L.; Finzel, B. C.; Howard, A. J.(1987) *J. Mol. Biol.*, **195**, 687.

52. Binda, C.; Coda, A.; Aliverti, A.; Zanetti, G.; Mattevi, A. (1998) *Acta Crystallogr. Sect. D*, **54**, 1353.

53. Nicholson, R. S.; Shain, I. (1964) *Anal. Chem*, **36**, 706.

CHAPTER V

MODULATION OF REDOX POTENTIAL IN ELECTRON TRANSFER

PROTEINS: EFFECTS OF COMPLEX FORMATION ON

THE ACTIVE SITE MICROENVIRONMENT

OF CYTOCHROME b_5

Introduction

Pioneering work which demonstrated facile heterogeneous electron exchange between cytochrome c and modified electrodes was reported by Eddowes and Hill [1] and Yeh and Kuwana [2]. Eddowes and Hill proposed that 4, 4'-bipyridyl adsorbs on to the surface of gold electrodes, hence preventing the adsorption and concomitant denaturation of cytochrome c. Yeh and Kuwana reported the reversible cyclic voltammetry of cytochrome c at clean indium oxide electrodes [2]. These two seminal reports stimulated a large effort aimed at understanding important aspects related to protein electrochemistry, including the role played by electrode modifiers in promoting rapid heterogeneous electron transfer, molecular recognition between electrode and protein surfaces, and the nature of the association between electrode and protein. These research efforts, carried out by many investigators, have been recently reviewed [3-6].

127

In contrast to cytochrome c, several electron transfer proteins possess localized patches of negatively charged residues on the surface near the active sites. The direct cyclic voltammetry of such proteins has been achieved by implementing a variety of different experimental schemes. For example, thiols with general structures of the type HS-R-X have been extensively used as electrode modifiers [33-35]. In these types of modifiers, the thiol group acts like a surface-active functional group that interacts with the electrode (typically gold or platinum) to form self-assembled monolayers. The role of the functional group X is to communicate with the electroactive protein via the formation of electrostatic or hydrogen bonding interactions. R is typically an organic structure linking the surface-active thiol and the protein "sensing" functionality. Examples of this type of surface modifier include 2-aminoethane [36] and peptides such as (Lys-Cys)$_2$ [34], which were used to promote the reversible voltammetry of plastocyanin and cytochrome b_5, respectively. One approach to obtaining the reversible cyclic voltammetry of negatively charged proteins at negatively charged pyrolytic graphite electrodes is by the addition of multivalent ions such as Ca^{+2}, Mg^{+2}, or $[Cr(NH_3)_6]^{+3}$ to the solution contained in the electrochemical cell [7-10].

When the electrochemistry of rat liver outer mitochondrial membrane (OM) cytochrome b_5 was studied at polycrystalline gold electrodes modified with β-mercaptopropionate, it was observed that the reduction potential of this protein shifted cathodically as a function of increasing polylysine concentration [11]. Polylysine was added to the electrochemical cell in order to promote interactions between the negatively charged β-mercaptopropionate electrode surface and the negatively charged surface of cytochrome b_5. It was initially postulated that the formation of a complex between cytochrome b_5 and polylysine would neutralize charges on the surface of the protein, including those originating from the heme

propionates, hence resulting in the observed cathodic shift of reduction potential [11].

Subsequently, electrochemical and NMR spectroscopic studies were carried out with OM cytochrome b_5 and a derivative of this protein, where the heme propionates were esterified to the corresponding dimethyl ester (DiMe cytochrome b_5). These studies were performed with the aim of elucidating the role played by surface and heme propionate charges in modulating the reduction potential of cytochrome b_5. Potentiometric studies performed with cytochrome b_5 demonstrated that the reduction potential of this protein, measured in the presence of polylysine, was significantly more positive than the reduction potential measured in the absence of polylysine. In contrast, potentiometric measurements demonstrated that the reduction potential of DiMe cytochrome b_5 was independent of the concentration of polylysine [12]. These findings indicated that electrostatic interactions between polylysine and the heme propionate in cytochrome b_5 modulate the reduction potential of this protein. Furthermore, the fact that the reduction potential of DiMe cytochrome b_5 (measured potentiometrically) is independent of the concentration of polylysine also indicates that neutralization of acidic residues on the surface of the protein exerts a minimum influence in the reduction potential cytochrome b_5. The latter is in agreement with studies that demonstrate that eliminating, and even reversing the charge of these residues by site-directed mutagenesis, does not have an effect on the reduction potential of cytochrome b_5 [13].

NMR experiments carried out with cytochrome b_5 containing heme labeled with ^{13}C at the heme propionate groups, conclusively demonstrated that only one of the heme propionates in cytochrome b_5 undergoes electrostatic interaction with polylysine [13]. In fact, the NMR experiments demonstrated that the heme propionate capable of interacting with polylysine

129

is located on the solvent exposed heme edge of cytochrome b_5. The solvent exposed heme propionate is part of a highly localized patch of negative electrostatic potential surrounding the heme, which is delineated by Glu-44, Glu-48, Glu-56, Asp-60, and the solvent exposed heme propionate. It is noteworthy that these residues [14] and the solvent-exposed heme propionate [15-17] have been implicated in the binding of mitochondrial cytochrome b_5 to cytochrome c. The formation of this inter-protein complex precedes the oxidation of ferrous cytochrome b_5 by ferric cytochrome c [15,18].

Voltammetric measurements performed with the gold disk electrodes modified with β-mercaptopropionate, showed that the reduction potential of both cytochrome b_5 and DiMe cytochrome b_5 is modulated by the concentration of polylysine in the electrochemical cell. Although the modulation of the reduction potential of cytochrome b_5 was expected, the modulation of the reduction potential of DiMe cytochrome b_5 was striking because the potentiometric studies described above showed that the reduction potential of DiMe cytochrome b_5 was independent of the concentration of polylysine. On the basis of these findings, it was proposed that the reduction potential of cytochrome b_5 was modulated by the formation of a complex between cytochrome b_5 and polylysine at the electrode surface. The formation of this complex neutralizes the charge on the heme propionate located on the exposed heme edge, and lowers the dielectric of the exposed heme microenvironment by excluding water from the complex interface. These two factors act synergistically to destabilize the positive charge of the ferric heme with respect to the neutral ferrous heme, hence encouraging a cathodic shift in the reduction potential of cytochrome b_5. The neutralization of the solvent-exposed heme propionate upon formation of a complex between cytochrome b_5 and polylysine was conclusively demonstrated on the basis of NMR

spectroscopic experiments performed with cytochrome b_5 containing ^{13}C-labeled heme [12,17].

The effect of the dielectric constant on the reduction potential of cytochrome b_5 was demonstrated by the corresponding V45L/V61L double mutant [12]. The reduction potential of this mutant protein, measured potentiometrically, was shown to be 50 mV more negative than that of the wild-type protein. Furthermore, X-ray crystallographic studies demonstrated that the heme in the double mutant was more accessible to water (increased dielectric of the heme microenvironment), hence providing indirect support for the idea that the reduction potential of cytochrome b_5 was also modulated by dehydration of the exposed heme-edge upon formation of a transient complex with the electrode surface [12].

A mutant of OM cytochrome b_5, in which the exposed heme edge has been closed by engineering hydrophobic contacts between Ile residues at positions 45 and 61 and the heme edge, is described. Evidence obtained from X-ray crystallographic and electrochemical studies carried out with the V45I/V61I double mutant provide conclusive evidence demonstrating that the dehydration of the exposed heme edge upon formation of a transient complex with polylysine at the electrode surface does indeed contribute to modulate the reduction potential of cytochrome b_5.

Experimental Procedure

Site directed mutagenesis to produce the V45I/V61I mutant was previously performed in this laboratory. The V45I/V61I double mutant of OM cytochrome b_5 was expressed and purified identically to the wild type protein, as discussed in Chapter II.

The dimethyl ester derivative of the V45I/V61I mutant was prepared as follows [12]: purified rat OM cytochrome b_5 was placed in a 50 ml conical tube on ice. The pH was

lowered to 2.0 with the addition of ice-cold 1 N HCl and 2-butanone (-20 °C) was added to extract the heme. The 2-butanone turned brown in color. The apoprotein (in transparent aqueous layer) was dialyzed against 4 L of 0.6 mM NaHCO$_3$, 1 mM EDTA, pH 10.3 at 4 °C for about 1h. This was followed by dialysis against 4 L of 0.6 mM NaHCO$_3$. The apoprotein was further dialyzed against 20 mM NaH$_2$PO$_4$, pH 7.2 overnight. A solution of Fe (III) protoporphyrin (IX) dimethyl ester (5 mg) was prepared in (10 ml) dimethyl sulfoxide (DMSO). Aliquots of the Fe (III) protoporphyrin (IX) dimethyl ester solution was added to the apoprotein at 35 °C. The incorporation of the dimethyl ester was monitored spectroscopically by following the absorbance ratio A_{280}/A_{412}. The reaction took approximately 20 h to complete. The V45I/V61I dimethyl ester was loaded onto the Sephadex G-50 column and eluted with size exclusion buffer. The fractions were collected, concentrated, and stored at 4 °C.

Site-Directed Mutagenesis

The recombinant plasmid MRL1 [37] and the transformer site-directed mutagenesis kit (Clonetech) were used to obtain a gene coding for the V45I/V61I double mutant of OM cytochrome b$_5$.

X-ray Crystallography

X-ray quality crystals of the V45I/V61I double mutant of OM cytochrome b$_5$ were grown using the vapor diffusion method applying conditions identical to those used in the crystallization of the wild-type protein [17] and the V45L/V61L double mutant [12]. In short, the protein (approx. 20 mg ml^{-1}) was mixed 1:1 by volume with precipitant solution [20% (w/v) polyethylene glycol (MW 8,000), 0.2 M magnesium acetate, and 0.1 M PIPES, pH 6.8] in 8 µl drops. The drops were allowed to equilibrate overnight, with 500 µL of

precipitant solution, in vapor diffusion chambers and then micro-seeded with cytochrome b_5 crystals. Crystals grew to a typical size of 0.5 x 0.2 x 0.2 mm^3 in a few days. The crystal belongs to space group $P2_12_12_1$ and diffracts to 1.8 Å resolution.

Cyclic Voltammetry

Cyclic Voltammetry was carried out with a BAS-CV50W potentiostat (Bioanalytical Systems, West Lafayette, IN). Glass-slides (2.50 cm x 2.50 cm) coated on one side with indium-doped tin oxide (ITO) semiconductor films exhibiting a typical resistance of less than 10 ohms were purchased from Delta Technologies (Stillwater, MN) and used as working electrodes. A platinum wire auxiliary electrode and a Ag/AgCl reference electrode containing a fiber junction were purchased from Cypress Systems (Lawrence, KS). The electrochemical cell was described in the previous chapter. The ITO working electrode was conditioned by sonicating for 30 min in each of the following solutions: 1% alconox in deionized water, ethanol, and deionized water. The clean electrodes were subsequently dried with a stream of nitrogen and used immediately.

The solution in the electrochemical cell was deaerated by bubbling high-purity nitrogen for 30 minutes and subsequently blanketed with nitrogen in order to maintain anaerobicity. Solutions used in the electrochemical studies were typically prepared in 100 mM MOPS at a pH of 7.0 and contained 100 μM of the protein. Protein concentrations were determined with the aid of UV-Vis spectrophotometry using an extinciton coefficient (ε =130 mM^{-1} cm^{-1}) previously reported for ferric cytochrome b_5 [19]. The concentration of polylysine was obtained from the weight of substance and the molecular weight provided by Sigma.

133

Spectroelectrochemistry

Transmission mode spectroelectrochemical titrations were carried out with a custom-made spectroelectrochemical cell constructed from a glass cuvette (1.0 cm path-length) equipped with a platinum-foil working electrode and a Ag/AgCl reference electrode. The cell design was modeled after that reported previously by Stankovich [20]. The potentiometric titrations were performed by the addition of the appropriate volumes of a 10 mM solution of sodium dithionite to a solution consisting of the appropriate protein (15 μM) and the appropriate redox mediators. For poteniometric titrations carried out with the V45I/V61I double mutant of OM cytochrome b_5, the solution contained either 200 μM [Ru(NH$_3$)$_6$]Cl$_3$, 25 μM 2,5 dihydroxy-*p*-benzoquinone (E$^{o\prime}$ = -0.060 V vs. NHE), and 25 μM anthraquinone-2,6-disulfonate (E$^{o\prime}$ = -0.184 V vs NHE) or 200 μM [Ru(NH$_3$)$_6$]Cl$_3$ and 15 μM pyocyanin (E$^{o\prime}$ = -0.030 V vs NHE). Solutions used for the potentiometric titration of the DiMe ester derivative of the V45I/V61I double mutant contained 200 μM [Ru(NH$_3$)$_6$]Cl$_3$, and 25 μM 2,5-dyhydroxy-*p*-benzoquinone (E$^{o\prime}$ = -0.060 V vs NHE).

The mediator Pyocyanin was prepared by the following procedure: One gram *N*-methylphenazonium methosulfate was dissolved in 300 ml of 10 mM Tris Cl, pH 8, and placed in a large glass container on ice. A watch glass full of water was placed above the *N*-methylphenazonium methosulfate to act as a heat filter. This was illuminated with a spotlight (250 W) for 3 to 5 h, time will depend on light source. The generation of pyocyanin at 695 nm was followed by UV-Vis. The solution was extracted with 325 ml of chloroform, and the latter saved (muddy blue). The chloroform was extracted twice with 125 ml of 0.1 N HCl, which turned a rosy pink. The chloroform was usually a dirty pale brown at this stage. The aqueous phase was adjusted to pH 8, where the pyocyanin was a beautiful blue

color. It is important not to go too alkaline or the product converts to phenazine. Tris buffer was used as the titrant. The blue aqueous phase was extracted with chloroform. The chloroform was dryed with 5 g anhydrous Na_2SO_4. The Na_2SO_4 was removed by filtration and washed with a little more chloroform. The chloroform fractions were combined and evaporated to dryness in a rotary evaporator. Yield 30%.

Results and Discussion

Research carried out, demonstrated that the reduction potential of cytochrome b_5 is modulated by the formation of a transient complex with polylysine at the electrode surface [11, 12]. The modulation of reduction potential stems from the degree of exposure of the heme in cytochrome b_5 to the aqueous environment. In fact, one edge of the heme forms part of the molecular surface, and consequently is in contact with the aqueous environment. This particular feature in the structure of cytochrome b_5, together with the results obtained from previously reported [12] electrochemical studies carried out with this protein, led us to postulate that formation of a transient complex with polylysine at the electrode surface modulates its reduction potential [12]. The modulation mechanism was proposed to originate from neutralization of the charge on the solvent exposed heme propionate and from dehydration of the protein surface surrounding the exposed heme edge. Direct evidence for the role played by the heme propionate in modulating the reduction potential of cytochrome b_5 upon complex formation was obtained from a combination of electrochemical and NMR experiments. By comparison, evidence demonstrating that sequestering the exposed heme edge from water modulates that the reduction potential was indirect.

Consequently, an important aim in the study presented here was to engineer a

cytochrome b$_5$ mutant in which the exposed heme edge would be sequestered from water by hydrophobic interactions between the heme edge and polypeptide side chains. The availability of a mutant protein exhibiting the desired structural properties was expected to furnish direct experimental information regarding the role played by the exposed heme edge in modulating the reduction potential of cytochrome b$_5$. Molecular models constructed to guide the site-directed mutagenesis experiments suggested that the V45I/V61I double mutant of OM cytochrome b$_5$ was likely to possess the desired structural features.

The rationale for constructing a gene coding for this double mutant is described in what follows. The X-ray crystal structure of wild type OM cytochrome b$_5$ [17] shows that one of the methyl groups (C$_{\gamma 1}$) in the side chains of Val-45 and Val-61 pack against the top and bottom of the heme (Fig. 1B). The same methyl groups in Val-45 and Val-61 also make hydrophobic interactions with His-39 and His-63, respectively. These hydrophobic interactions taken together create a hydrophobic wall that prevents access by water into the heme binding pocket (Fig. 1B). When Val-45 and Val-61 are replaced by Leu, the X-ray crystal structure of the double mutant [12] shows that the longer Leu side chains adopt a conformation that leaves the volume previously occupied by the C$_{\gamma 1}$ carbon in Val-45 and Val-61 unoccupied (Fig. 1A). The effect of replacing Val for Leu at positions 45 and 61, therefore, is to create water cavities in the interior of the heme binding pocket. This observation underscores the idea that subtle (conserved) changes in amino acid composition can have significant changes in structure that ultimately exert an effect on protein function. For instance, the water cavities created in the interior of the heme binding pocket of the V45I/V61I mutant increase the dielectric constant of the heme microenvironment, therefore resulting in a -50 mV shift in the reduction potential (function) of OM cytochrome b$_5$ [12].
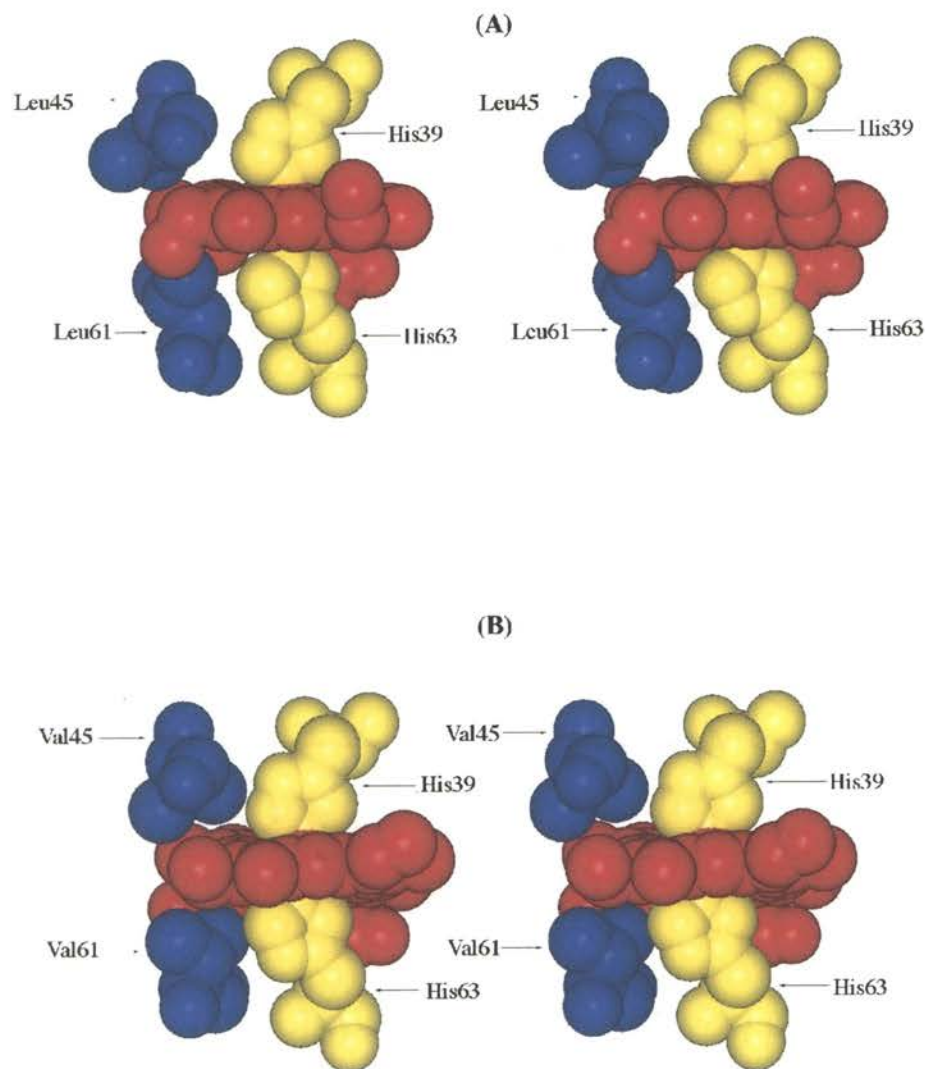
Figure 1. Cross sectional stereo views obtained from the X-ray crystal structures of **(A)** V45L/V61L double mutant of OM cytochrome b₅ (PDB ID code: 1AWP) and **(B)** wild type OM cytochrome b₅ (PDB ID code: 1B5M). The stereo view shown in **B** demonstrates that the isopropyl methyl groups ($C_{\gamma 1}$) in Val-45 and Val-61 pack against His-39 and His-63, respectively. The stereo views shown in **A** demonstrate that replacement of Val for Leu at positions 45 and 61 leaves the position previously filled by the $C_{\gamma 1}$ carbon of Val vacant. The voids introduced by the conformation of the Leu side chains result in increased water accessibility to the interior of the heme binding cavity and in a -50 mV shift in the reduction potential of the mutant with respect to the wild type protein [12].

137

In order to engineer a mutant cytochrome b_5 displaying a heme edge with restricted water accessibility, it is desirable to create hydrophobic interactions between amino acids lining the exposed heme edge and this part of the heme cofactor. To accomplish this task, however, it is not only necessary to introduce the desired hydrophobic interactions at the heme edge, but it is also important to avoid the creation of voids in the interior of the molecule. Molecular models built with coordinates from the X-ray crystal structure of wild type and V45I/V61I cytochrome b_5, suggest that placing Ile at positions 45 and 61 is likely to accomplish the task of closing the heme edge, while maintaining packing integrity inside the heme binding pocket. In fact, a model of the V45I/V61I double mutant indicates that the *sec*-methyl in the Ile side chains is likely to occupy the volume normally filled by the isopropyl methyl in Val-45 and Val-61 in the wild type protein. Furthermore, the model also indicates that iso-propyl side chains at positions 45 and 61 are likely to shield the heme edge from the aqueous environment. A gene coding for the V45I/V61I double mutant was therefore constructed and the corresponding protein expressed in *E. coli* and then purified to homogeneity. The protein was subsequently studied by X-ray crystallography and electrochemistry.

X-ray Crystallography

X-ray diffraction data was collected at room temperature using a RAXIS IV image plate system. The data was processed with the HKL program package [32]. Since the unit cell parameters of the V45I/V61I crystal form are marginally different (less than 2% in any given dimension), from those of the previously reported V45L/V61L crystal form (ID: 1AWP), the initial phases of the new structures were calculated from the model of the V45L/V61L structure. There are two identical cytochrome b_5 molecules in a crystallographic asymmetric

unit with V_m of 2.6 Å³ Da⁻¹. Refinement was carried out with the program CNS (V.1.0) [33], and 4.6% of the total reflections were randomly selected to monitor the free-R factor. Non-crystallographic symmetry restraint was not applied since the number of observations exceeded the degrees of freedom. Simulated annealing (from 5000 K) was used at the initial stage of the refinement to reduce bias for the template model. Solvent molecules were introduced after the R-factor dropped below 23% and were all modeled as water molecules. The average B factor of the Ile-45 side chain was 34 Å² and that of Ile-61 was 43 Å². In both cases, molecule B displayed a higher B factors than molecule A (there are two cytochrome b₅ molecules per crystallographic asymmetric unit). The side chain methylene groups in Ile-45 and Ile-61 were well adopted and show good electron density. In three of the four Ile residues of interest (Ile-45 and Ile-61 in molecules A and B) the secondary methyl carbon displayed a slightly lower B factor than the other side chain atoms beyond C_β. Bulk solvent correction and correlated B-factor refinement were used in the final stage of refinement. The statistics of the diffraction data and refinement results are summarized in Table 1.

In the V45I/V61I mutant (Fig. 2a), the sec-methyl carbon ($C_{\gamma2}$) in Ile-45 is located 3.84 Å away from the $C_{\epsilon1}$ atom in His 39. By comparison, in the wild type protein the isopropyl-methyl carbon ($C_{\gamma1}$) in Val-45 is 3.85 Å away from the $C_{\epsilon1}$ atom in His 39 (Fig 2b). Consequently, the secondary methyl group of Ile-45 in the double mutant maintains compact packing that restricts water accessibility into the heme binding pocket. This is also illustrated by the space filling views corresponding to the V45I/V61I mutant (Fig 2C) and the wild type protein (Fig. 2D). In the wild type protein (Fig 2B and D), methyl carbon $C_{\gamma2}$ in the Val-45 is located 4.71Å and 3.75Å from the heme meso and heme vinyl-β carbons, respectively. In the mutant protein, the $C_{\gamma1}$ and $C_{\delta1}$ carbons in the Ile-45 are closer to the

139

Table 1 Data collection and refinement statistics

(a) Data statistics

Space group	P2$_1$2$_1$2$_1$	
Unit cell (a, b and c in Å)	46.2, 70.8 and 72.4	
Resolution/Å	24.2-1.8	
R$_{merge}$ (%)	6.5	(48)[a]
No. Of reflections	21091	
Completeness (%)	93.0	(91.8)
<I>/δ	20.6	(1.8)

(b) Refinement statistics

R$_{working}$ (%)	20.8	for 20051 reflections
R$_{free}$ (%)	23.9	for 1040 reflections

No. Of non-hydrogen atoms

Protein	694 x 2
Heme	43 x 2
Solvent	78

Rms deviation from ideal values

Bond length/Å	0.0056
Bond angle/degree	1.18
Average B-factor/Å^2	
Protein atoms	34
Heme	37
Solvent molecules	40

[a] Numbers in parentheses are the corresponding numbers for the highest resolution shell (1.85-1.80 Å). The highest resolution shell with R$_{merge}$ below 20% is that corresponding to 2.13-2.03 Å.
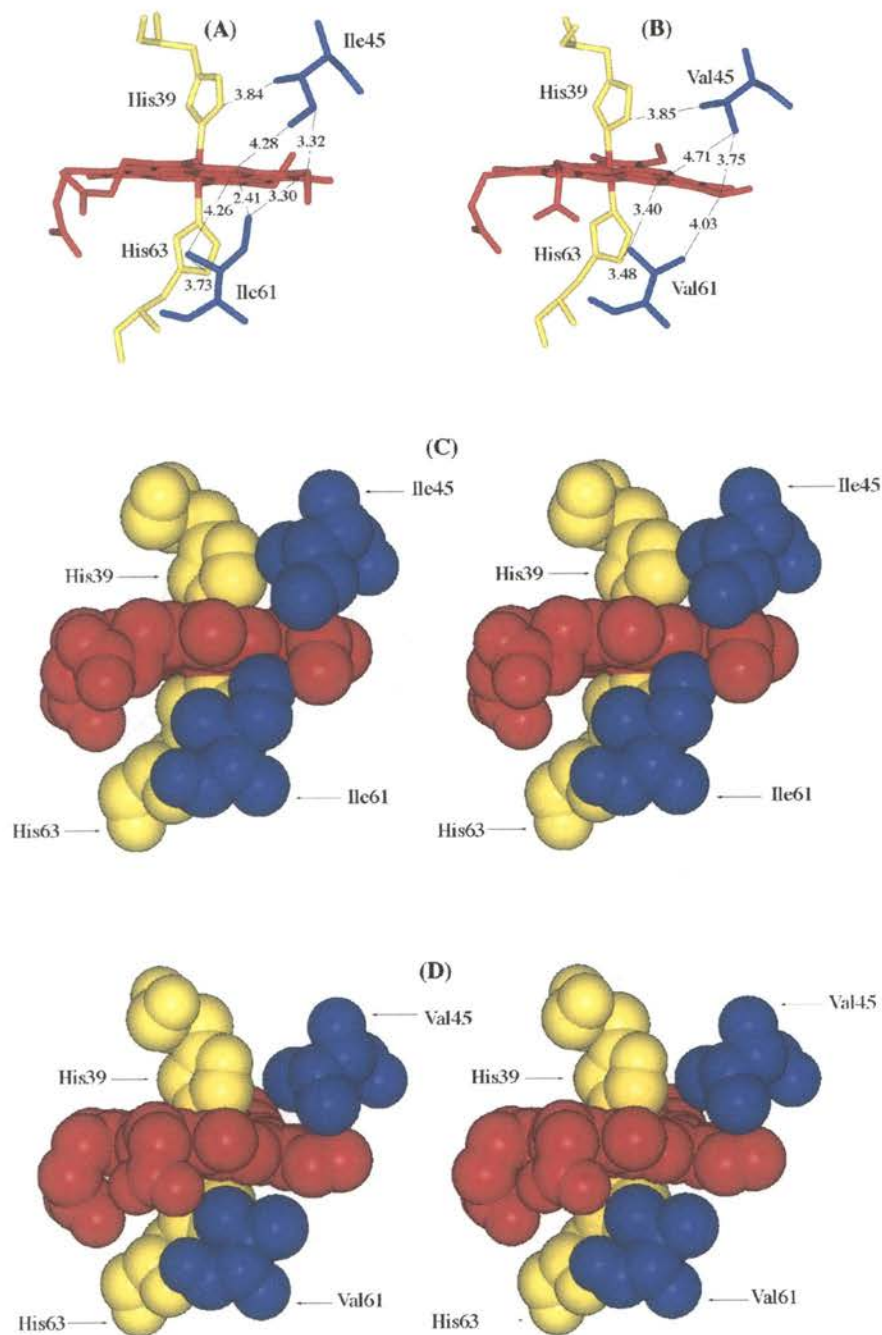
Figure 2. The cross sectional views shown in **A** and **B** allow the comparison of important distances in the structures of V45I/V61I mutant **(A)** with corresponding distances in the structures of wild type OM cytochome b₅ **(B)**. Space filling views shown in **C** and **D** correspond to the views shown in A and B, respectively. These representations provide visual confirmation that the secondary methyl groups in Ile-45 and Ile-61 restrict water accessibility to the interior of the heme pocket. It is also evident that Ile at positions 45 and 61 shield the heme edge from the aqueous environment, whereas Val at the same positions leaves the heme edge highly accessible to water.

141

heme meso (4.28 Å) and heme vinyl-β (3.32 Å) carbons (Fig 2A andC). The X-ray crystal structure of the mutant also reveals that the secondary methyl carbon ($C_{\gamma2}$) in Ile-61 is located 3.73 Å from the $N_{\gamma1}$ atom in His-63 (Fig 2A), therefore occupying a position similar to that taken by the isopropyl $C_{\gamma1}$ carbon of Val-61 (3.48 Å from His-63 $N_{\gamma1}$) in the wild type protein (Fig.2B). Consequently, the secondary methyl group of Ile-61 restricts water accessibility to the interior of the heme binding pocket in the V45I/V61I double mutant. Furthermore, the $C_{\gamma1}$ carbon in Ile-61 is located 2.41 Å from the heme-meso carbon and 3.30 Å from the heme vinyl-β carbon (Fig 2A and C). The shorter comparable distances in the wild-type protein (Fig 2a and Fig 3a) are from Val 61 $C_{\gamma1}$ carbon to heme meso carbon (3.40 Å) and from Val-51 $C_{\gamma2}$ carbon to heme-vinyl-β carbon (4.03 Å).

From the above, it is evident that the secondary methyl group in the side chains of Ile-45 and Ile-61 occupy the volume taken by the isopropyl methyl groups of Val-45 and Val-61 in the wild type protein, therefore preventing water access to the interior of the heme cavity. In addition, it is also clear that hydrophobic contacts between the heme edge and the side chains of Ile at positions 45 and 61 sequester a large section of the heme edge from the aqueous environment. Consequently, it is anticipated that the structural properties engineered into the V45I/V61I mutant are going to be useful in unraveling the role played by the solvent exposed heme edge in modulating the redox potential of cytochrome b_5.

Electrochemistry

In previous electrochemical studies carried out with OM cytochrome b_5, cyclic voltammograms of the protein were obtained at gold-disk electrodes modified with β-mercaptopropionate [15,16,34]. Interactions between the negatively charged protein and electrode surface were promoted by the addition of polylysine to the electrochemical cell.

For the present study, cyclic voltammograms of OM cytochrome b_5 have been obtained with the aid of indium-doped tin oxide (ITO) electrodes. The negative charge on the surface of indium oxide electrodes [26] was initially exploited by Yeh and Kuwana [2], who used it in order to obtain the unmediated electrochemistry of cytochrome c, a positively charged protein. In subsequent studies, the voltammetry of negatively charged proteins had been obtained at indium oxide electrodes by addition of a polycation in order to overcome the electrostatic repulsion between negatively charged proteins and electrode surfaces [27, 28, 29].

Typical background subtracted cyclic voltammograms obtained from solutions containing a mixture of polylysine and the V45I/V45I double mutant, or polylysine and the DiMe ester derivative of the V45I/V45I mutant are shown in Figure 3 and 4. The ratio of the cathodic to anodic peak currents (i_{pc}/i_{pa}) is unity and the peak to peak separation (ΔEP) is 63 mV. For all proteins, the cathodic peak current is proportional to the square root of the scan rate, indicating that the electrochemical process is diffusion controlled. In agreement with results previously obtained with the β-mercaptopropionate [11,12], cyclic voltammograms obtained at ITO electrodes demonstrate that the reduction potential of OM cytochrome b_5 and that of its DiMe derivative shift cathodically with increasing concentrations of polylysine (Figure 5 a and b). Similar observations were made for the reduction potential of the V45I/V61I double mutant (Fig. 5c). In sharp contrast, the reduction potential of the DiMe ester derivative of the V45I/V61I double mutant, measured by cyclic voltammetry, is nearly independent of polylysine concentration (Fig. 5d). When cyclic voltammetry is used to measure the reduction potential of OM cytochrome b_5, reduction values shift from -102 to -26 mV (76 mV), as the concentration of polylysine is increased (Fig 5a). This is in

143
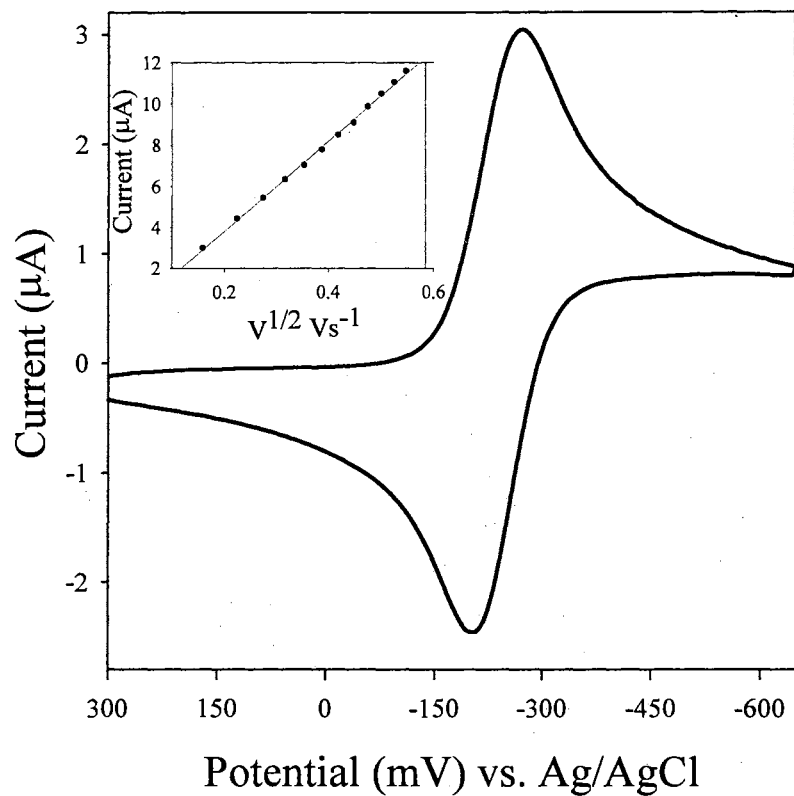
Figure 3. Background subtracted cyclic voltammogram of the V45I/V61I double mutant of OM cytochrome b_5. The cyclic voltammogram was obtained at an ITO electrode from a solution containing 100 μM of the mutant, and polylysine at a scan rate of 20 mV/s.

144
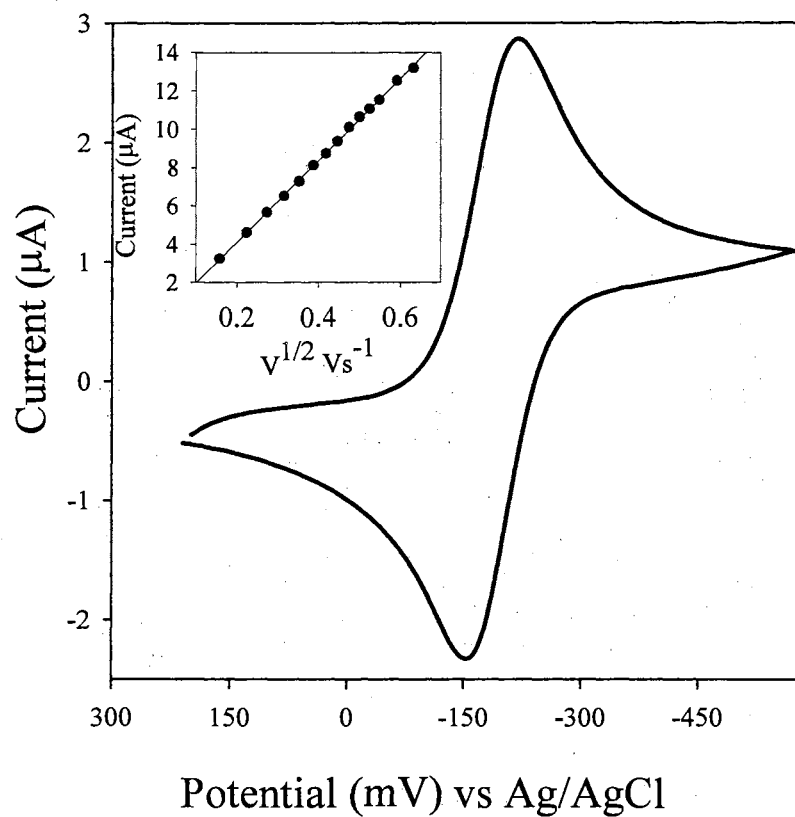
Figure 4. Background subtracted cyclic voltammogram of the DiMe ester derivative of the V45I/V61I mutant of OM cytochrome b_5. The cyclic voltammogram was obtained at an ITO electrode from a solution containing 100 μM of the mutant, and polylysine at a scan rate of 20 mV/s.
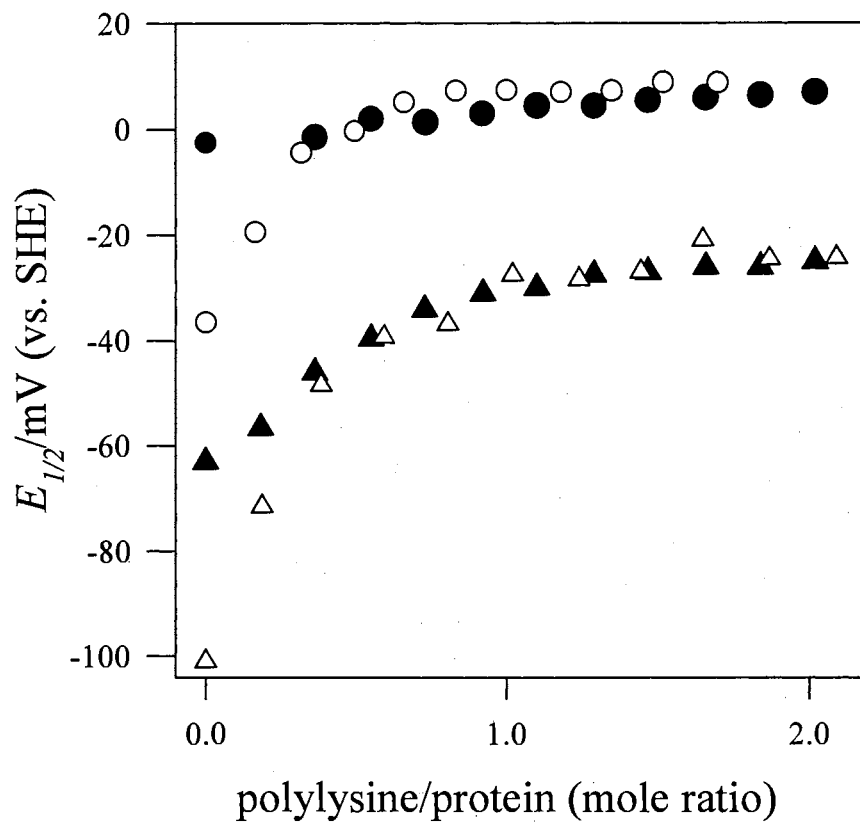
Figure 5. Titration of (a) OM cytochrome b_5 (Δ), (b) DiMe cytochrome b_5 (O), (c) V45I/V61I cytochrome b_5 (▲), and (d) DiMe V45I/V61I cytochrome b_5 (●) with polylysine (MW 3970). The first point in each titration curve was obtained from a potentiometric titration, as described in the experimental procedures section.

good agreement with previous results obtained with the aid of gold-disk electrodes modified with β-mercaptopropionate [11,12]. Since polylysine is also necessary to promote the electrochemistry of cytochrome b_5 at the ITO electrodes, the reduction potentials corresponding to the absence of polylysine in Fig. 5 were obtained from potentiometric (spectroelectrochemical) titrations. The reduction potential of DiMe OM cytochrome b_5 (measured potentiometrically) is -37 mV vs. NHE, a value 65 mV more positive than the corresponding value for the wild type protein. The cathodic shift in reduction potential brought about by esterification of the heme propionates is well documented and has been attributed to the destabilization of the positive charge on the ferric heme upon neutralization of the negative charge on the heme proprionates [21,22,30,31]. When cyclic voltammetry is used to measure the reduction potential of DiMe OM cytochrome b_5, the values shift from -37 to +4 mV (41 mV), as the concentration of polylysine is increased (Fig. 5b). This behavior corroborates the idea that the neutralization of the solvent exposed heme propionate is not the only factor modulating the reduction potential of OM cytochrome b_5 when this molecule forms a transient complex with polylysine at the electrode surface.

Potentiometric measurements demonstrated that the reduction potential of the V45I/V61I mutant is -63 mV vs NHE (Fig.6). Consequently, the mutant exhibits a reduction potential 40 mV more positive than that displayed by wild type OM cytochrome b_5. The more positive reduction potential of the mutant protein is in agreement with the fact that its heme experiences a lower dielectric constant because it is more shielded from the aqueous environment, as demonstrated by its X-ray crystal structure. When cyclic voltammetry is used to measure the reduction potential of the V45I/V61I mutant, the values shift from -63 to -24 (39 mV), as the concentration of polylysine is increased (Fig.5c). In contrast, the

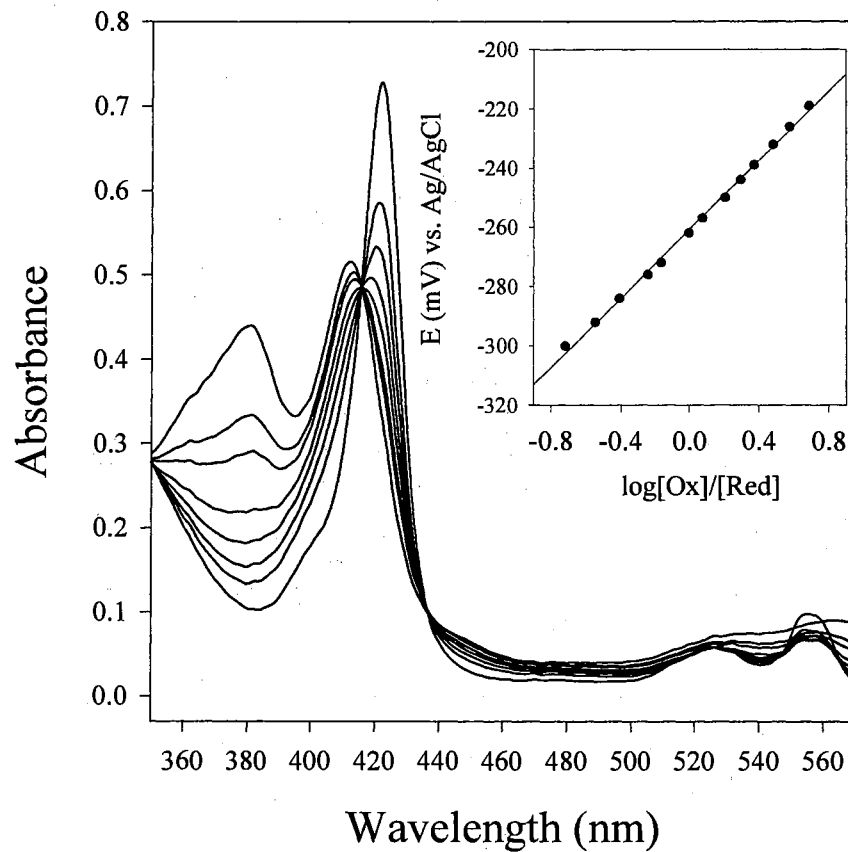**Figure 6.** Spectra obtained from the titration of V45I/V61I mutant in the presence of $[Ru(NH_3)_6]Cl_3$ and pyocyanine. Phosphate buffer, pH 7.0, $\mu = 0.1$ was used for the experiment. Inset: Nernst plot of the data. The midpoint potential calculated from this plot is -64 mV *vs* NHE. The Nernst slope is 60 mV. The absorbance at 422 nm was monitored.

voltammetric values obtained for the DiMe ester derivative of the V45I/V61I double mutant are nearly independent of the concentration of polylysine (Fig. 5d). The Nernst plot for the DiMe is shown in Figure 7.

In order to understand the experimental observations described above, it is useful to consider how the structures of the wild type and mutant proteins affect the properties of the transient complex formed with polylysine at the electrode surface. The X-ray crystal structure of the mutant protein clearly shows that as a result of closer packing between the side chains of Ile-45 and Ile-61 and the heme meso and heme vinyl groups, the heme cofactor is more protected from the aqueous environment than its counterpart in wild type OM cytochrome b_5. This is illustrated in the space-filling representations shown in Fig. 2C and D and in Fig. 8. The side chain of Ile-61 (Fig. 2C and 8a) packs against the heme meso and the heme vinyl groups, hence restricting water accessibility to those heme substituents. The methylene group ($C_{\gamma 2}$) in the side chain of Ile-45 packs against the top of the heme-vinyl group; furthermore, the terminal methyl group in the Ile-45 side chain ($C_{\delta 1}$), acts as a hydrophobic barrier that restricts water accessibility to the heme-meso and heme-vinyl groups. By comparison, the shorter side chains of Val at positions 45 and 61 in the wild type protein (Fig. 2D and 8B) impose a structure where the heme meso and heme vinyl groups are highly exposed to the aqueous environment. For heterogeneous electron transfer to take place at the electrode surface, cytochrome b_5 must diffuse toward the electrode surface where a transient complex is formed prior to the electron transfer event. Evidence for diffusion control stems from the proportionality of the cathodic peak current with the square root of the scan rate (inset in Fig. 3 and 4). In the transient complex formed at the electrode surface, cytochrome b_5 is expected to form electrostatic interactions with polylysine via the
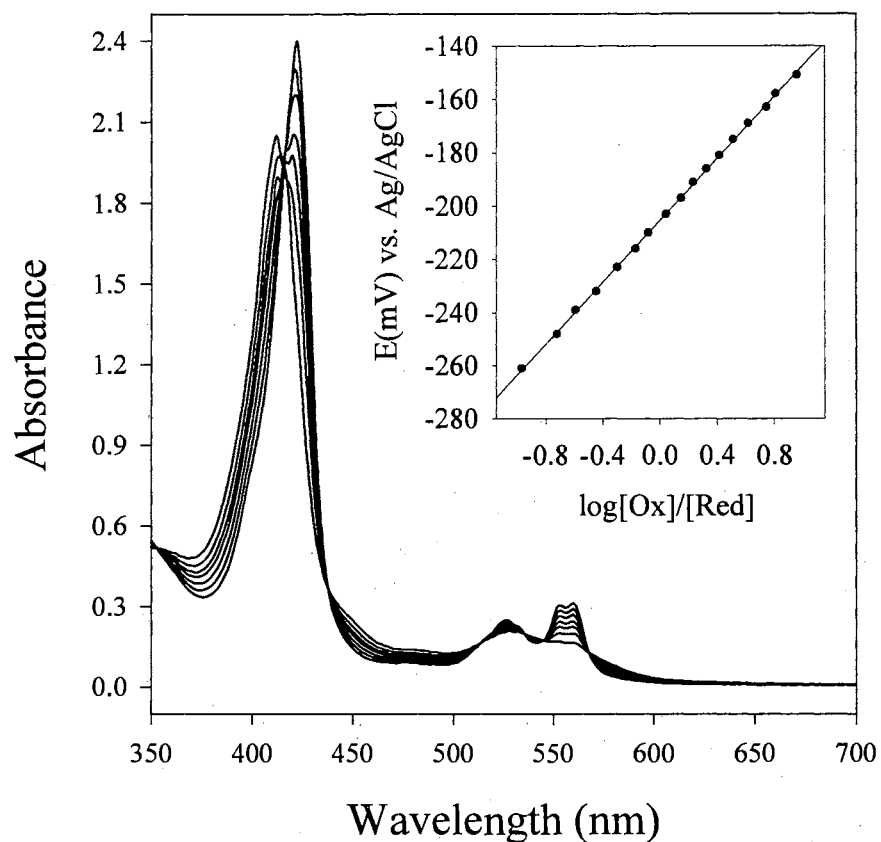
Figure 7. Spectra obtained from the titration of DiMe ester in the presence of [Ru(NH$_3$)$_6$]Cl$_3$ and 2,5-dyhydroxy-p-benzoquinone. Phosphate buffer, pH 7.0, μ = 0.1 was used for the experiment. Inset: Nernst plot of the data. The midpoint potential calculated from this plot is -4 mV vs NHE. The Nernst slope is 58 mV. The absorbance at 422 nm was monitored.
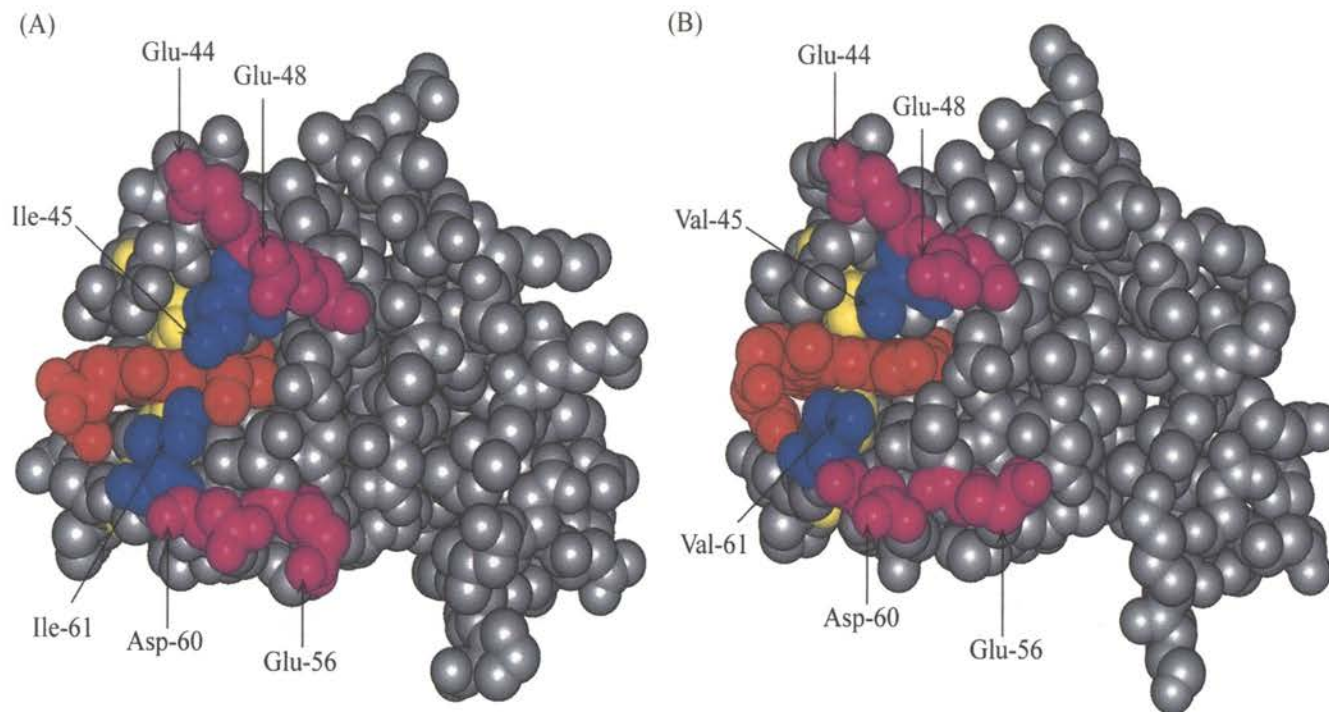
Figure 8. (A) View of the V45I/V61I double mutant of OM cytochrome b₅ showing the relative positions of the heme (red) Ile-45 and Ile-61 (blue) and acidic residues Glu-44, Glu- 48, Glu-56 and Asp-60 (magenta). This view shows that the side chains of Ile at positions 45 and 61 protect the heme meso and heme vinyl groups from the aqueous environment. **(B)** This view of wild type OM cytochrome b₅ demonstrates that the heme edge in this molecule is largely exposed to the aqueous environment.

solvent exposed heme propionate, Glu-44, Glu-48, Glu-56, and Asp-60; the position of these acidic residues with respect to the heme is shown in Fig. 8. The formation of a complex neutralizes the charge on the heme propionate and excludes water from the interface between polylysine and cytochrome b_5, which is delineated by the above mentioned acidic residues. Exclusion of water from the complex interface, therefore, has a large effect on the dielectric constant experienced by the heme microenvironment. In other words, before the complex is formed, the heme edge in the wild type protein is solvated by water, whereas within the complex the heme edge is in a more hydrophobic environment, hence experiences a lower dielectric constant. The reduced value of the dielectric constant is less efficient in stabilizing the positive charge on the ferric heme, therefore destabilizing the ferric oxidation state with respect to the ferrous oxidation state. Consequently, the protein within the complex is more easily reducible, as manifested in the more positive reduction potential.

Direct experimental evidence in support of this argument comes from the fact that the reduction potential of the DiMe ester derivative of the V45I/V61I double mutant is nearly independent of polylysine concentration (Fig. 5D). The heme edge of the DiMe ester derivative of the V45I/V61I mutant is also delineated by the solvent exposed heme propionate, Glu-44, Glu-48, Glu-56, and Asp-60. In contrast to the wild type protein, however, the heme edge in the mutant is not readily solvated by water (Fig. 8) because of the hydrophobic contacts that it makes with the side chains of Ile-45 and Ile-61. This is evident not only from the X-ray crystal structure of the mutant but also from the fact that the reduction potential of this protein is 40 mV more positive than that of the wild type protein. As a result, the dielectric constant experienced by the heme microenvironment in the V45I/V61I double mutant is not expected to change significantly upon formation of a

complex with polylysine. In fact, this is manifested in the nearly independent behavior of the reduction potential of the DiMe ester derivative of V45I/V61I as a function of polylysine concentration. In comparison, when the reduction potential of the V45I/V61I mutant is measured by voltammetry, the values are dependent on polylysine concentration (Fig. 5c). The modulation of reduction potential in this case originates almost exclusively from the neutralization of the negative charge on the solvent exposed heme propionate, upon formation of a complex with polylysine.

Relative Contributions to Modulation of Redox Potential

Previous studies carried out with native [17] and mutated [18] bovine microsomal cytochrome b_5 and their corresponding DiMe ester derivatives revealed that the proteins with esterified hemes possess a reduction potential of 64-67 mV more positive than proteins containing normal heme. Furthermore, studies conducted with cytochrome b_5 reconstituted with modified hemes demonstrated that neutralization of only one heme propionate is typically accompanied by a 27-35 mV cathodic shift in reduction potential [23]. In this context, it is interesting to analyze the magnitude of the shifts observed with the wild type, V45I/V61I mutant, and corresponding DiMe ester derivatives of OM cytochrome b_5. Inspection of Fig. 5 reveals that OM cytochrome b_5 undergoes a total shift of 76 mV (Fig. 5a), whereas the reduction potential of the corresponding DiMe ester is modulated by 41 mV (Fig. 5b). Assuming that the shift in the potential of the DiMe ester of OM cytochrome b_5 originates primarily from the dehydration of the complex interface, then it is possible to subtract 41 mV from the 76 mV shift displayed by OM cytochrome b_5. This indicates that neutralization of the solvent exposed heme propionate in OM cytochrome b_5 by polylysine results in a 35 mV shift in reduction potential. This value is in good agreement with the

153

expected shift resulting from the neutralization of one heme propionate. In a similar manner, inspection of Fig. 5c reveals that the reduction potential of the V45I/V61I mutant is modulated by a total of 39 mV, whereas the reduction potential of the DiMe ester derivative of the mutant protein is modulated by a total of 8 mV. Assuming that the shift observed for the DiMe ester derivative of V45I/V61I originates from a small change in the dielectric constant experiences by the heme environment upon complex formation, then the neutralization of the heme propionate in the mutant protein must modulate the reduction potential by 31 mV. These observations imply that in OM cytochrome b_5, the exclusion of water from the complex interface exerts an effect that is comparable, if not larger, than the one originating from neutralization of the charge on the solvent exposed heme propionate.

Conclusion

It is known that the reduction potential of electroactive cofactors is affected by the dielectric constant of the environment that surrounds them. For instance, it has been reported that the reduction potential of the heme in cytochrome c is 240 mV more positive in the folded protein than in its unfolded counterpart [24]. This large shift has been attributed to water exclusion from the heme environment. In fact, the availability of X-ray crystal structures for several different cytochrome c allowed these authors to demonstrate that the reduction potential of heme proteins can be tuned by approximately 500 mV, through variations in the exposure of heme to the aqueous environment [24]. The results presented in this report suggest that in addition to the large modulation of reduction potential resulting from embedding the heme cofactor in the interior of a poly-peptide, an additional modulation of redox potential may originate from protein-protein interactions. This secondary

modulatory mechanism is likely to be more noticeable in proteins where the redox-active cofactor is partially exposed to the aqueous environment. When such proteins bind a redox partner immediately prior to electron exchange, the partially exposed cofactor is likely to be buried at the interface of the interprotein complex. The change in dielectric constant experienced by the cofactor, in turn, will impose a shift in the reduction potential of the corresponding protein. It has also been demonstrated that the binding of cytochrome c to cytochrome b_5 lowers the reorganization energy of the intramolecular electron transfer reaction between a ruthenium complex appended to cytochrome b_5 and the heme center in this protein [18, 25]. These investigators proposed that the change in reorganization energy originates from the exclusion of water from the cytochrome b_5-cytochrome c complex interface. The modulation of the reduction potential of cytochrome b_5 by its exposed heme edge, therefore, is in good agreement with the conclusions obtained from kinetic experiments of Durham and coworkers [18, 25]. In fact, if the electrochemical and kinetic observations are taken together, it is possible to conclude that the reduction potential exhibited by cytochrome b_5 is likely to be significantly more positive when it is bound to cytochrome c than when it is measured with classical potentiometric techniques. Consequently, in order to attain a detailed description of electron transfer between cytochrome b_5 and cytochrome c it may be necessary to consider that the formation of an interprotein complex has an effect in the reorganization energy and in the driving force of the reaction.

References

1. Eddowes, M. J.; Hill, H. A. O (1977) *J. Am.Chem. Soc. Chem. Comm.*, 771.

2. Yeh, P.; Kuwana, T. (1977) *Chemistry Letters*, 1145.

3. Armstrong, F. A. (1990) *Struc. Bond*, **72**, 137.

4. Hawkridge, F. M.; Taniguchi, I. (1995) Comments *Inorg. Chem.* **17**, 163.

5. Bond., A. M. (1994) *Inorg. Chim. Acta*, **226**, 293.

6. Bowden, E. F. (1997) *Interface*, 40.

7. Armstong, F. A.; Hill, H. A. O.; Walton, N.J. (1984) *J. Chem. Soc. Chem.Commun.*, 976.

8. Armstong, F. A.; Cox. P. A.; Hill, H. A. O.; Lowe, V. J.; Oliver, B. N. (1987) *Electroanal.Chem.*, **217**, 331.

9. Armstong, F. A.; Hill, H. A. O.; Oliver, B. N.; Walton, N.J. (1984) *J. Am. Chem. Soc.*, **106** 921.

10. Armstong, F. A.; Lannon, M. J. (1987) *J. Am. Chem. Soc.*, **109**, 7211.

11. Rivera, M.; Wells, M. A.; Walker, F. A. (1994) *Biochemistry* **33**, 2161.

12. Rivera, M.; Seetharaman, R.; Ghirdhar, D.; Wirtz, M.; Zhang, X.; Wang, X. (1998) *Biochemistry*, **37**, 1485.

13. Rodgers, K. K.; Sliger, S. G. (1991) *J. Am. Chem. Soc.*, **113**, 9419.

14. Rodgers, K. K.; Sliger, S. G. (1991) *J. Mol. Biol.*, **221**, 1453.

15. Mauk, M. R.; Mauk, A. G. (1986) *Biochemistry*, **25**, 7085.

16. Mauk, A. G.; Mauk, M. R.; Moore, G. R.; Northrup, S. H. (1995) *J. Bioenerg. Biomemr.*, **27**, 311.

17. Rodriquez-Maranon, M.J.; Feng, Q.; Stark, R. E.; White, S. P.; Zhang, X.;

Foundling, S.I.; Rodriques, V.; Schilling III, C. L.; Bunce, R. A.; Rivera, M. (1996) *Biochemistry,* **35**, 16378.

18.   Durham, B.; Fairris, J. L.; Mclean, M.; Millet, F.; Scott, J. R.; Sligar, S. G.; Willie, A. (1995) *J. Bioenerg. Biomembr.,* **27**, 331.

19.   Beck von Bodman, S.; Schuler, M. A.; Jollie, D. R.; Sliger, S. G. (1986) *Proc. Natl. Acad. Sci.* U.S.A., **83**, 9443.

20.   Stankovich, M. T. (1980) *Anal. Biochem.,* **109**, 295.

21.   Reid, L. S.; Mauk, M. R.; Mauk, A. G. (1984) *J. Am. Chem. Soc,* **106**, 2182.

22.   Funk, W. D.; Lo, T. P.; Mauk, M. R.; Brayer, D. G.; Macgillivray, R. T. A.; Mauk, G.M. (1990) *Biochemistry,* **29**, 5500.

23.   Lee, K. B.; Jun, E.; La Mar, G. N.; Ressano, I. N.; Ravindra, K. P.; Smith, K. M.; Walker, F. A.; Buttlaire, D. H. (1991) *J. Am. Chem. Soc,* **113**, 3576.

24.   Tezcan, F. A.; Winkler, J. R.; Gray, H. B. (1998) *J. Am. Chem. Soc,* **120**, 13383.

25.   Scott, J. R.; Willie, A.; McLean, M.; Stayton, P.; Sligar, S. G.; Durham, B.; Millet, F.; (1993) *J. Am.Chem. Soc,* **115**,. 6820.

26.   Bowden, E. F.; Hawkridge, F. M.; Blount, H. N. (1984) *J. Electoanal. Chem.,* **161**, 355.

27.   Wirtz, M.; Klucik, J.; Rivera, M. (2000) *J. Am.Chem. Soc.,* **122**, 1047.

28.   Taniguchi, I.; Hirakawa, Y.; Iwakiri, K. I.; Tominago, M.; Nishiyama, K. (1994) *J. Chem. Soc. Chem.Commu.,* 953.

29.   Taniguchi, I.; Miyahara, A.; Iwakiri, K. L.; Hirakawa, K.; Nishiyama, K.; Akahashi, T.; Hase, T. (1997) *Chem. Lett.,* 929.

30.   Moore, G. R. (1983) *FEBS Lett.,* **161**, 171.

31.   Costa, C.; Moore, G. R. (1998) *Inorg.Chim. Acta,* **275**, 256.

32.   Otwinowshi, Z.; Minor, W. (1997) *Methods Enzymol.,***276**, 307.

33.   Armstrong, F. A.; Hill, H. A. O.; Walton, N. J. (1988) *Acc. Chem. Res.,* **21**, 407.

34.   Bagby, S.; Barker, P. D.; Di Gleria, K.; Hill, H. A. O.; Lowe, V. (1988)*Biochem. Soc. Trans.,* **16**, 958.

35.   Bond, A. M.; Hill, H. A. O.; Page, D. J.; Psalti, I. S.; Walton, N. J. (1990) *Eur. J. Biochem..,* **191**, 737.

36.   Hill, H. A. O.; Page, D. J.; Walton, H. J.; Whitford, D. (1985) *J. Electroanal. Chem.,* **187**, 315.

37.   Rivera, M.; Barillas-Mury, C.; Christensen, K. A.; Little, J. W.; Wells, M. A.; Walker, F. A. (1992) *Biochemistry,* **31**, 12233.

VITA

MARC-OLIVER SASCHA WIRTZ

Candidate for the Degree of

Doctor of Philosophy

Thesis: ELECTROCHEMICAL ACTIVATION OF PROTEINS AT
ELECTRODE SURFACES THROUGH ELECTROSTATIC
PROMOTION AND DISCRIMINATION

Major Field: Chemistry

Biographical:

Personal Data: Born in Erlangen, Germany, October 17, 1972, the son of Donald
and Rita Wirtz.

Education: Graduated from Vicenza High School, Vicenza, Italy in 1990;
received a Bachelor of Science Degree in Chemistry from Cameron
University, Lawton, Oklahoma in 1996; completed requirements for the
Doctor of Philosophy Degree at Oklahoma State University in December,
2000.

Professional Experience: August 1996 to present, graduate research and teaching
assistant, Oklahoma State University.

Professional Organizations: Phi Lamda Upsilon; American Chemical Society.